APPLICATION OF SPIRITUAL PRINCIPLES TO THE WORK OF TEACHING

MAURICE COLBOURNE

Application of Artificial Neural Networks for Online Voltage Stability Monitoring and Enhancement of an Electric Power System

By

Saikat Chakrabarti, B. E., M. E.

A thesis submitted in partial fulfillment
of the requirements for the degree of
Doctor of Philosophy

Faculty of Engineering and Applied Science
Memorial University of Newfoundland
St. John's, Newfoundland, Canada

October, 2006

Your file Votre référence
ISBN: 978-0-494-30424-2
Our file Notre référence
ISBN: 978-0-494-30424-2

Abstract

Due to economic reasons arising out of deregulation and open market of electricity, modern day power systems are being operated closer to their stability limits. When a fault occurs, there is a great possibility of occurrence of cascading outages, as observed in the August 2003 Blackout in the North-East USA and Canada. Power system voltage stability is one of the challenging problems faced by the utilities. Innovative methods and solutions are required to evaluate the voltage stability of a power system and implement suitable strategies to enhance the robustness of the power system against voltage stability problems. This is the motivation behind the research carried out as a part of the PhD program and presented in this dissertation.

Artificial neural networks (ANNs) have gained widespread attention from researchers in recent years as a tool for online voltage stability assessment. Two major areas requiring investigation are identified after doing a thorough survey of the existing literature on online voltage stability monitoring using ANN. The first one is the effective method of selecting important features among numerous possible measurable parameters as potential inputs to the ANN. The second one is the feasibility of using a single ANN for monitoring voltage stability for multiple contingencies. In the first phase of the research, a regression-based method of computing sensitivities of the voltage stability margin with respect to different parameters is proposed. Using the sensitivity information, important features are chosen selectively to train separate Multilayer Perceptron Networks (MLP) to monitor voltage stability for different contingencies.

In the second phase of the research, an enhanced Radial Basis Function Network (RBFN) is proposed for online voltage stability monitoring. Important features of the proposed RBFN are: (1) the same network is trained for multiple contingencies, thus eliminating the need for training different ANNs for different contingencies, (2) the number of neurons in the hidden layers is decided automatically using a sequential learning strategy, (3) the RBFN can be adapted online, with changing operating scenario, (4) a network pruning strategy is used to limit the growth of the network size as a result of the adaptation process.

In the next phase of the research, a sensitivity-based voltage stability enhancement method is proposed, considering multiple contingencies. Considering the limitations of the existing analytical methods, the sensitivities of the voltage stability margin with respect to parameters are found by using the RBFN proposed in the second phase of the research. Using the sensitivity information, correct amounts of generation rescheduling are found by using linear optimization. Case studies are presented throughout different sections of the thesis to illustrate the application of the proposed methods.

Acknowledgements

First of all I would like to take this opportunity to express my sincerest gratitude and indebtedness to Dr. Benjamin Jeyasurya for his continuous encouragement, guidance and supervision throughout my PhD program. I also acknowledge the assistance from the members of my supervisory committee, Dr. Glyn George and Dr. M. Tariq Iqbal. I extend my appreciation to the School of Graduate Studies, Memorial University of Newfoundland for their support in this program. I am also grateful to the Dean and Associate Dean, Faculty of Engineering and Applied Science, for their help in this program. The financial Assistance from the Natural Sciences and Engineering Research Council of Canada is acknowledged.

I sincerely acknowledge the help and advice received from Ms. Moya Crocker regarding the administrative matters throughout my program. Assistance from Ms. Lillian Beresford and Ms. Sonja Knutson of the International Student Advising Office regarding issues related to international studentship is highly appreciated. I offer my sincerest thanks to Dr. J. E. Quaicoe and Dr. Vlastimil Masek for their constructive suggestions during my Comprehensive Examination.

I am grateful to my friends and fellow graduate students for their cooperation, valuable suggestions and constant encouragement. I am grateful to my parents and sisters for their continued encouragement and support throughout my program. Finally it is time to thank all who have contributed directly or indirectly towards completion of this work.

CONTENTS

List of Figures

List of Tables

List of Symbols and Abbreviations

E	Sending end voltage
V	Receiving end voltage
δ	Power angle
λ	Eigenvalue of a matrix
Λ	Diagonal matrix containing all the Eigenvalues of a matrix
$\mathbf{J}$	Powerflow Jacobian matrix
v_m	Vector of modal voltage variation
q_m	Vector of modal reactive power variation
K	Load multiplication factor
M	Voltage stability margin in MW
ΔM	Required enhancement in the voltage stability margin
$\mathbf{f}$	Powerflow equations
ω	Left eigenvector of the powerflow Jacobian matrix
β	Coefficients of regression
Z	Condition number of a matrix
S_i^j	Sensitivity of the voltage stability margin with respect to the i^{th} parameter for the j^{th} contingency
S_{pmin}	Minimum cutoff value of sensitivity for selecting load active power as feature for the ANN
S_{qmin}	Minimum cutoff value of sensitivity for selecting load reactive power as feature for the ANN

T_j^p	Set of load active power demands chosen as features for the ANN for the j^{th} contingency
T_j^q	Set of load reactive power demands chosen as features for the ANN for the j^{th} contingency
c	Number of contingencies considered, including the base case
φ	Activation functions for the Multilayer Perceptron neural netwok
$g(\mathbf{X},\mathbf{t})$	Radial Basis Function at the data center **t** for input **X**
σ	Spread parameter of the Radial Basis Function
e_{min}	The minimum tolerable error for the output of the Radial Basis Function Network
ε_{max}	The initial value of the distance parameter for adding a new hidden unit to the Radial Basis Function Network
ε_{min}	Minimum allowable value of the distance parameter
$\mathbf{G}$	Matrix of Basis Functions
$\mathbf{I}_q$	Identity matrix of dimension $[q \times q]$
$\mathbf{o}_j$	The output vector of the j^{th} hidden unit of the Radial Basis Function Network
r_{min}	The threshold contribution to the output of the Radial Basis Function Network for pruning a hidden unit
P_{gi}	Real power generation of the i^{th} generator
$C(P_{gi})$	Cost of generation for the i^{th} generator, in \$/hr
HVDC	High Voltage Direct Current
TSO	Transmission System Operator
LTC	Load Tap Changer
PSAT	Power System Analysis Toolbox

SVC	Static Var Compensator
EMS	Energy Management System
ANN	Artificial Neural Network
MLP	Multilayer Perceptron
SEP	Stable Equilibrium Point
UEP	Unstable Equilibrium Point
PCA	Principal Component Analysis
VSM	Voltage Stability Margin
RBFN	Radial Basis Function Network
RAN	Resource Allocating Network
MRAN	Minimum Resource Allocation Network
LMS	Lease Mean Square

Chapter 1

Power System Voltage Stability

1.1 Introduction

At any point of time, a power system operating condition should be stable, meeting various operational criteria, and it should also be secure in the event of any credible contingency. Present day power systems are being operated closer to their stability limits due to economic and environmental constraints. Maintaining a stable and secure operation of a power system is therefore a very important and challenging issue. Voltage instability has been given much attention by power system researchers and planners in recent years, and is being regarded as one of the major sources of power system insecurity. Voltage instability phenomena are the ones in which the receiving end voltage decreases well below its normal value and does not come back even after setting restoring mechanisms such as VAR compensators, or continues to oscillate for lack of damping against the disturbances. Voltage collapse is the process by which the voltage falls to a low, unacceptable value as a result of an avalanche of events accompanying voltage instability [1]. Once associated with weak systems and long lines, voltage problems are now also a source of concern in highly developed networks as a result of heavier loading.

The main factors causing voltage instability in a power system are now well explored and understood [1-13]. A brief introduction to the basic concepts of voltage stability and some of the conventional methods of voltage stability analysis are presented in this chapter. Simulation results on test power systems are presented to illustrate the

problem of voltage stability and the conventional methods to analyze the problem. Limitations of conventional methods of voltage stability analysis are pointed out and the scope of the use of Artificial Neural Networks as a better alternative is discussed.

1.2 Classification of voltage stability

The time span of a disturbance in a power system, causing a potential voltage instability problem, can be classified into short-term and long-term. The corresponding voltage stability dynamics is called short- term and long-term dynamics respectively [2-5]. Automatic voltage regulators, excitation systems, turbine and governor dynamics fall in this short-term or 'transient' time scale, which is typically a few seconds. Induction motors, electronically operated loads and HVDC interconnections also fall in this category. If the system is stable, short-term disturbance dies out and the system enters a slow long-term dynamics. Components operating in the long-term time frame are transformer tap changers, limiters, boilers etc. Typically, this time frame is for a few minutes to tens of minutes. A voltage stability problem in the long-term time frame is mainly due to the large electrical distance between the generator and the load, and thus depends on the detailed topology of the power system.

Figure 1.1 shows the components and controls that may affect the voltage stability of a power system, along with their time frame of operation [1]. Examples of short-term or transient voltage instability can be found in the instability caused by rotor angle imbalance or loss of synchronism. Recent studies have shown that the integration of highly stressed HVDC links degrades the transient voltage stability of the system [1].

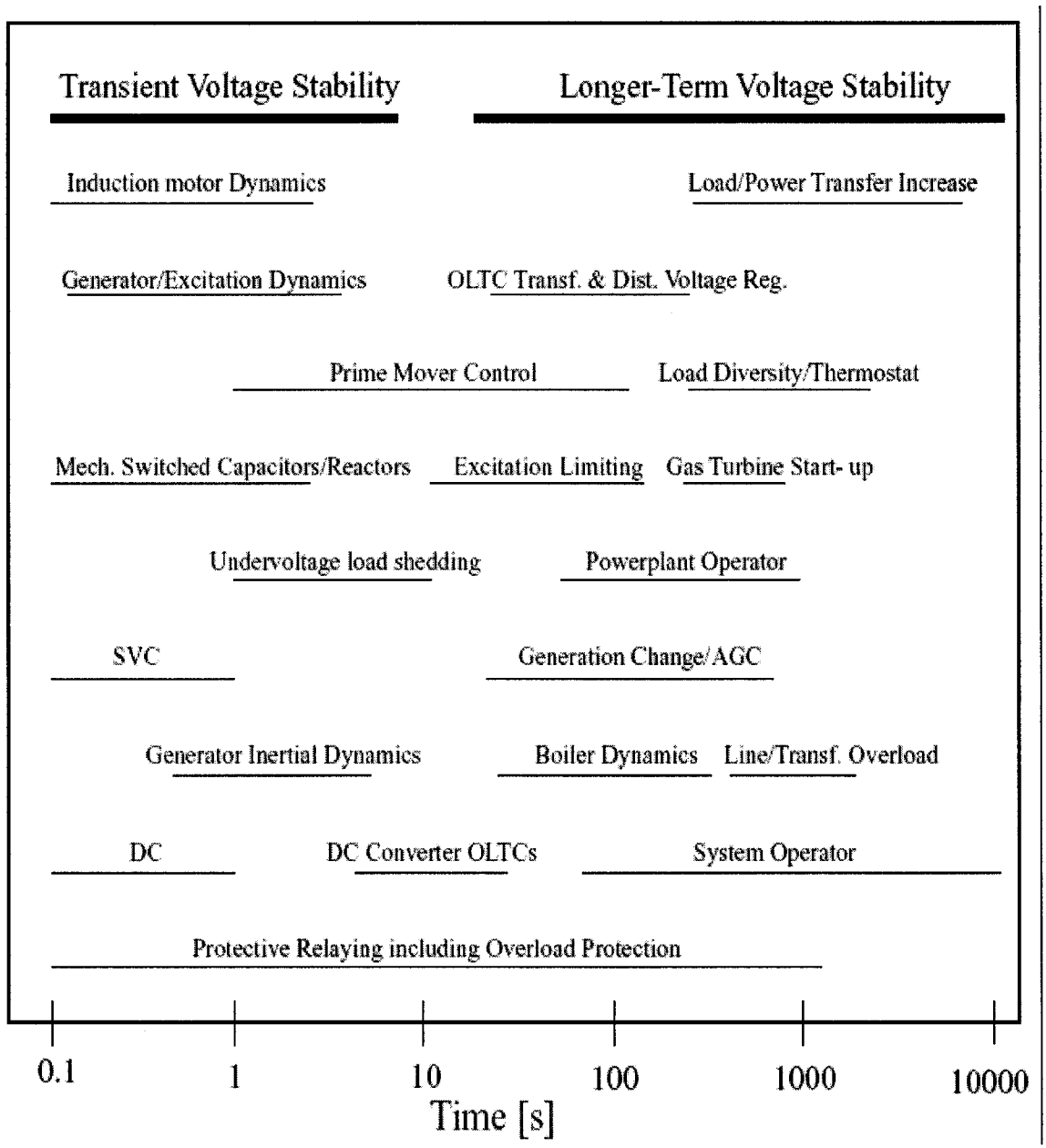

Figure 1.1: Time responses of different controls and components to voltage stability [1]

There is not much scope for operator intervention in transient voltage instability. The transmission system operator (TSO) mainly relies on automatic emergency actions to avoid incumbent voltage instability. The automatic corrective actions are taken through

protective devices to preserve operation of largest possible part of the power system by isolating the unstable part [6].

Long-term voltage instability (or mid-term or post-transient, as it is sometimes called) problems can occur in heavily loaded systems where the electrical distance is large between the generator and the load. The instability may be triggered by high power imports from remote generating stations, a sudden large disturbance, or a large load buildup (such as morning or afternoon pickup). Operator intervention may be possible if the time scale is long enough. Timely application of reactive power compensation or load shedding may prevent this type of voltage instability.

From the point of view of techniques used to analyze the voltage stability, it is often useful to categorize the problem into small-disturbance and large-disturbance voltage stability [2]. Small disturbance or steady state voltage stability deals with the situation when the system is subjected to a small perturbation, such that the system can be analyzed by linearizing around the pre-disturbance operating point. Steady state stability analysis is helpful in getting a qualitative picture of the system, i.e., how stressed the system is, or how close the system is, to the point of instability. Examples of steady state stability can be found in power systems experiencing gradual change in load.

Large-disturbance stability deals with larger disturbances such as loss of generation, loss of line etc. To analyze the large-disturbance stability, one has to capture the system dynamics for the whole time frame of the disturbance. A suitable model of the system has to be assumed and a detailed dynamic analysis has to be carried out in order to get a clear picture of the stability.

1.3 Voltage stability of a simple 2-bus system

The basic concept of voltage stability can be explained with a simple 2-bus system shown in Figure 1.2. The load is of constant power type. Real power transfer from bus 1 to 2 is given by [4],

$$P = \frac{EV}{X}\sin\delta \tag{1.1}$$

Reactive power transfer from bus 1 to 2 is given by,

$$Q = -\frac{V^2}{X} + \frac{EV}{X}\cos\delta \tag{1.2}$$

where, $\mathbf{E} = E\angle\delta$ is the voltage at bus 1,

$\mathbf{V} = V\angle 0$ is the voltage at bus 2,

X= impedance of the line (neglecting resistance),

δ = power angle.

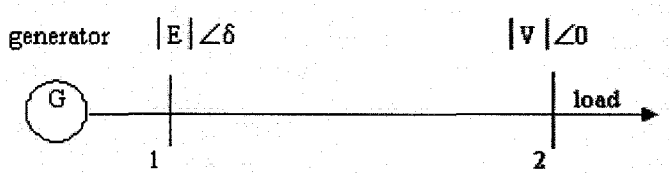

Figure 1.2: 2-bus test system

Normalizing the terms in (1.1) and (1.2) with

$v = V/E$, $p = P.X/E^2$ and $q = Q.X/E^2$, one obtains,

$$p = v \sin \delta \tag{1.3}$$

$$q = - v^2 + v \cos \delta \tag{1.4}$$

Squaring the two equations above and rearranging,

$$v^2 (\sin^2 \delta + \cos^2 \delta) = p^2 + (q + v^2)^2$$

$$\text{or, } v^4 + v^2 (2q - 1) + (p^2 + q^2) = 0 \tag{1.5}$$

Positive real solutions of v from (1.5) are given by,

$$v = \sqrt{\frac{1}{2} - q \pm \sqrt{\frac{1}{4} - p^2 - q}} \tag{1.6}$$

A plot of v on the p-q-v plane is shown in Figure 1.3 [4]. Corresponding to each point (p,q), there are two solutions for voltage, one is the high voltage or stable solution, which is the actual voltage at the bus, and the other one is the low voltage or unstable solution. The equator, along which the two solutions of v are equal, represents maximum power points. Starting from any operating point on the upper part of the surface, an increase in p or q or both brings the system closer to the maximum power point. An increase in p or q beyond the maximum power point makes the voltage unstable.

The preceding discussion illustrates voltage instability caused by an increase in system loading. In a real power system, voltage instability is caused by a combination of many additional factors which includes the transmission capability of the network, generator reactive power and voltage control limits, voltage sensitivity of the load,

characteristics of reactive compensation devices, action of voltage control devices such as transformer under load tap changers (ULTCs) etc.

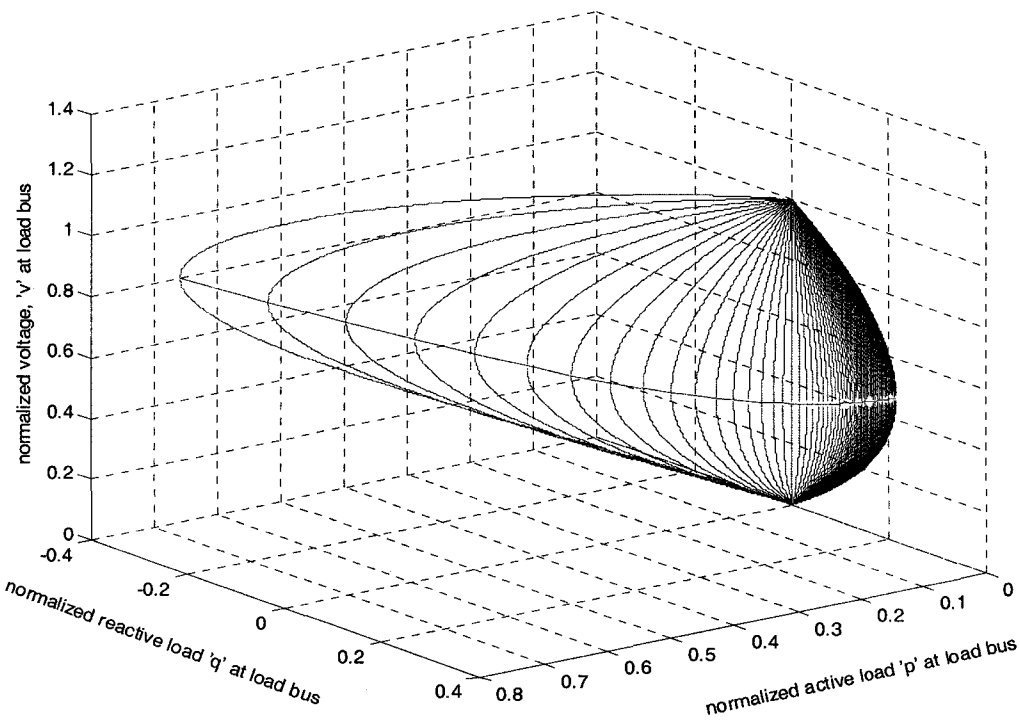

Figure 1.3: Variation of bus voltage with active and reactive loading for the 2-bus test system

1.4 Tools for voltage stability analysis

Different methods exist in the literature for carrying out a steady state voltage stability analysis. The conventional methods can be broadly classified into the following types.

1. P-V curve method.
2. V-Q curve method and reactive power reserve.

3. Methods based on singularity of power flow Jacobian matrix at the point of voltage collapse.
4. Continuation power flow method.

1.4.1 P-V curve method

This is one of the widely used methods of voltage stability analysis. This gives the available amount of active power margin before the point of voltage instability. For radial systems, the voltage of the critical bus is monitored against the changes in real power consumption. For large meshed networks, P can be the total active load in the load area and V can be the voltage of the critical or representative bus. Real power transfer through a transmission interface or interconnection also can be studied by this method.

For a simple two-bus system as shown in Figure 1.2, equation (1.6) gives real solutions of v^2, provided $(1 - 4q - 4p^2) \geq 0$.

Assuming a constant power factor load such that $q/p = k$ (constant), the inequality can be expressed as,

$$p \leq \frac{1}{2}((1+k^2)^{1/2} - k) \tag{1.7}$$

For values of 'p' satisfying (1.7), there are two solutions of v as follows:

$$v_1 = (1/2 - pk + (1/4 - pk - p^2)^{1/2})^{1/2} \tag{1.8}$$

and $$v_2 = (1/2 - pk - (1/4 - pk - p^2)^{1/2})^{1/2} \tag{1.9}$$

For real values of v_1 and v_2, the terms under the square roots should be positive.

Hence, $(1/2 - pk - (1/4 - pk - p^2)^{1/2}) \geq 0$

or, $p^2(k^2 + 1) \geq 0$ (1.10)

which is always true.

Hence (1.7) is the inequality that determines the maximum value of p.

Thus, representing the load as a constant power factor type, with a suitably chosen power factor, the active power margin can be computed from (1.7). For different values of load power factors, i.e., for different corresponding values of 'k', the normalized values of load active power are shown in Figure 1.4.

In practice, it is possible to find the Thevenin equivalent of any system with respect to the bus under consideration. It is to be noted that the generations are rescheduled at each step of change of the load. Some of the generators may hit the reactive power limit. The network topology may keep changing with respect to the critical bus, with change in the loading, thereby reducing the accuracy of the method. This method works well in the case of an infinite bus and isolated load scenario.

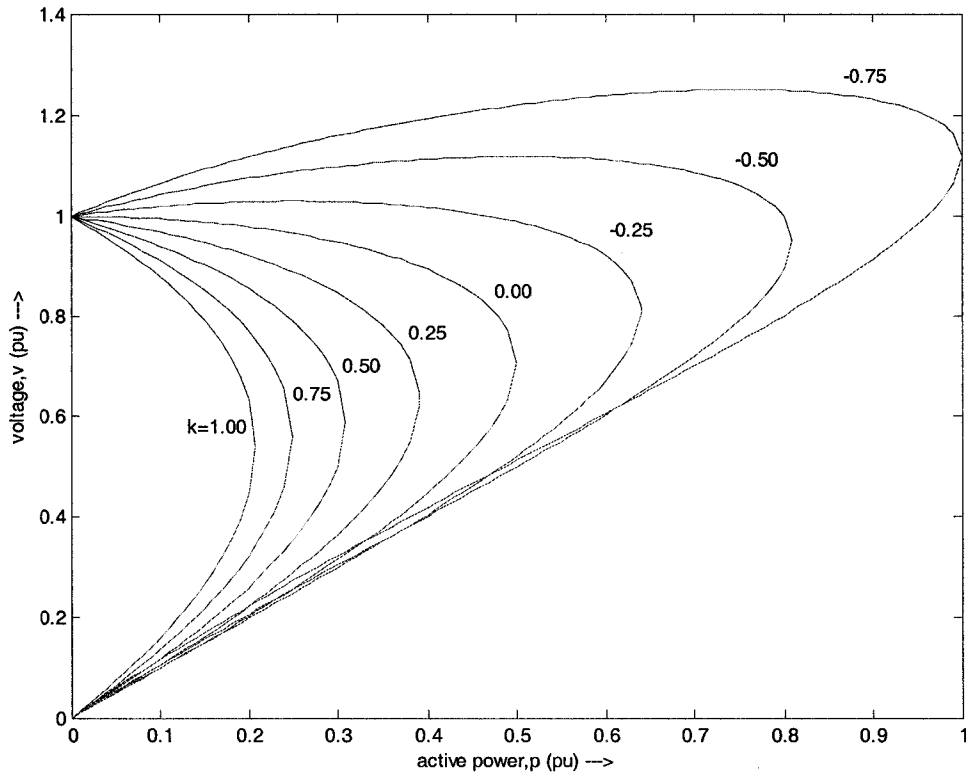

Figure 1.4: Normalized P-V curves for the 2-bus test system

1.4.2 V-Q curve method and reactive power reserve

The V-Q curve method is one of the most popular ways to investigate voltage instability problems in power systems during the post transient period [1, 4, 5]. Unlike the P-V curve method, it doesn't require the system to be represented as two-bus equivalent. Voltage at a test bus or critical bus is plotted against reactive power at that bus. A fictitious synchronous generator with zero active power and no reactive power limit is connected to the test bus. The powerflow program is run for a range of specified voltages with the test bus treated as the generator bus. Reactive power at the bus is noted from the

power flow solutions and plotted against the specified voltage. The operating point corresponding to zero reactive power represents the condition when the fictitious reactive power source is removed from the test bus.

Voltage security of a bus is closely related to the available reactive power reserve, which can be easily found from the V-Q curve of the bus under consideration. The reactive power margin is the MVAR distance between the operating point and either the nose point of the V-Q curve or the point where capacitor characteristics at the bus are tangent to the V-Q curve [1]. Stiffness of the bus can be qualitatively evaluated from the slope of the right portion of the V-Q curve. The greater the slope is, the less stiff is the bus, and therefore the more vulnerable to voltage collapse it is. Weak busses in the system can be determined from the slope of V-Q curve.

For the simple two-bus system shown in Figure 1.2, equations of V-Q curves for constant power loads can be derived as follows. From (1.3) the power angle δ is computed for specified active power and used in (1.4). For a range of values of voltage and different active power levels, normalized V-Q curves are shown in Figure 1.5. The critical point or nose point of the characteristics corresponds to the voltage where dQ/dV becomes zero. If the minimum point of the V-Q curve is above the horizontal axis, then the system is reactive power deficient. Additional reactive power sources are needed to prevent a voltage collapse. In Figure 1.5, curves for p=1.00 and p=0.75 signify reactive power deficient busses. Busses having V-Q curves below the horizontal axis have a positive reactive power margin. The system may still be called reactive power deficient, depending on the desired margin.

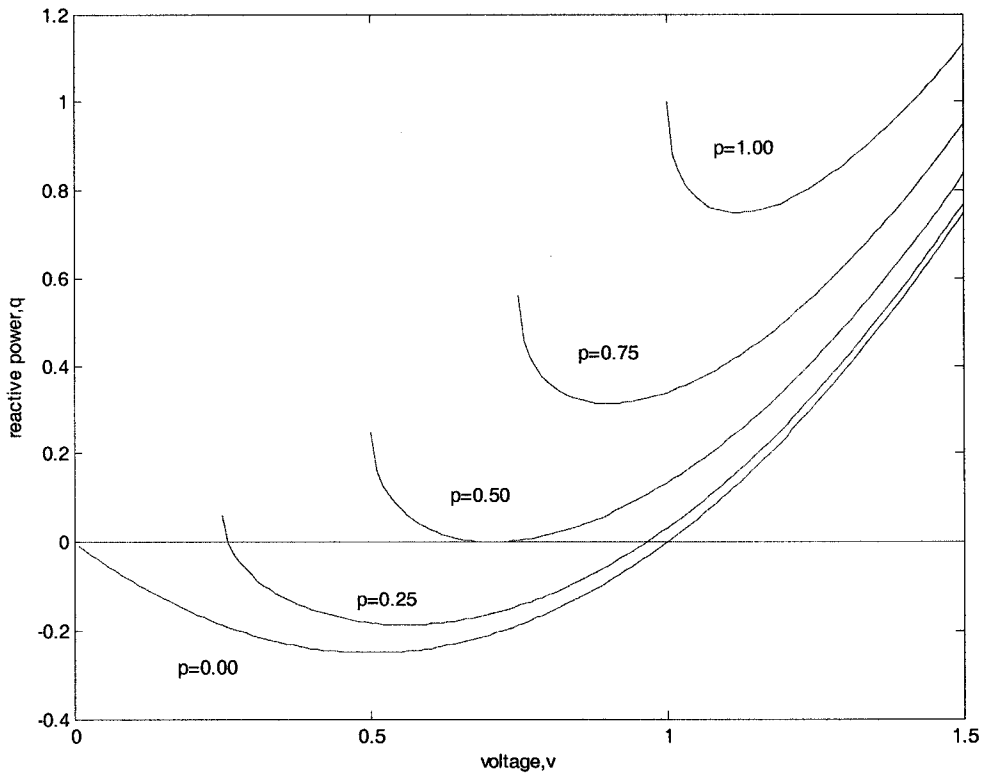

Figure 1.5: Normalized V-Q curves for the 2-bus test system

1.4.3 Method based on singularity of powerflow Jacobian matrix at the point of voltage collapse

A number of methods have been proposed in the literature that uses the fact that the power flow Jacobian matrix becomes singular at the point of voltage collapse. Modal analysis [2, 5, 14] of the Jacobian matrix is one of the most popular methods.

1.4.3.1 Modal analysis

For a (n x n) square matrix **A**, left and right eigenvectors are defined as follows:

$$\mathbf{Ax} = \lambda\mathbf{x} \tag{1.11}$$

$$\mathbf{yA} = \lambda\mathbf{y} \tag{1.12}$$

where λ = eigenvalue of the matrix **A**, **x** (n x 1) = right eigenvector, **y** (1 x n) = left eigenvector.

The characteristic equation of both (1.11) and (1.12) is,

$$\det(\mathbf{A}-\lambda\mathbf{I}) = 0 \tag{1.13}$$

The solution of (1.13), i.e., $\lambda_1,\lambda_2,\ldots,\lambda_n$ are the eigenvalues of **A**. For different eigenvalues λ_i, i = 1,...,n, the right and left eigenvectors are defined as, $\mathbf{x}_i$, i = 1,...,n and $\mathbf{y}_i$, i = 1,...,n. In matrix form, the right eigenvector matrix, $\mathbf{X} = [\mathbf{x}_1, \mathbf{x}_2,\ldots, \mathbf{x}_n]$ and the left eigenvector matrix, $\mathbf{Y} = [\mathbf{y}_1^T,\mathbf{y}_2^T,\ldots, \mathbf{y}_n^T]^T$.

It can be shown that, $\mathbf{x}_j$ and $\mathbf{y}_i$ are orthogonal, such that,

$\mathbf{y}_i.\mathbf{x}_j = 0, \qquad \forall\ i \neq j$

$\neq 0, \qquad \forall\ i = j$

In practice, eigenvectors are normalized so that $\mathbf{y}_i.\mathbf{x}_i = 1, \quad \forall\ i = 1,\ldots,n.$

Hence, $\mathbf{Y.X} = \mathbf{I}$, or, $\mathbf{Y} = \mathbf{X}^{-1}$ (1.14)

Now, $\mathbf{A.X} = [\lambda_1\mathbf{x}_1\ \lambda_2\mathbf{x}_2\ \ldots\ldots\lambda_n\mathbf{x}_n\ ] = \mathbf{X}.\Lambda$ (1.15)

where $$\Lambda = \begin{bmatrix} \lambda_1 & 0 & \ldots & 0 \\ 0 & \lambda_2 & \ldots & 0 \\ & & \ldots\ldots & \\ 0 & 0 & \ldots & \lambda_n \end{bmatrix}$$

or, $\mathbf{A} = \mathbf{X}\,\Lambda\,\mathbf{X}^{-1} = \mathbf{X}\,\Lambda\mathbf{Y}$ (1.16)

Powerflow equations can be written in matrix form as follows.

$$\begin{bmatrix}\Delta\mathbf{P}\\ \Delta\mathbf{Q}\end{bmatrix}=\begin{bmatrix}J_{p\delta} & J_{pV}\\ J_{q\delta} & J_{qV}\end{bmatrix}\begin{bmatrix}\Delta\boldsymbol{\delta}\\ \Delta\mathbf{V}\end{bmatrix} \quad (1.17)$$

where $\Delta\mathbf{P}$ and $\Delta\mathbf{Q}$ are the changes in the real and reactive powers respectively, $\Delta\delta$ and $\Delta\mathbf{V}$ are the deviations in bus voltage angles and bus voltage magnitudes respectively.

For calculating V-Q sensitivities, one can assume $\Delta\mathbf{P} = 0$

Hence, $\mathbf{J}_{p\delta}.\,\Delta\delta + \mathbf{J}_{pV}.\Delta\mathbf{V} = 0$

or, $\Delta\delta = -\,\mathbf{J}_{p\delta}^{-1}.\mathbf{J}_{pV}.\Delta\mathbf{V}$ (1.18)

Now, $\Delta\mathbf{Q} = \mathbf{J}_{q\delta}.\Delta\delta + \mathbf{J}_{qV}.\Delta\mathbf{V} = \mathbf{J}_{q\delta}(-\,\mathbf{J}_{p\delta}^{-1}.\mathbf{J}_{pV}).\Delta\mathbf{V} + \mathbf{J}_{qV}.\Delta\mathbf{V} = \mathbf{J}_{R}\,.\Delta\mathbf{V}$

where, $\mathbf{J}_R = \mathbf{J}_{qV} - \mathbf{J}_{q\delta}.\mathbf{J}_{p\delta}^{-1}.\mathbf{J}_{pV}$

Hence, $\Delta\mathbf{V} = \mathbf{J}_R^{-1}\Delta\mathbf{Q}$ (1.19)

Now, assuming $\mathbf{J}_R = \mathbf{A}$ and using (1.16) one gets, $\mathbf{J}_R = \mathbf{X}\,\Lambda\mathbf{Y}$

or, $\mathbf{J}_R^{-1} = \mathbf{Y}^{-1}\Lambda^{-1}\mathbf{X}^{-1} = \mathbf{X}\Lambda^{-1}\mathbf{Y}$

Using (1.19), $\Delta\mathbf{V} = \mathbf{X}\,\Lambda^{-1}\mathbf{Y}\,\Delta\mathbf{Q}$

or, $\mathbf{Y}\Delta\mathbf{V} = \Lambda^{-1}\mathbf{Y}\Delta\mathbf{Q}$;[since, $\mathbf{X}=\mathbf{Y}^{-1}$]

Hence, $\mathbf{v}_m=\Lambda^{-1}\mathbf{q}_m$

where, $\mathbf{v}_m$ = vector of modal voltage variation

$\mathbf{q}_m$ = vector of modal reactive power variation

$$\text{Now, } \Lambda^{-1} = \begin{bmatrix}\lambda_1^{-1} & \ldots & 0\\ 0 & \lambda_2^{-1} & \ldots 0\\ 0 & 0 & \ldots \lambda_n^{-1}\end{bmatrix}$$

Thus, $\mathbf{v}_{mi} = \lambda_i^{-1}\mathbf{q}_{mi}$, $\forall$ i = 1,...,n

For any i, if $\lambda_i > 0$, then the variation of $\mathbf{v}_{mi}$ and $\mathbf{q}_{mi}$ are in the same direction and the system is voltage stable. When $\lambda_i < 0$ for any i, the system is voltage unstable.

To illustrate the use of the singularity-based voltage stability analysis method, modal analysis is applied on the 10-bus test system [2, 14] shown in Figure 1.6. Data for the 10-bus test system are given in Tables 1.1 to 1.5. Table 1.6 shows the eigenvalues of the reduced Jacobian matrix against load multiplication factor, K. Load multiplication factor is the ratio by which load is increased at 1 pu voltage. Real parts of the eigenvalues are designated as E_1, E_2,..., E_7. Normalized values of the two smallest eigenvalues are plotted against load multiplication factor in Figure 1.7. Computationally obtainable minimum values of eigenvalues correspond to a load multiplication factor of 1.146. An increase in load beyond this load level makes the receiving end voltage unstable. The magnitude of the minimum eigenvalue is therefore used as an indicator of the proximity of an operating point to the point of voltage collapse.

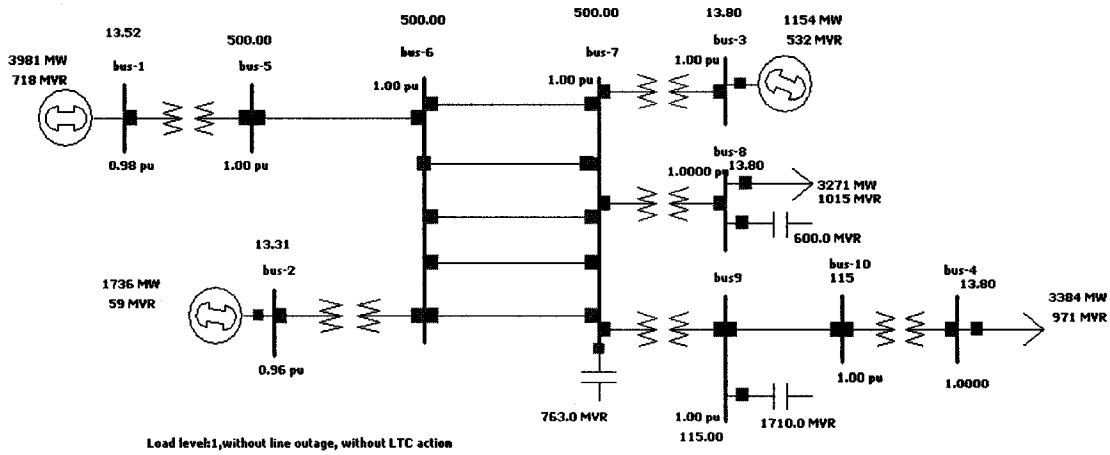

Figure 1.6: Single line diagram of the 10-bus test system

Table 1.1: Transmission lines data (R, X and B in pu on 100MVA base) for the 10-bus test system

End buses	R	X	B
5-6	0.0000	0.0040	0.0000
6-7	0.0015	0.0288	1.1730
9-10	0.0010	0.0030	0.0000

Table 1.2: Transformer data (R, X in pu on 100 MVA base) for the 10-bus test system

End buses	R	X	Ratio
1-5	0.0000	0.0020	0.8857
2-6	0.0000	0.0045	0.8857
3-7	0.0000	0.0125	0.9024
7-8	0.0000	0.0030	1.0664
7-9	0.0000	0.0026	1.0800
10-4	0.0000	0.0010	0.9750

Table 1.3: Shunt capacitor data for the 10-bus test system

Bus	MVAR
7	763
8	600
9	1710

Table 1.4: Base case Load data for the 10-bus test system

Bus	P (MW)	Q (MVAR)
8	3271	1015
4	3384	971

Table 1.5: Base case Generator data for the 10-bus test system

Bus	P (MW)	V (pu)
1	3981	0.9800
2	1736	0.9646
3	1154	1.0400

Table 1.6: Eigenvalues of the reduced Jacobian matrix of the 10-bus test system for different load levels

Load multiplication factor, K	E_1	E_2	E_3	E_4	E_5	E_6	E_7
0.9	2364	1407.1	951.37	26.9	161.27	634.92	390.65
1.0	2203.6	1330.8	425.01	25.062	148.21	598.07	374.9
1.1	2039.5	1253.1	903.38	22.724	134.36	560.11	360.82
1.12	1982.8	1224.6	896.14	21.718	129.64	546.49	356.42
1.14	1885.6	1173.8	881.53	19.795	121.52	522.62	348.03
1.145	1803.7	1129.5	867.34	17.983	114.62	502.09	340.19
1.146	1768.2	1110.4	861.03	17.143	111.59	493.21	336.72

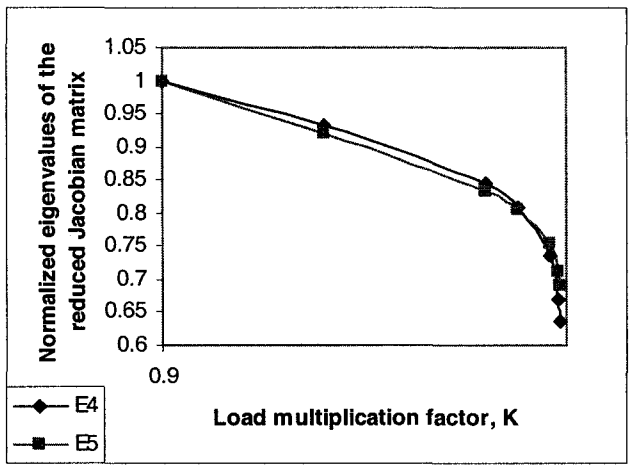

Figure 1.7: Variation of the real parts of the smallest two eigenvalues of the reduced Jacobian matrix against load multiplication factor for the 10-bus test system

1.4.4 Continuation powerflow

It is numerically difficult to obtain a powerflow solution near the voltage collapse point, since the Jacobian matrix becomes singular. Continuation powerflow is a technique by which the powerflow solutions can be obtained near or at the voltage collapse point [2, 4, 15].

Powerflow equations can be represented as,

$$\mathbf{P}_s = \mathbf{P}(\delta,\mathbf{V}) \quad \text{and} \quad \mathbf{Q}_s = \mathbf{Q}(\delta,\mathbf{V}) \tag{1.20}$$

where $\mathbf{P}_s$, $\mathbf{Q}_s$ are specified active and reactive powers of busses, δ and $\mathbf{V}$ are bus voltage angles and magnitudes respectively.

Equation (1.20) can be expressed as,

$$\mathbf{f}(\delta,\mathbf{V}) = \mathbf{PQ}_{spc} \tag{1.21}$$

where $\mathbf{PQ}_{spc} = [\mathbf{P}_s, \mathbf{Q}_s]^T$.

Considering variation of load as one of the parameters of the power flow equations, (1.21) can be rewritten as,

$$\mathbf{f}(\delta,\mathbf{V}) = \mathrm{K}\mathbf{PQ}_{spc} \tag{1.22}$$

where K is the loading parameter. For base case loading, K = 1.

Equation (1.22) can be written as,

$$\mathbf{F}(\delta,\mathbf{V},\mathrm{K}) = 0 \tag{1.23}$$

$$\text{Hence, } \Delta\mathbf{F} = \frac{\partial\mathbf{F}}{\partial\boldsymbol{\delta}}\Delta\boldsymbol{\delta} + \frac{\partial\mathbf{F}}{\partial\mathbf{V}}\Delta\mathbf{V} + \frac{\partial\mathbf{F}}{\partial\mathrm{K}}\Delta\mathrm{K} \tag{1.24}$$

$$\text{Now, } \Delta\mathbf{F} = \mathbf{F}(\delta^0,\mathbf{V}^0,\mathrm{K}^0) - \mathbf{F}(\delta,\mathbf{V},\mathrm{K}) = -\mathbf{F}(\delta,\mathbf{V},\mathrm{K}) \tag{1.25}$$

where $(\delta^0,\mathbf{V}^0,\mathrm{K}^0)$ is the solution of (1.23).

Using the above in equation (1.24) and writing in matrix form,

$$\begin{bmatrix} \frac{\partial \mathbf{F}}{\partial \boldsymbol{\delta}} & \frac{\partial \mathbf{F}}{\partial \mathbf{V}} & \frac{\partial \mathbf{F}}{\partial \mathrm{K}} \end{bmatrix} \begin{bmatrix} \Delta\boldsymbol{\delta} \\ \Delta \mathbf{V} \\ \Delta \mathrm{K} \end{bmatrix} = \left[-\mathbf{F}(\boldsymbol{\delta}, \mathbf{V}, \mathrm{K}) \right] \tag{1.26}$$

This can be written as,

$$\mathbf{J} \,.\, [\Delta\delta \;\; \Delta\mathbf{V} \;\; \Delta\mathrm{K}]^{\mathrm{T}} = [-\mathbf{F}(\delta, \mathbf{V}, \mathrm{K})]$$

or, $$[\Delta\delta \;\; \Delta\mathbf{V} \;\; \Delta\mathrm{K}]^{\mathrm{T}} = \mathbf{J}^{-1} . [-\mathbf{F}(\delta, \mathbf{V}, \mathrm{K})] \tag{1.27}$$

where **J** is the Jacobian matrix.

Near the point of voltage collapse, the Jacobian matrix, **J** approaches singularity; hence it is difficult to calculate $\mathbf{J}^{-1}$ near the collapse point. To overcome the problem one more equation is added assuming one of the variables as fixed. This variable is called the continuation variable.

Assuming that the i^{th} variable is the continuation variable, one can write,

$$[\mathbf{e}_i] \, [\Delta\delta \;\; \Delta\mathbf{V} \;\; \Delta\mathrm{K}]^{\mathrm{T}} = 0 \tag{1.28}$$

where $[\mathbf{e}_i]$ is the vector having i^{th} element as 1 and all other elements as zero.

Augmenting equation (1.28) to (1.27),

$$\begin{bmatrix} \mathbf{J} \\ \mathbf{e}_i \end{bmatrix} [\Delta\boldsymbol{\delta} \;\; \Delta\mathbf{V} \;\; \Delta\mathrm{K}]^{\mathrm{T}} = \begin{bmatrix} -\mathbf{F}(\boldsymbol{\delta}, \mathbf{V}, \mathrm{K}) \\ 0 \end{bmatrix} \tag{1.29}$$

The difference vector $[\Delta\delta \;\; \Delta\mathbf{V} \;\; \Delta\mathrm{K}]^{\mathrm{T}}$ is found from (1.29) and added with the initial assumption of vector $[\delta, \mathbf{V}, \mathrm{K}]$ to get the predictor.

The predictor may not be exactly on the desired solution curve. To get the exact solution, the following corrector equations are added with the set of equations (1.23).

$x_i = \mu$ or $x_i - \mu = 0$

where μ is the assumed fixed value of the continuation variable.

Thus the system of equations becomes,

$\mathbf{F}(\delta,\mathbf{V},K) = 0$, and, $x_i - \mu = 0$

In the above set of equations, the number of variables is equal to the number of equations. Thus it can be solved by the Newton-Raphson method, having the predictor as the initial guess.

Continuation power flow allows the load voltage to be computed even when the power flow Jacobian matrix is singular. The complete PV curve, including the nose point and the lower part of the curve, can be drawn using continuation power flow. Figure 1.8 shows the complete PV curve of bus-4 for the 10-bus test system, using PSAT [16] that uses continuation power flow.

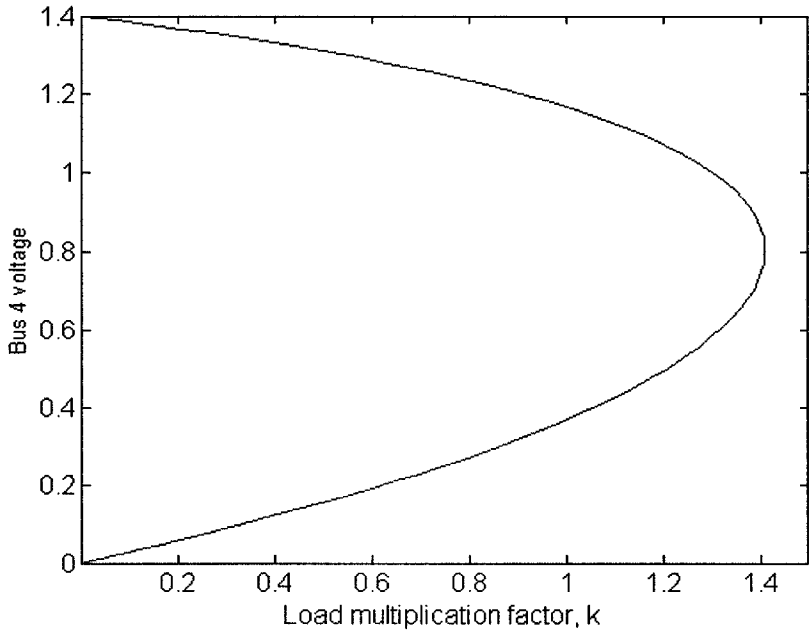

Figure 1.8: PV curve of bus-4 for the 10-bus test system, obtained by using continuation power flow

1.5 Detailed voltage stability analysis of the 10-bus test system for different loading conditions

Voltage stability analysis is carried out for the 10-bus test system described earlier in this chapter. Different transformer tap settings for different load levels and corresponding generations for the 10-bus test system are given in Tables 1.7 to 1.9 [2, 17]. Simulations are carried out with and without load tap changers (LTCs) between bus 4 and bus 10. The effect of line outage on voltage stability is also studied.

Simulations are done in PowerWorld Simulator [18]. Base case conditions for three load levels are as follows.

- All the transformers are at fixed tap [Table 1.7].
- The load at bus 8 [Table 1.8] is of constant power type, while that of bus 4 is 50% constant power and 50% constant current.

Simulation results are recorded at four different operating conditions (or 'snapshots') at three different load levels and are presented in Tables 1.10 to 1.12. The effect of LTC between bus 10 and 4 on voltages at different busses, as well as the reactive power generation and consumption in nearby busses are studied.

At 'snapshot 1', i.e., when there is no line outage in the system and the LTC is kept at fixed tap position, bus 4 voltage reduces with increased loading. At load level 3, the voltage level is very low and it needs LTC operation to restore the voltage.

When the LTC is turned on, there is a considerable increase in load bus (bus 4) voltage. With higher voltage, load power consumption increases (because of 50% constant current load), which leads to the reduction of voltages in the adjacent busses. At reduced voltage, output of the shunt capacitor reduces, thereby stressing the generators to produce more reactive power.

With outage of one line between bus 6 and bus 7, less power is available to the load from the two generators at the other end of the system, thus the voltages reduce at the load end busses. Output of the shunt capacitor falls because of reduced voltage and as a result load voltage deceases further. Generators are more stressed and produce more reactive power to compensate for the loss.

Even with operation of LTC after line outage, load voltage is not restored significantly. A reason for this is the shortage of available reactive power at the load end

because of the line outage and reduced efficiency of capacitors due to reduced voltage. In an attempt to raise the voltage, LTC increases load power consumption. If the load is slightly increased, it can be seen that this reduces the voltage further and eventually the system faces a voltage collapse.

Modal analysis was carried out on the reduced Jacobian matrix of the system for different operating conditions and the results are shown in Table 1.13. It can be seen that the minimum eigenvalue of the reduced Jacobian matrix reduces with load. It can be used as an indicator of the closeness of the operating point to the point of voltage collapse.

Table 1.7: Transformer data for different load levels for the 10-bus test system (R, X in pu on 100 MVA base)

End busses	R	X	Tap setting
10-4	0.0000	0.0010	0.9750 (load level: 1) 0.9938 (load level: 2) 1.0000 (load level: 3)

Table 1.8: Load data for different load levels for the 10-bus test system

Bus	P (MW)	Q (MVAR)	Load level
8	3271	1015	1
	3320	1030	2
	3335	1035	3
4	3384	971	1
	3435	985	2
	3460	993	3

Table 1.9: Generator data for different load levels for the 10-bus test system

Bus	P (MW)	V (pu)	Load level
1	3981	0.9800	1
	4094	0.9800	2
	4252	0.9800	3
2	1736	0.9646	1
	1736	0.9646	2
	1736	0.9646	3
3	1154	1.0400	1
	1154	1.0400	2
	1154	1.0400	3

Table 1.10: Load voltages and reactive power outputs of generator 2 and 3 at load level 1

Contingency	V4	V8	V7	QG3 (MVAR)	QG2 (MVAR)
Without outage, fixed tap	0.98	1.03	1.11	390	-94
Without outage, LTC active	1.00	1.01	1.10	505	31
Line outage, fixed tap	0.95	0.96	1.05	700	440
Line outage, LTC active	0.93	0.92	1.00	700	723

Table 1.11: Load voltages and reactive power outputs of generator 2 and 3 at load level 2

Contingency	V4	V8	V7	QG3 (MVAR)	QG2 (MVAR)
Without outage, fixed tap	0.96	1.03	1.11	390	-93
Without outage, LTC active	0.99	0.99	1.08	627	164
Line outage, fixed tap	0.91	0.91	1.00	700	724
Line outage, LTC active	0.92	1.01	1.09	543	146

Table 1.12: Load voltages and reactive power outputs of generator 2 and 3 at load level 3

Contingency	V4	V8	V7	QG3 (MVAR)	QG2 (MVAR)
Without outage, fixed tap	0.95	1.02	1.11	401	-81
Without outage, LTC active	0.99	0.98	1.07	700	249

Table 1.13: Eigenvalues of the reduced Jacobian matrix for different contingencies and load levels for the 10-bus test system

	Without outage, fixed tap	Without outage, LTC active	Line outage, fixed tap	Line outage, LTC active
Load level 1	2203.6	2272.3	2190.9	2249.1
	1330.8	1313.1	1230.3	1206.2
	925.01	919.68	899.14	893.12
	25.062	24.737	21.788	21.376
	148.21	143.97	135.57	130.19
	598.07	588.45	560.6	547.69
	374.9	371.46	347.46	343.47
Load level 2	2151.1	2284.1	2191.8	2219.2
	1329.8	1293.5	1206.4	1193.5
	924.85	913.89	893.15	889.96
	24.979	24.308	21.228	21.002
	148.54	139.86	130.69	127.86
	598.04	578.28	548.21	541.37
	374.75	367.68	343.41	341.31
Load level 3	2130.8	2294.4	2194.9	2203.7
	1327.8	1281.2	1191.4	1187
	924.32	910.3	889.43	888.33
	24.903	24.043	20.877	20.797
	148.34	137.29	127.63	126.66
	597.18	571.89	540.44	538.08
	374.38	365.35	340.92	340.2

1.6 Limitations of the conventional voltage stability analysis methods

Most of the conventional voltage stability analysis methods suffer from the following drawbacks [19, 20, 21].

- Most of the above-mentioned techniques are computationally demanding. In a real-time environment where the system state may change every hour, or even every few minutes, computation of these indices may considerably burden the Energy Management System (EMS).
- All of the conventional methods mentioned above need detailed mathematical models of the power system components, which is not always feasible to obtain in a complex power system. For example, detailed functional dependence of the power system loads on the voltage is rarely available in practice and the commonly used constant power model is far from accurate.
- Available information relevant to the state of the power system is often available in input/output form, rather than in the form of any relationship that can be expressed by simple mathematical functions. Interpolation of any unforeseen case is not always possible only by using these input/output patterns.
- Online implementation of the conventional voltage stability indices would be based on real-time measurements of power system parameters. These measurements can be of three types, (1) analog measurements of real and reactive power flows in lines, real and reactive power injection at busses, bus voltage magnitudes etc, (2) logic measurements, such as status of switches and breakers, tap positions of LTCs etc, and (3) pseudo-measurements such as forecasted loads

and generation etc. Analog and logic measurements are telemetered to the control center, which may be far away, and thus may contain errors. Decisions based on the conventional voltage stability assessment tools are therefore subjected to a lack of reliability. A method that is somewhat insensitive to errors in input data is more reliable for assessing voltage stability of the system.

1.7 Voltage stability monitoring using Artificial Neural Networks

Artificial neural networks (ANN) have gained widespread attention from researchers in recent years as a tool for online voltage stability and voltage security assessment. Due to the non-linear nature of the voltage stability assessment problem, neural networks are superior to conventional analytical methods of voltage stability analysis, as described below:

- ANNs can learn complex non-linear relationships through a set of input/output examples. Functional relationships between system parameters are not always easy to determine, and ANNs do not require those while learning the relationships. By a series of weight adjustments during training of a parallel-distributed architecture, ANNs can virtually approximate any kind of non-linear complex relationship.
- ANNs have in-built noise rejection capability, which makes them robust in a distributed power network where data collection or transmission error is a possibility. As mentioned earlier, there may be errors in the data telemetered to the control center. Due to the relative insensitivity of the neural network output to

the errors in the input data, ANNs are more reliable compared to conventional voltage stability analysis tools.

- It takes a considerable time to train an ANN with a large number of training examples. Once trained, execution time of the ANNs subjected to any input is much less, which makes it an attractive alternative compared to conventional voltage stability analysis methods.
- The most important and useful property of ANNs is perhaps the ability to interpolate unforeseen patterns. Once trained with a sufficient number of example patterns that covers the entire range of input variables, ANNs can interpolate any new pattern that falls in the domain of its input features.
- Parallel processing units of the trained ANNs can be implemented using general purpose or application-specific hardware, and thus can relieve some computational burden of the EMS computers.

1.8 Motivation for the research

Due to the ever-changing operating conditions and various unforeseen factors associated with a huge power-network, off-line stability studies can no longer ensure a secure operation of the power system. Security of a power system is defined as its ability to perform normally, meeting all the criteria of a healthy power system, even after occurrence of any credible contingencies such as line outage, loss of generation etc. Earlier, system robustness and reliability was of principal concern in power system security studies. Nowadays, 'risk aversion' of the system subjected to different

contingencies has become more important, and consequently, security is being treated as a real-time function of power system state variables [22]. Offline studies normally tend to be conservative, since highly stressed systems are considered while carrying out security analysis, and they are incomplete also in the sense that not all equipment outages can be taken into consideration. Online security assessment is based on real-time direct measurements, and therefore, gives better estimates of power system states and existing topology.

Voltage instability has been identified as the major factor behind a number of recent power system collapses, and is being regarded as a very important factor in power system security studies. Online voltage stability monitoring is therefore becoming an integral part of a modern day Energy Management System (EMS).

Online voltage stability monitoring using the Artificial Neural Network is the focus of a major part of the present research. Considering the limitations of the existing works, the research aims at developing an improved, efficient and robust scheme for online voltage stability monitoring using ANN. For secure operation of the power system, the voltage stability should be maintained in the event of potential contingencies. The proposed scheme is therefore designed to monitor voltage stability for multiple contingencies. Certain desired qualities of the ANN, such as automatic selection of the network size, online adaptation of the ANN etc. are incorporated in the proposed scheme for online voltage stability monitoring in the advanced phase of the research.

For a secure and reliable operation of the power system, it is not sufficient only to monitor the voltage stability. If the power system is deemed to be insecure in the event of

any credible contingency, preventive actions should be taken to steer the system away from instability. A sensitivity-based generation rescheduling scheme for multiple contingencies is proposed in the later part of the research. The ANN architecture developed in the earlier part of the research finds use in computing parameter sensitivities of the voltage stability margin. The ANN-based method of computing sensitivities overcomes many limitations of the existing analytical methods for finding sensitivities.

The thesis is organized as follows. Chapter 2 gives a brief review of the existing work on online voltage stability monitoring using ANN, and existing methods of generation rescheduling for voltage stability enhancement. Chapter 3 proposes an ANN-based scheme for online voltage stability monitoring of a power system. A new regression-based method of selection of features is also proposed. Chapter 4 describes a scheme for online voltage stability monitoring for multiple contingencies using ANN, which has the advantages of automatic selection of network size, online training or adaptation, and network pruning strategy. Chapter 5 proposes a sensitivity-based generation rescheduling scheme for voltage stability enhancement. Chapter 6 summarizes and highlights the contributions of the dissertation, followed by future directions of research. The analytical concepts are validated throughout the thesis with simulation results on test power system.

Chapter 2

Overview of Literature

2.1 Introduction

Artificial Neural Networks (ANN) have gained increased attention from power system operators, planners and researchers in recent years for various power system applications such as security assessment, load forecasting, fault diagnosis, and unit commitment [19, 23, 24, 25]. Online voltage stability monitoring is an integral part of the power system security assessment, and is the topic of interest for a major part of the present thesis. The secure operation of a power system requires detection of potentially dangerous operating conditions and contingencies, along with preventative and/or corrective actions to steer the system away from any such situations. Enhancement of voltage stability of a power system is the topic of research for the later part of the thesis. Among different existing methods, generation rescheduling is taken in this research as a means to enhance voltage stability of a power system. This chapter presents an overview of the existing literature on online voltage stability monitoring using ANN, followed by a brief review of the existing methods for voltage stability enhancement.

2.2 Online voltage stability monitoring using the ANN

There are a number of works on online voltage stability monitoring using ANN reported in the literature [26-33]. The problem of online voltage stability monitoring using ANN consists of three aspects, namely, selection of suitable voltage collapse proximity indicator, selection of the input features that affect the voltage stability of the power system, and a suitable neural network to establish mapping between these two. The standard Multilayer Perceptron (MLP) network trained by a back-propagation algorithm has been mostly used by the researchers. Works reported in the literature differ from each other in different combinations of methods of selecting input features and the voltage stability indicator. A review of some of the previous works related to the present research is presented in this chapter.

In [26], Artificial Neural Networks (ANN) are used to assess the maximum MW loadability of a power system. Multilayer feed-forward network trained with error back-propagation algorithm is used in the work. Modal analysis is carried out to identify most voltage-sensitive areas, and the parameters which affect the voltage stability most, are selected for training the ANN. The proposed scheme is applied on the 39-bus New England test system. The following are the parameters used as input features:

1. Ratio of total reactive power generation and total reactive power generation capability installed (ignoring slack bus reactive power generation).

2. Ratio of reactive power generation at the most critical generator and maximum reactive power limit of that generator. Most critical generator is assumed to be the one with the lowest voltage.
3. Lowest reactive power reserve among all the generators.
4. Number of generators operating at maximum reactive power limit.
5. Lowest voltage at the base case loading.
6. Number of busses with voltage below 1pu.
7. Total active power demand in MW.
8. Total reactive power demand in MVAR.
9. Total active power loss in MW.
10. Total reactive power loss in MVAR.
11. Ratio of the most critical branch MVA flows to the total MVA demand (calculated by the powerflow program).
12. Ratio of most critical branch MVA flows to the maximum total MVA demand before voltage collapse.

The neural network configuration is determined by considering convergence rate, error criteria etc. One hidden layer with 5 neurons is found to be optimum for the study. The output layer represents the maximum possible MW loading for the system. Critical branch loading and reactive power reserve in critical generators are found to be very important features affecting voltage stability of the system. Training data are generated for different contingencies involving different line and generator outages and different loading levels. For all the cases, the above-mentioned twelve inputs are noted along with

the maximum MW loadability limit found by using commercial software. An accuracy of better than 90% is achieved with the help of ANN for prediction of MW loadability limit.

Popovic et. al in [27, 28] describe a methodology for online monitoring and assessment of voltage stability margin of a power system with the help of ANNs. The complete vector of input variables, **y**, consists of bus voltage magnitudes (V), angles (δ), active powers (P) and reactive powers (Q). Outputs of the ANN are voltage stability margin, M and real part of minimum eigenvalue, S_c, of linearized dynamic model of the system. The voltage stability margin, M is useful in assessing the steady state voltage stability of the power system, and is defined by,

$$M = \frac{P_m - P_{total}}{P_m}, \tag{2.1}$$

where P_{total} is the total active power demand at the current operating point,

P_m is the maximum possible loading.

Four different ANN configurations are used in the training stage and two different combinations of these four ANNs are used to assess the voltage stability margin. A self-organized ANN is used to reduce the dimension of input variables. The four basic blocks of ANNs are schematically shown below and described briefly.

UR: A self-organized ANN, **UR** takes the complete vector of input features, **y**, as input and produces reduced vector of input variables, $\mathbf{y}_R$, for the current topology.

NT: **NT** is a three-layer feed-forward ANN that takes the complete vector of system variables, **y**, as input and produces binary identification code, K_t, for the system topology.

NY: **NY** is a three-layer feed-forward ANN that takes the complete vector of input features, **y** and topology code, K_t as inputs and produces voltage stability margin, M and real part of minimum eigenvalue, S_c, of linearized dynamic model of the system.

NR: **NR** is a three-layer feed-forward ANN that produces voltage stability margin, M and real part of the critical eigenvalue, Sc, when subjected to reduced vector of input features, $\mathbf{y}_R$ as input.

The four basic ANNs are shown schematically below.

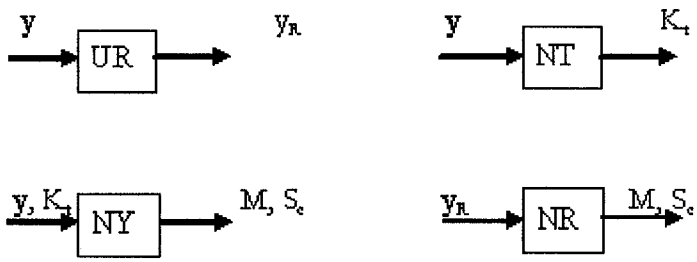

Two combinations of these four basic blocks are used for voltage stability assessment as described below.

AY: In this combination, the same ANN is trained and used for all the contingencies. ANN blocks **NT** and **NY** are combined as illustrated in the schematic diagram below.

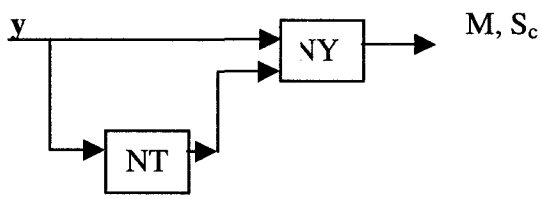

AR: In this configuration, different ANNs are trained and used separately for different system topologies. The ANN block **NT** is used to identify existing system topology, and for each topology, a separate combination of **UR** and **NR** block is used to assess voltage

stability based on the reduced set of input features as illustrated in the schematic diagram below.

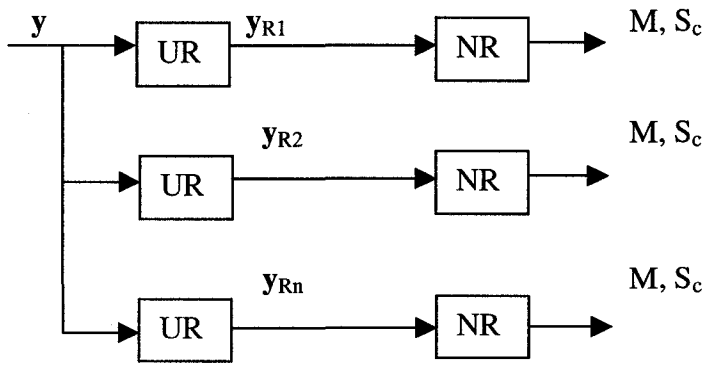

Chosen input features are classified into different groups as a first step. Data that are close to the mean or center of the group are eliminated. Average reduction of the input dimension is 95%. Static and dynamic stability margins are calculated from linearized static and dynamic models of the power system respectively. For ANNs detecting system topology, a sigmoid activation function is used for hidden layers and a pure linear activation function for the output layer. For ANNs used for voltage stability assessment, activation functions for hidden layer and output layer are a tangent hyperbolic function and a pure linear function respectively. The error back-propagation algorithm with a variable learning rate is used for training the supervised ANNs.

Stability assessment is carried out by using two methods: indirect and direct. In the indirect method, input features are determined by fast decoupled power flow and then the stability margin is evaluated. In the direct method, power injections in all the busses are used as input features, without carrying out any power flow calculations. While carrying out the training of ANNs, contingencies considered are base configuration, all

single outages of lines and generators, and most probable combinations of double outages. Loads are varied from night time minimum to day time maximum for the relevant contingency.

The proposed method is applied to the high voltage power system on the eastern part of the former Yugoslavia. The system has 92 busses, 12 equivalenced generator busses and 174 lines. Stability analysis is carried out by using both **AY** and **AR** algorithms described earlier. The **AR** algorithm is found to be more efficient than the **AY** algorithm in terms of accuracy and speed of calculation. The only problem associated with the **AR** algorithm is the large number of separate ANNs that has to be used if a large number of system topologies is considered. Simulation results show that voltage stability margins predicted by ANNs comply fairly with actual values. Moreover, efficiency and accuracy of the proposed method with a reduced data set are better, compared to the method with a complete data set.

In [29], a feedforward MLP network is used to estimate the Energy measure, which is used as an indicator to the proximity of the operating point of the power system to the point of voltage collapse. A heavily loaded power system tends to have at least two power flow solutions: the 'operable' solution corresponds to the stable equilibrium point (SEP), and the other solution, generally referred to as the low voltage solution corresponds to the unstable equilibrium point (UEP). A typical voltage collapse scenario is characterized by a saddle node bifurcation between the two solutions. Conceptually, Energy measure shows the height of the potential barrier between operable solution and

the low voltage solution. The height of the potential barrier decreases as the power system gets closer to the point of instability. Voltage instability occurs when the disturbance energy is sufficient to escape the barrier.

The MLP network consisted of 13 input nodes, 13 hidden nodes, and one output node. Bus voltages and real and reactive powers at busses are used as input features to the ANN. The output is the Energy margin corresponding to the operating point characterized by the inputs. A variety of loading conditions are considered while generating the training data. The proposed scheme is applied on a sample 5 bus system.

An ANN is used in [30] for estimating the power system loading margin. A three layer ANN is used and trained with a back-propagation algorithm. The input features used for training the ANN are the generator terminal voltages, real and reactive power of generators and loads, and the reactive power reserve of generators. Principal Component Analysis (PCA) is used to reduce the dimension of the input features. PCA projects the set of input features into a new set of coordinates in such a way that the variance of projections is stationary, i.e., either maximum or minimum. Projections of features on coordinates, for which variances are higher, are chosen as inputs.

The input features are segregated into three classes, viz., generator voltage, generator P/Q/Qreserve and load P/Q, before applying PCA separately to each class. Considerable reduction of input dimension is achieved in this work by applying PCA. The Levenberg-Marquardt algorithm is used during the training process to ensure fast convergence. The possibility of including system topology in the input features is tried,

but the ANN is not found to be able to learn binary topology information. Separate ANNs are therefore used for different system topologies. Four different topologies, including the base case, are studied with the help of four ANNs trained separately. Powerflow solutions for different contingencies and loading margins for different operating conditions are calculated by a commercial software, which uses continuation power flow.

The proposed ANN is applied to the IEEE 118-bus system. The major part of the available simulation data are used for training the ANN and the remaining part is used for testing. The simulation results show that the output of the proposed scheme matches well with the actual load margins. Average errors for all the four ANNs are less than 3%.

In [31], a multi-layer feed-forward network trained with the back-propagation algorithm is used to establish direct mapping between system loading condition and the Voltage Stability Margin (VSM), based on the Energy method. The selection of input features is based on the sensitivity of the Energy function with respect to the features. Critical parameters, i.e., parameters with respect to which VSM has higher sensitivities, are chosen as input features. A three-layer feed-forward network trained with error back-propagation algorithm is used in this paper. A direct mapping is established during the training procedure between input features and Energy margin for the power system. The three-layer ANN architecture contains one hidden layer with five neurons having a unipolar sigmoid activation function. The output layer consists of a single neuron with a unipolar sigmoid activation function, giving the Energy function as the output.

Sensitivity analysis is carried out for VSM with respect to the input parameters before selecting the features. Real and reactive power of busses for which VSM has greater sensitivity, are chosen as input features. The proposed ANN architecture is used for IEEE 5-, 14-, 30-, 57- and 118-bus systems. The simulation results match closely with the expected values of Energy margins under normal operating conditions. Under a heavily loaded condition however, the ANN does not give satisfactory results. The reason for this is found to be the sensitivity of the ANN itself with respect to loading levels in the system. A proposed remedial measure for this problem is the classification of load into low, medium and high levels and using three ANNs trained separately for these three load levels. Considerable improvement in performance is observed after using separate ANNs for corresponding different load levels.

In [32], reactive power margin of a chosen load area is estimated by using active power flows in selected lines as inputs to the ANN. Reactive power margin for a selected load area of the New England 39-bus system is estimated using three different methods and the results are compared. The three methods are linear regression, Kohonen network and feed-forward ANN. The ANN is found to give the best result in terms of accuracy. The steps followed in the proposed method of online estimation of reactive power margin using ANN are as follows.

- A load centre consisting of three busses, i.e., busses 17, 18 and 27 is chosen for which reactive power margin is monitored.

- The reactive power margins in the load centre and all the other busses for the base case, all N-1 contingencies and a few selected N-2 contingencies are computed by using V-Q curve method.
- The Busses having very low reactive power margin are identified as weak busses and the flows in the lines connected to the weak busses for each contingency are taken as input features.
- A feed-forward ANN is trained with the selected line power flows to give corresponding reactive power margin at the load centre as the output.

It was found that very similar line flows for different contingencies had radically different reactive power margins. Selection of flows in lines connecting to the weakest busses or in the lines, outage of which cause very low reactive power margins provide a basis for selecting important input features. Implementation of the proposed method on the 39-bus New England test system shows satisfactory results in terms of estimating voltage stability margin.

2.3 Voltage stability enhancement using optimization techniques

For secure operation of a power system it is not only necessary to detect potentially dangerous situations, but also to steer the system away from a possible instability. There are different measures against voltage instability in a power system, both in real time, and in the planning and design stage [4]. Real time measures can be preventive or corrective in nature. Corrective actions are needed to prevent immediate loss of voltage stability. Preventive actions are then taken to enhance the voltage stability margin. The preventive

and corrective control of voltage stability mainly constitute one or more of the following options: rescheduling real power generation, changing load tap changer (LTC) settings, adjusting phase shifter angles, reactive compensation and load shedding. In the present research, generator real power rescheduling is taken as the means for enhancing voltage stability of a power system. Many of the reported works on the use of optimization for voltage stability enhancement use the sensitivity of the voltage stability margin with respect to different control parameters as a means to enforce voltage stability constraint into the optimization method. An introduction to the most commonly used method of finding the sensitivity is therefore given below, followed by a brief review of some of the relevant works reported on the use of generation rescheduling for voltage stability enhancement.

2.3.1 Sensitivity of the voltage stability margin with respect to parameters

The sensitivities with respect to control parameters are found for the system 'stress'. Conceptually, the system is more 'stressed' with the increase of the real and reactive power injections at busses. Voltage stability margin is taken as the additional stress the system can withstand before experiencing instability.

The power flow equations can be expressed as

$$\mathbf{f}(\mathbf{u},\mathbf{p})=0, \tag{2.2}$$

where $\mathbf{u}$ is the vector of power system states such as voltages (V) and angles (δ), $\mathbf{p}$ is the vector of parameters such as real and reactive power injections at busses.

It has been well accepted that at the point of voltage instability, the power system undergoes bifurcation or the dynamical behavior of the power system undergoes a qualitative change [4,15]. Let $(\mathbf{u}^0, \mathbf{p}^0)$ be the base case operating condition and $(\mathbf{u}^*, \mathbf{p}^*)$ be the point of bifurcation such that,

$$\mathbf{p}^* = \mathbf{p}^0 + S^* \mathbf{d}. \tag{2.3}$$

Here $\mathbf{d}$ is the direction of change of parameters and S^* is the loading margin or the voltage stability margin of the operating condition $(\mathbf{u}^0, \mathbf{p}^0)$ along the direction $\mathbf{d}$.

At the point of bifurcation,

$$\mathbf{f}(\mathbf{u}^*, \mathbf{p}^*) = \mathbf{f}(\mathbf{u}^*, \mathbf{p}^0 + S^* \mathbf{d}) = 0 \tag{2.4}$$

Differentiating above,

$$\mathbf{f_u} d\mathbf{u} + \mathbf{f_p} (d\mathbf{p}^0 + dS^* \mathbf{d}) = 0, \tag{2.5}$$

where $\mathbf{f_u}$ and $\mathbf{f_p}$ are Jacobian matrices of $\mathbf{f}$ with respect to $\mathbf{u}$ and $\mathbf{p}$ respectively.

Noting that at the point of bifurcation, the minimum eigenvalue of $\mathbf{f_u}$ becomes zero, and premultiplying (2.5) by the left eigenvector ω corresponding to zero eigenvalue,

$$\omega^T \mathbf{f_u} d\mathbf{u} + \omega^T \mathbf{f_p} (d\mathbf{p}^0 + dS^* \mathbf{d}) = 0 \tag{2.6}$$

Rearranging the terms in (2.6) and noting that $\omega^T \mathbf{f_u} = 0$, at the point of bifurcation, the sensitivities of the voltage stability margin, S^*, with respect to the parameters at the base case operating condition, $\mathbf{p}^0$, can be stated in the form of the following equation [4, 34].

$$\left[\frac{\partial S^*}{\partial p_1^0}, \frac{\partial S^*}{\partial p_2^0}, \ldots, \frac{\partial S^*}{\partial p_n^0}\right]^T = -\frac{\mathbf{f}_p^T \boldsymbol{\omega}}{\boldsymbol{\omega}^T \mathbf{f}_p \mathbf{d}} \tag{2.7}$$

2.3.2 Voltage stability enhancement methods utilizing generation rescheduling

There are a number of works reported on the use of optimization to coordinate control actions for preventive and corrective measures against voltage instability [35-41]. Current research concentrates on the use of ANN to find voltage stability margin sensitivities to be used for generation rescheduling in order to enhance voltage stability of a system. The following discussion therefore mainly considers those methods of voltage stability enhancement, which use generation rescheduling as part of the overall preventive and corrective control scheme.

Optimization is used in [35] to design a preventive and corrective control scheme for voltage stability. The objective of the optimization method is to minimize the control cost, while satisfying the system and equipment constraints along with maintaining the voltage stability margin. The costs of different control actions are not the same. For example, the cost of shedding a load may be higher than the other control actions such as changing the transformer tap. Hence different cost factors are chosen for different control variables. The objective function to minimize is as follows:

$$\sum_{j=1}^{n} (w_j (\Delta p_j)^2) \tag{2.8}$$

where Δp_j is the change in the j^{th} control action, and w_j is the cost curve weighting factor for the j^{th} control variable.

The different control actions considered for the preventive and corrective scheme for voltage stability are: active power generations, reactive power generations, LTC transformer taps, phase shifter angles, shunt compensation, and load shedding. Constraints on the following parameters are enforced into the optimization program:

- Active power generations of the units.
- Phase shifter angles.
- Line power flows.
- Reactive power generation of the units.
- LTC transformer taps.
- Transformer power flow.
- Bus voltage magnitudes.
- Voltage stability margins.
- Shed loads.

The proposed method is applied on 100-bus, 901-bus, 1635-bus, 2097-bus and 4112-bus systems. Simulation results show that desired improvements in the voltage stability margins are achieved.

A scheme for preventive and corrective control of voltage instability is proposed in [36]. Sensitivities of the voltage stability margin to control parameters are computed first to determine the best control actions. Computation of the sensitivities is in the same

line as described in section 2.3.1. A linear optimization method minimizing total control cost is then used to coordinate the control actions. Given a system operating condition, referred to as the base case, different credible contingencies are first examined. For an unsolvable contingency, corrective actions are taken to restore system solvability. Preventive actions are then taken to increase the voltage stability margin to a desired level. Fast-acting load shedding and reactive power compensation are used as means for corrective control of voltage stability. Relatively slower actions such as generation rescheduling and generator secondary voltage controls are taken as preventive measures against voltage instability. The proposed method is applied on the New England 39-bus system and the simulation results demonstrate the effectiveness of the method in mitigating voltage collapse.

In [37], generation rescheduling and load curtailment are used as means to enhance voltage stability margin of the system. The best control actions to restore security margin with respect to credible contingencies are found by using linear optimization. Sensitivities of the voltage stability margin with respect to the control parameters are used to implement voltage stability constraints in the optimization procedure. The rescheduled generations make the system secure for multiple contingencies. The objective function to be minimized is the total cost of control actions as follows, assuming unity costs for simplicity.

$$\text{Minimize} \quad \sum_{j=1}^{n} (\Delta p_j) \tag{2.9}$$

where Δp_j is the j^{th} control action.

The voltage security constraints for multiple contingencies are incorporated in the following equality constraint:

$$\sum_{j=1}^{n} S_{ij}\Delta p_j \geq \Delta M_i \,, \forall i = 1,...,c \tag{2.10}$$

where S_{ij} is the sensitivity of the voltage stability margin with respect to the control parameter p_j , for the i^{th} contingency. Computation of the sensitivities is similar to the method described in section 2.3.1. ΔM_i is the minimum required enhancement in the MW margin for the i^{th} contingency, 'c' being the number of contingencies considered.

The proposed method of generation rescheduling and load curtailment is applied on 80-bus 'Nordic 32' system and Hydro-Quebec system. The test results show that the voltage stability margin is improved significantly for multiple contingencies.

A number of other works related to the voltage stability enhancement, and the use of optimization techniques in powers systems were also reviewed as part of the current research. T. V. Cutsem in [38] proposes an approach to corrective control of voltage stability through simulations and sensitivity information. The sensitivities of the reactive power generations with respect to demand are calculated, in order to determine the generators to be rescheduled. The potentially dangerous contingencies are identified using the eigenvalues of the linearized Jacobian matrix that includes the effect of LTCs on voltage stability of the system, and then control actions are taken to improve the voltage stability margin. In [39], a reactive reserve-based contingency constrained

optimal power flow is proposed for voltage stability enhancement. The concept is based on the fact that increase in reactive reserves is effective for enhancement of voltage stability margins. In the same line, an optimized reactive reserve management scheme is proposed in [40] to improve voltage stability of a power system. Significant improvement in voltage stability is observed by applying the method on test system. An optimal power flow incorporating voltage collapse constraints is proposed in [41]. Both saddle node bifurcation and limit-induced bifurcation leading to voltage instability are considered in the optimization procedure.

2.4 Summary and discussions

A review of the existing literature on voltage stability monitoring of a power system using ANN is presented in section 2.2. A number of limitations in the existing methods are identified, which needs further research. A systematic way of selection of input features for the ANN needs to be developed. A small number of features are used in some of the works, which may not be able to map the complex nonlinear relationship to the desired voltage stability indicator. The proposed method in [26] uses only 12 inputs to the ANN, which may not be sufficient for estimating the voltage stability margin for a larger system. Although diverse classes of features are addressed, only one numerical value representing the feature may not serve the purpose. For example, a number of generators may be operating close to their reactive power limits, a number of busses may experience lower-than-normal voltage, and a number of lines may be heavily loaded and could be very critical to the voltage stability of the system. The method proposed in [27, 28] is

applied to a real power system with 92 busses. The use of separate ANNs for different system topologies could be a challenging task if the number of possible topologies is very large. Loads are varied from night time minimum to day time maximum while training the ANNs for a specified contingency. A better accuracy in the output could be achieved by training the ANNs separately for different load levels. The proposed method in [30] is applied on IEEE 118-bus system. The use of Principal Component Analysis is proved to be a useful method of reduction of input data dimension. The use of separate ANNs for each topology could be a demanding task when a large number of system topologies is to be considered. The proposed method in [31] gives satisfactory results for the prediction of the voltage stability margin. Sensitivity analysis of the features is a useful tool for feature selection, especially for large systems. Use of separate ANNs for different loading levels increases accuracy of the output of the ANNs. The effect of different system topologies on the performance of the ANN is not addressed in this paper. The calculation of the voltage stability margin based on the Energy method is an involved task. A more straightforward method could be the use of the loading margin for the system. The method proposed in [32] attempts to find a systematic way of selecting input features. The worst N-1 contingencies in terms of available reactive power margin, along with lines connecting to weakest busses are chosen as important features.

The loading margin for the power system has been the most commonly used indicator of the proximity to voltage collapse in the literature. A three-layer feed-forward network trained with a back-propagation algorithm is mostly used in literature for predicting voltage collapse proximity. Performing sensitivity analysis of the voltage

stability indicator with respect to the input parameters is a reasonable method for feature selection [31]. A very important issue is, whether the system topology information can be included in the input features or not. Most of the studies show negative results. The use of separate ANNs for each topology has been suggested as remedial measure. When the number of relevant topologies is very large, this method is not feasible.

The review of the existing literature indicated the need for research in a number of aspects of online voltage stability monitoring using ANN. The number of parameters that may be used as inputs to the ANN may be very high in a large power system. Suitable data reduction techniques are therefore needed to reduce the dimension of the input data. Sensitivity analysis of the voltage stability margin with respect to the inputs is an effective way of reducing feature dimension. Use of the conventional MLP network for voltage stability monitoring for multiple contingencies has not been very successful and convincing. Different classes of ANN architectures therefore need to be explored to investigate the scope of using a single ANN for multiple contingencies.

A brief review of the literature on methods of enhancing voltage stability of a power system is presented in the section 2.3, with emphasis on the works reported on the use of generation rescheduling for voltage stability enhancement. Most of the optimization-based works reported for enhancement of voltage stability use sensitivity of the voltage stability margins with respect to control parameters to incorporate voltage stability constraints into the optimization program. The conventional method of computing parameter sensitivities of the voltage stability margin, as described in section 2.3.1, suffers from a number of drawbacks as follows:

1. It is numerically difficult to find the Jacobian matrix at the exact point of voltage instability. One has to resort to the continuation power flow to obtain the exact nose point, which is sensitive to the predictor or corrector step size.
2. A particular direction of increase in system 'stress' is considered to reach the bifurcation point and in most cases a linear direction is assumed. For a real power system with loads having different voltage to power sensitivities, this is an unrealistic assumption. It has been shown by researchers that inclusion of the voltage sensitive load models significantly affect the computation of the voltage stability margin of a power system [42-50]. A method of computing sensitivities, which can incorporate voltage sensitive load models, would be more accurate and realistic.
3. Obtaining the sensitivities for multiple contingencies and different operating conditions is a demanding task. Dynamic simulations may be needed in some cases to obtain the exact point of voltage instability, which is a time consuming task for a large power system having numerous potentially dangerous contingencies.

An efficient and accurate method to compute the sensitivities would be useful in better representation of the voltage stability constraint in the optimization program for voltage stability enhancement. Chapter 5 of this thesis describes a scheme to efficiently compute the sensitivities using ANN. Using the computed sensitivities, a voltage stability enhancement scheme is also proposed by rescheduling the real power outputs of the generators.

Chapter 3

Online Voltage Stability Monitoring Using Artificial Neural Network

3.1 Introduction

Online voltage stability monitoring using Artificial Neural Network (ANN) is the focus of a major part of the present research. A scheme for implementation of ANNs for real-time assessment of the voltage stability of a power system is proposed in this chapter. The standard Multilayer Perceptron (MLP) neural network is used for estimating the voltage stability margin of a power system. The load active and reactive powers are used as the input features to the ANN and the available MW margin is used as an indicator to the voltage stability of the system. A regression-based method is used to compute the sensitivities of the voltage stability margin with respect to different inputs. The load active and reactive powers, for which the corresponding sensitivities are higher, are chosen as the important features for the ANN. Considerable data reduction is obtained by the proposed feature selection method. The systematic way of selection of highly important features results in a compact and efficient ANN architecture. A number of critical contingencies are considered for voltage stability monitoring, and separate ANNs are used for each of the contingencies. The online voltage stability monitoring scheme is applied to the New England 39-bus power system and the simulation results are presented.

3.2 Proposed method for online voltage stability monitoring using the Artificial Neural Network

Selection of the suitable voltage stability assessment method is the first step towards developing an online voltage stability monitoring scheme. In this research, the loading margin is used as an indicator of the proximity of the system to the voltage collapse point. The active power (MW) margin to the voltage instability point is a straightforward and widely used method to assess the voltage stability of the system. At any operating point, the MW margin is defined as the additional MW load the system can withstand, before going unstable. Figure 3.1 shows the MW margin to the point of voltage instability for the indicated operating point.

Selected active and reactive load powers are taken as the input data set for the ANN. It is to be noted here that many other combinations of different measurable power system parameters such as generator reactive power reserves, line flows, bus voltages can be taken as input features to the ANN [26-33]. In fact, the choice of inputs to the ANN may be specific to the system. The proposed ANN should work as a tool for online voltage stability monitoring for various possible combinations of suitable inputs. The selected active and reactive load demands, used as inputs to the ANN give satisfactory results and hence are used in the current research. A sensitivity-based data reduction technique is applied to reduce dimension of the input data set. A three layer feed-forward ANN trained with the back-propagation algorithm is used to establish mapping between the input data set and the loading margin. Contingency analysis is carried out at the beginning to identify the most critical contingencies to be monitored, and separate ANNs

are used for the corresponding system topologies. The basic scheme of the online voltage stability monitoring is shown in the Figure 3.2, followed by detailed description of individual steps.

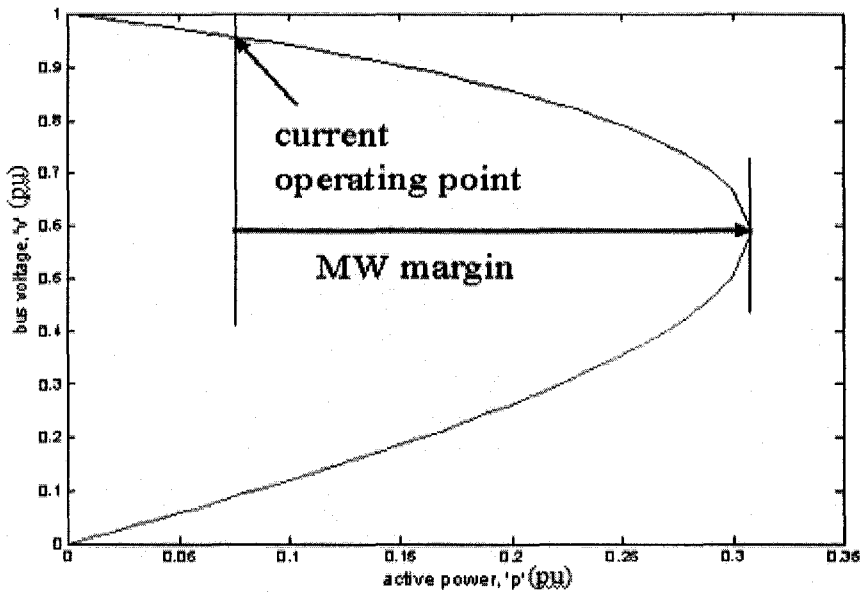

Figure 3.1: MW margin to the point of voltage instability

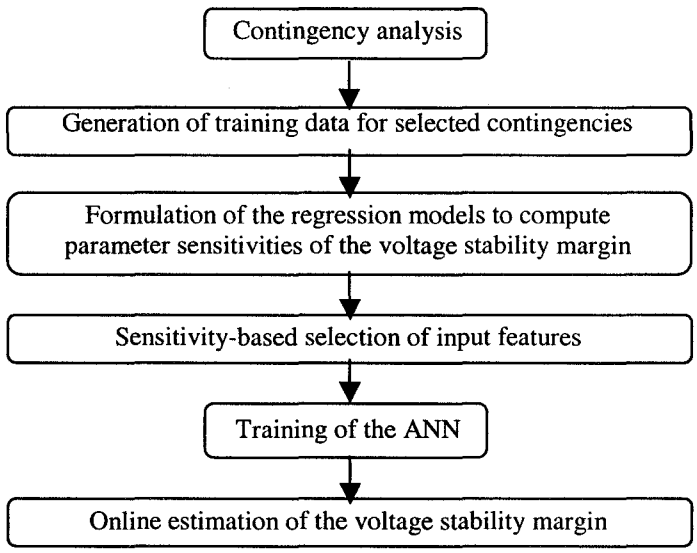

Figure 3.2: Feature selection and training the MLP neural network for online voltage stability monitoring

3.2.1 Contingency analysis

The analysis of credible contingencies is an integral part of the stability assessment of a power system. The analysis of 'N-1' contingencies, meaning, normal system minus one element, has been the standard procedure for the contingency analysis in many utilities [51]. For the present study, all single line outages are analyzed and are ranked in the decreasing order of severity in terms of the available MW margin to the point of voltage instability. For a large system, it is not possible to consider all the contingencies while carrying out security analysis. A selected number of worst-case contingencies are considered in this study. Numerous attempts have been made in the literature to train and use a single ANN for all the contingencies, with little success. Separate ANNs are therefore used for the selected number of critical contingencies.

3.2.2 Generation of training data

The training data sets for the ANN are generated for the base case and the selected contingencies separately. The load active and reactive power demands are varied randomly within specific limits to simulate different operating conditions in the system. The change in load is distributed among participating generators in proportion to their participation factors in the base case. The participation factor of a generator is defined as the ratio of its generation to the total generation in the system. Corresponding to each operating point, MW distance to the point of voltage instability is found by using PowerWorld simulator [18] and recorded as the desired output of the ANN. The load active and reactive powers, along with the MW margin to the point of voltage instability

constitute a training sample corresponding to a particular system topology.

3.2.3 Reduction of dimension of input data

The objective of input data reduction is to discard the data that are repetitive in nature and to choose only those data which contain maximum information regarding different patterns or variations of the whole set of input data. In other words, features that highly affect the voltage stability of the system are chosen as inputs to the ANN. In this research, the input variables are chosen using a regression-based sensitivity analysis of the input features, which overcomes many limitations of the conventional methods of computing sensitivities. A second order regression model is first developed for each system topology, and then the sensitivities of the voltage stability margin with respect to the regressor variables are found by differentiating the regression model.

3.2.3.1 Sensitivity analysis

Sensitivity of the voltage stability margin is found with respect to the parameters included in the input data set. Those inputs, for which the sensitivities are higher, are chosen as the important features. A commonly used method to compute sensitivities of the voltage stability margin with respect to different parameters has been the use of the singularity of the powerflow Jacobian matrix at the point of voltage instability [4, 34]. Section 2.3.1 describes this method of computing sensitivities. The main drawbacks of the method are discussed in section 2.4. In this work, a second order regression model is first designed to estimate voltage stability margin in terms of load active and reactive

powers. A higher order regression model can also be used for this purpose to increase the accuracy in estimation of the voltage stability margin, and consequently of the sensitivities. However, the computational burden increases with higher order regression models. The performance of a second order regression model was found satisfactory and hence used in the present work.

3.2.3.2 Formulation of the regression model for estimating voltage stability margin

A second order regression model is taken as follows:

$$y = \mathbf{p}\boldsymbol{\beta}_2\mathbf{p}^T + \mathbf{p}\boldsymbol{\beta}_1 + \beta_0, \tag{3.1}$$

where y is the MW margin to the point of voltage instability, $\mathbf{p}$ is the vector of real and reactive load powers, i.e.,

$$\mathbf{p} = [p_1, p_2, \ldots, p_{ld}, q_1, q_2, \ldots, q_{ld}], \tag{3.2}$$

with p_i and q_i being the active and reactive power demand respectively of the i^{th} load. β_0 is a constant, $\boldsymbol{\beta}_1$ is a vector and $\boldsymbol{\beta}_2$ is a diagonal matrix containing regression coefficients. Equation (3.1) can be viewed as a first order regression model as shown below:

Assuming, $\mathbf{x} = [1, p_1, \ldots, p_{ld}, q_1, \ldots, q_{ld}, p_1^2, \ldots, p_{ld}^2, q_1^2, \ldots, q_{ld}^2]$, (3.1) can be expressed as,

$$y = \mathbf{x}\boldsymbol{\beta}, \tag{3.3}$$

where $\boldsymbol{\beta}$ is the vector of regression coefficients.

The load active and reactive powers are taken as independent or regressor variables in the regression model and the MW margin is taken as the output. The vector $\boldsymbol{\beta}$ containing the coefficients of regression is the solution of the following equation.

$$\mathbf{y}=\mathbf{X}\boldsymbol{\beta}, \tag{3.4}$$

where $\mathbf{y}=[y_1,y_2,...,y_n]^T$ is the vector containing MW margins to voltage instability for 'n' different operating conditions. Defined below is the matrix **X**, each row of which represents a sample of regressor variables. Each column of **X**, starting with the second one, contains sample values of each regressor variable.

$$\mathbf{X}=\begin{bmatrix} 1 & x_{11} & x_{21} & \cdots & x_{k1} \\ 1 & x_{12} & x_{22} & \cdots & x_{k2} \\ \vdots & \vdots & \vdots & \cdots & \vdots \\ 1 & x_{1n} & x_{2n} & \cdots & x_{kn} \end{bmatrix} \tag{3.5}$$

and $$\boldsymbol{\beta}=[\beta_0,\beta_1,...,\beta_k]^T \tag{3.6}$$

The least square estimate of $\boldsymbol{\beta}$ is given by [52],

$$\boldsymbol{\beta}=\left(\mathbf{X}^T\mathbf{X}\right)^{-1}\mathbf{X}^T\mathbf{y} \tag{3.7}$$

In case of complete or partial linear dependency between columns of the matrix **X**, (3.7) has poor numerical properties and the coefficients of regression found from (3.7) do not represent the true relationship between the dependent and the independent variables. This phenomenon is a commonly encountered problem in regression, known as 'multicollinearity' [52]. For the present work, precautions are taken to avoid multicollinearity while generating the training data for the regression model.

The regressor variables, i.e., each column of **X**, are centered and scaled. If x_{ij} is the j^{th} value of the regressor variable, $\overline{x}_i=\sum_{j=1}^{n}(x_{ij}/n)$ is subtracted from x_{ij} and $(x_{ij}-\overline{x}_i)$ is

divided by S_i, where $S_i=\sqrt{\sum_{j=1}^{n}(x_{ij}-\bar{x}_i)^2}$. This centering and scaling result in $\mathbf{X}^T\mathbf{X}$ being a correlation matrix. Multicollinearity, if present in the training samples, is detected by the condition number of the correlation matrix as shown below:

$$Z=\frac{\lambda_{max}}{\lambda_{min}}, \tag{3.8}$$

where Z is the condition number, λ_{max} and λ_{min} respectively are the maximum and minimum eigenvalues of the correlation matrix $\mathbf{X}^T\mathbf{X}$.

After generation of each sample pattern, (3.8) is evaluated and the sample is discarded if the condition number Z is very high. The value of the condition number above 1000 is considered very high for the current research. This is a commonly used value of condition number for detecting multicollinearity. The prediction-error of the regression model is also minimized by avoiding multicollinearity.

Following the above procedure, the regression model is designed for sufficient variety of operating conditions for the power system. Separate regression models are designed for different potential contingencies as well as for the base case. For the present work, only N-1 contingencies are considered. It is possible to include other types of contingencies also in the proposed method. Training data for the regression models are generated separately for the base case and for different contingencies. In the next step, the regression models are used to find sensitivities of the voltage stability margin with respect to regressor variables, as described in the next section.

3.2.3.3 Computation of sensitivities

Once the regression model is designed for all possible operating conditions, sensitivities of voltage stability margin with respect to the load active and reactive powers are found by differentiation of (3.1). The sensitivity of the voltage stability margin 'y' with respect to the i^{th} regressor variable p_i is given by,

$$S_i = \frac{\partial y}{\partial p_i} = 2\beta_{2(i,i)} p_i + \beta_{1(i)}, \tag{3.9}$$

The sensitivities above are found for the base case and all other contingencies considered. It is to be noted that the expression for sensitivity given in (3.9) does not depend on any particular choice of direction of increase in system stress. Although a certain direction is assumed for increasing system stress while generating the training data, different directions can be assumed for different operating conditions and the directions do not have to be linear, as is commonly used in the case of the sensitivity expression given in (2.7). One more advantage is that one does not have to find the Jacobian matrix exactly at the point of bifurcation. Once designed for a sufficient variety of operating conditions, the regression model can be used for any new operating condition to determine the required sensitivities.

3.2.3.4 Sensitivity-based selection of input features

Equation (3.9) gives the sensitivities of the voltage stability margin with respect to the regressor variables. The load real and reactive power demands, for which sensitivities of the voltage stability margin are higher, are selected as inputs to the ANN. Let S_{min} be the

minimum sensitivity criterion for selection of an input. The i^{th} feature qualifies as an input to the ANN, only if the following criterion is satisfied:

$$\|S_i\| \geq S_{min} \tag{3.10}$$

where $\|S_i\|$ is the absolute value of the sensitivity S_i of the voltage stability margin with respect to the i^{th} feature.

For the present work, the sensitivity-based feature selection method above is applied separately to the real and reactive power demands. Different minimum cutoff values of sensitivity, viz., S^j_{pmin} and S^j_{qmin} are used to select the real and reactive power demands respectively, for the j^{th} contingency. The set T^p_j of active power demands included in the input feature set for the j^{th} system topology is defined as:

$$T^p_j = \{p_i : \|S_i\| \geq S^j_{pmin}, i = 1,...,ld\}; j = 1,...,c \tag{3.11}$$

where 'ld' is the number of load busses in the system, and 'c' is the number of contingencies considered for voltage stability monitoring, including the base case.

Similarly, the set of reactive power demands chosen as input features for the RBFN is defined as:

$$T^q_j = \{q_i : \|S_i\| \geq S^j_{qmin}, i = 1,...,ld\}; j = 1,...,c \tag{3.12}$$

3.2.4 Training the ANN

An MLP network consisting of one input layer, one output layer and a hidden layer has been found suitable for the power system voltage stability monitoring problems [26-33]. Denoting the neurons in the input, hidden and output layers for a three-layer MLP

network by i, j and k respectively, the output of neuron k in the output layer can be written as,

$$y_k = \varphi_k\left(\sum_{j=0}^{mj} w_{kj}\varphi_j\left(\sum_{i=0}^{mi} w_{ji}\varphi_i\left(\sum_{l=0}^{ml} w_{il}y_l\right)\right)\right) \tag{3.13}$$

where 'mj' is the number of neurons in the hidden layer, 'mi' is the number of neurons in the input layer and 'ml' is the dimension of input to the input layer. φ_i, φ_j and φ_k are the activation functions for input, hidden and output layers respectively.

During the learning phase, the ANN is trained with the reduced vector of input features and the corresponding MW margins as target outputs. The error back-propagation algorithm is used to train the MLP network [53-55]. The generalization property of the ANN is improved by using an 'early stopping' criterion during the training [56]. The selected samples of input features are divided into three sets. $1/4^{th}$ of the data are used as the validation set, $1/4^{th}$ as the testing set, and the remaining half as training set. The validation error is monitored during the training phase and the training is stopped when the validation error starts increasing after a specified number of iterations. Overfitting in the ANN is avoided by using this technique.

3.2.5 Voltage stability assessment using output of the ANN

The objective of the proposed scheme is to monitor the power system voltage stability in real time. The output of the ANN is the available MW margin to the point of voltage instability. An operating point, which has a sufficient MW margin, is taken as voltage stable. The amount of the MW margin for which the power system can be classified as

voltage stable is based on past experience and engineering considerations. In some cases, the system might be operated closer to their stability limit due to economic reasons; hence the required MW margin may be small. A system may also have a larger MW margin requirement due to regulatory requirements.

3.3 Simulation results

The proposed scheme for online voltage stability monitoring has been applied to the New England 39-bus test system [57]. The single-line diagram of this test power system is shown in Figure A.1 in Appendix A. The system consists of 19 load busses, 10 generators and 46 lines. Base case load is 5036.9 MW and base case generation is 5620 MW. For generating training data for the ANNs, active and reactive powers at the load busses are varied randomly within ± 20% of the base case values. Any change in total load demand in the system is distributed among the participating generators in proportion to their participation factors in the base case. For each operating condition, active and reactive powers at the busses are recorded as input features. The loads are assumed to be of constant power factor type. The available MW margin to the point of voltage instability is found for each operating condition using PowerWorld simulator [18] and recorded as the desired output of the ANN corresponding to that operating condition. Test results are reported in this section for the base case operating condition and for four different contingencies as described in Table A.1 in Appendix A. The contingencies are selected in such a way that they reflect significant changes in the system topology. For example, all the contingencies considered in this study involve outage of a radial line, which

disconnects the corresponding generator also from the system. The lost generation is supplied by the available generators in proportion to their participation factors.

For the base case and each contingency, separate regression models are designed. The random variations imparted on load active and reactive power demands, while generating the sample data, ensure that the samples are not linearly correlated. Any possible occurrence of multicollinearity is detected by the condition number of the correlation matrix, and the corresponding sample is discarded. The sensitivities of the voltage stability margin with respect to the active and reactive load power demands are computed by differentiating the regression models at the operating point of interest. Table A.2 in Appendix A shows the computed sensitivities of the voltage stability margin with respect to different parameters for the contingencies considered. Pi and Qi in Table A.2 represent real and reactive power demands of the i^{th} load respectively. Table A.3 shows the number of inputs selected for different cut-offs for the absolute values of the sensitivities, for different contingencies. The subsequent results given in this section are based on the cut-off values of $S_{p\ min}$ and $S_{q\ min}$ given in Table A.4 for different contingencies. Different set of cut-off values were tried while designing the ANN. The best results in terms of maximum and average output error are obtained by using the values shown in Table A.4.

The ANN for each network topology is trained with the help of the reduced data set by error back-propagation algorithm. The numbers of neurons in the input, hidden and output nodes are 7, 10 and 1 respectively, which were found by trial and error method to give the best results. Figure 3.3 shows the change in the sum of squared errors with each

epoch of training for the ANN used for the base case. Figure 3.4 shows the simulation results for the base case topology, where estimated values by the ANN are graphically compared with the actual MW margins for the system. Figures 3.5 to 3.8 show the simulation results for contingencies C1 to C4. Table 3.1 shows the numerical values of the actual and the predicted MW margins plotted in Figures 3.4 to 3.8. Table 3.2 gives the summary of simulation results for the base case and different contingencies. It is observed that the output errors of the ANNs are within reasonable limits.

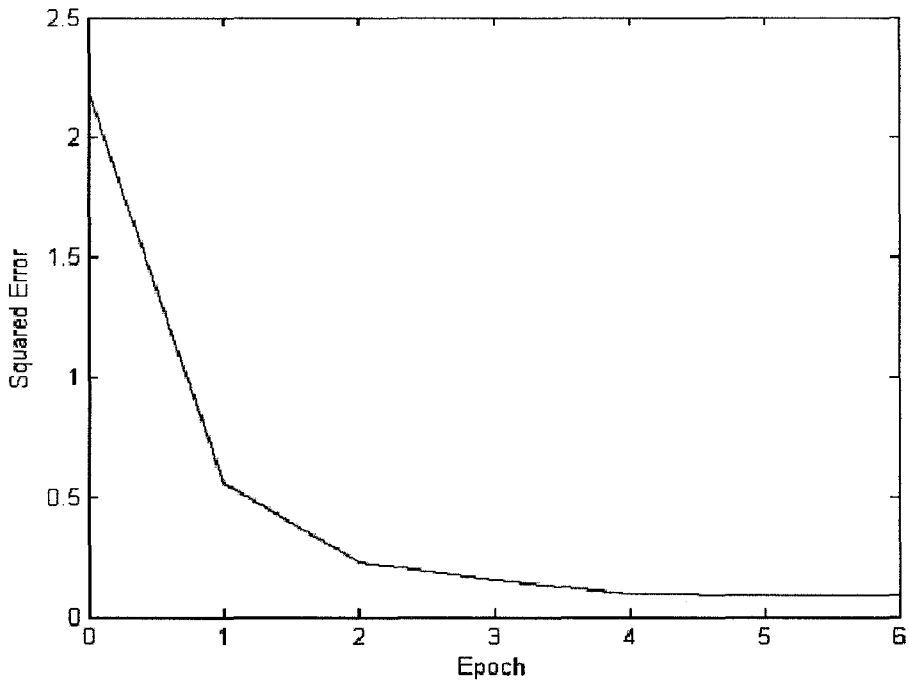

Figure 3.3: Sum of squared errors during training of the ANN used for the Base case of New England 39-bus test system

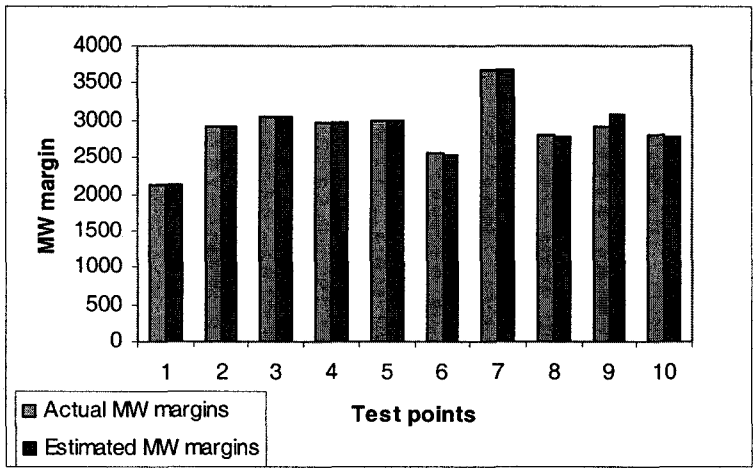

Figure 3.4: Estimated and actual values of the MW margins for the base case of New England 39-bus test system using the MLP neural network

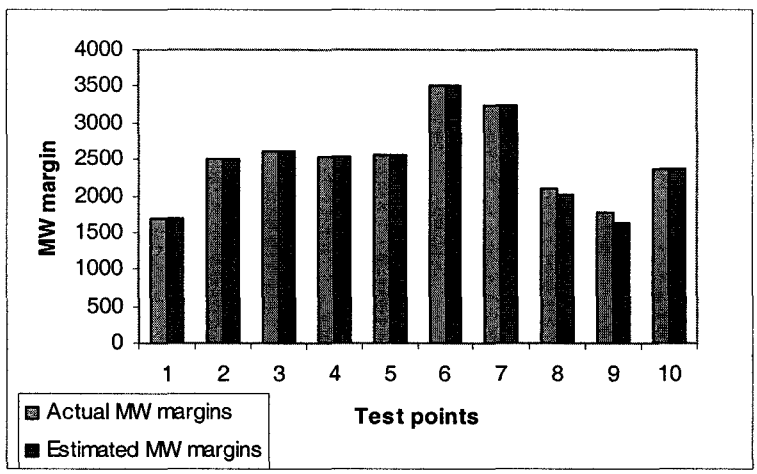

Figure 3.5: Estimated and actual values of the MW margins for the contingency C1 of the New England 39-bus test system using the MLP neural network

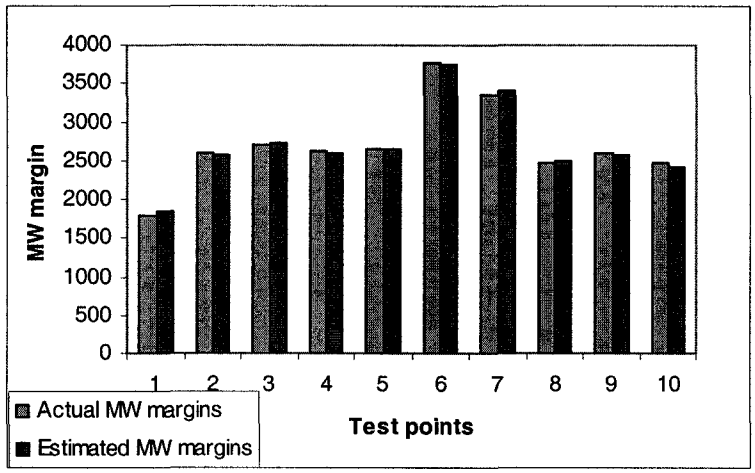

Figure 3.6: Estimated and actual values of the MW margins for the contingency C2 of the New England 39-bus test system using the MLP neural network

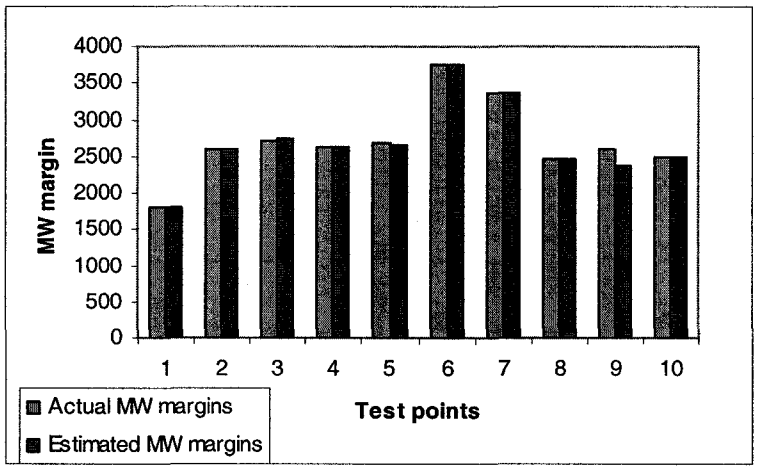

Figure 3.7: Estimated and actual values of the MW margins for the contingency C3 of the New England 39-bus test system using the MLP neural network

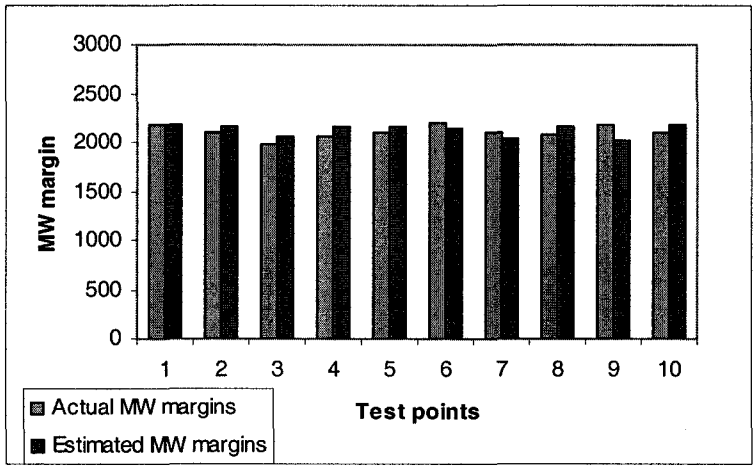

Figure 3.8: Estimated and actual values of the MW margins for the contingency C4 of the New England 39-bus test system using the MLP neural network

Table 3.1: Sample values of the actual and the estimated MW margins using the MLP neural networks, for different topologies for the New England 39-bus test system

Base case		Contingency C1		Contingency C2		Contingency C3		Contingency C4	
Actual	Estimated	Actual	Estimated	Actual	Estimated	Actual	Estimated	Actual	Estimated
2112	2114.1	1700	1700	1799	1838.4	1810	1816.8	2178	2182.4
2912	2907.4	2500	2497	2587	2577.2	2600	2600	2104	2160.5
3047	3035.3	2612	2612	2712	2733	2725	2730.2	1972	2057.3
2962	2969.2	2535	2535	2635	2596.9	2637	2633.8	2067	2163.1
2987	3003.2	2562	2562	2662	2658.7	2675	2669.1	2098	2171.6
2547	2542.7	3512	3511.4	3760	3727.7	3762	3761.4	2203	2146.7
3685	3680.6	3250	3249.7	3350	3399.1	3360	3356.9	2112	2046.9
2797	2776.8	2100	2024.6	2472	2499.7	2475	2478.4	2077	2155.2
2925	3067	1775	1625.2	2600	2582.6	2612	2384.7	2187	2026.2
2800	2787.3	2375	2374.9	2475	2412.9	2485	2487.6	2108	2186.3

Table 3.2: Summary of the test results for base case and different contingencies by using the MLP neural network

ANN for different topologies	Maximum % error	Average % error
Base case	4.85	0.77
Contingency C1	8.43	1.21
Contingency C2	2.50	1.15
Contingency C3	8.70	0.99
Contingency C4	7.35	3.58

3.4 Conclusions

A scheme for online voltage stability monitoring of a power system using the ANN is proposed in this chapter. Separate ANNs are used for voltage stability monitoring for different contingencies. For each contingency, an MLP neural network consisting of one input layer, one hidden layer, and one output layer is used for estimating the voltage stability margin. The reduced vectors of the active and reactive load demands are used as the inputs to the ANN, and the available MW margin to the point of voltage instability is taken as the output. A sensitivity-based method of selection of important features for the ANN is proposed. The conventional method of computing parameter sensitivities of the voltage stability margin has many limitations, as discussed in section 2.4 in the previous chapter. A regression-based method is proposed to compute the sensitivities, which overcomes many limitations of the conventional method, such as fixed direction of increase in system stress, and numerical difficulty in finding the exact point of voltage instability. The sensitivity-based selection of the important inputs provides a systematic way of reducing the number of features. The ANN architectures designed by this method have smaller size with sufficient accuracy and high execution speed. The test results indicate the effectiveness of the proposed method for online voltage stability monitoring.

For the secure operation of the power system, it is very important that the utilities monitor the voltage stability of the system on a continuous basis [51]. The proposed regression-based sensitivity analysis method can give realistic and accurate information regarding the dependency of the voltage stability margin on the parameters considered. Based on the sensitivity information, the important parameters are chosen as input

features for the ANN. The utility can acquire the values of these parameters from the measurement units or the state estimator at regular intervals of time, and obtain the estimates of the available voltage stability margin for the critical contingencies using the proposed scheme.

Chapter 4

Multicontingency Voltage Stability Monitoring Using an Enhanced Radial Basis Function Network

4.1 Introduction

There are many works reported on online voltage stability monitoring in the literature, exploring the capability of the ANN to approximate the functional relationship between a voltage stability indicator and the measurable power system parameters that affect the chosen voltage stability indicator [26-33]. Chapter 3 describes a scheme for online voltage stability monitoring using the Multilayer Perceptron (MLP) neural network. A major limitation of the use of ANNs for online voltage stability monitoring arises due to the fact that the functional relationship itself gets changed from one topology to the other. This results in the requirement of an additional ANN for each new topology. When a contingency occurs, the system topology may change. For a large power system with numerous potentially dangerous credible contingencies, it poses the practical problem of implementing large number of ANNs for voltage stability monitoring.

A scheme for real-time assessment of voltage stability of a power system for multiple contingencies using a single ANN is presented in this chapter. A Radial Basis Function Network (RBFN) is used to provide an estimate of the voltage stability margin for different contingencies. The active and reactive power demands of the loads are used as input features to the RBFN and the available MW margin to the point of voltage instability is used as an indicator of the voltage stability of the system. The proposed

scheme has the ability to get adaptive training when subjected to any new training pattern. Risk of network size growing bigger with time as a result of network adaptation is eliminated by using a network pruning strategy. The online voltage stability monitoring scheme is applied to the New England 39-bus power system and the test results are presented.

4.2 Radial Basis Function Network

Radial Basis Function Networks (RBFN) are a special class of feed-forward neural networks. An RBFN consists of three layers: an input layer, a hidden layer and an output layer. The network is capable of performing nonlinear mapping of the input features into the output. The hidden layer contains neurons with nonlinear functions called basis functions, whose arguments involve the Euclidian distance between the applied input pattern and the centre of the basis function. The Gaussian function is the most commonly used basis function for the RBFNs. It has been established by researchers that an RBFN with sufficient number of Gaussian basis functions in the hidden layer can be used as a universal approximator [53-55].

Let there be 'q' Gaussian basis functions in the hidden layer of an RBFN and let $\{\mathbf{t}_i\}_{i=1}^{q}$ be the centres of the basis functions. The Gaussian Radial Basis Function at the centre $\mathbf{t}_i$ for an input $\mathbf{X}$ is defined as,

$$g(\mathbf{X},\mathbf{t}_i)=g(\|\mathbf{X}-\mathbf{t}_i\|)=\exp\left(-\frac{\|\mathbf{X}-\mathbf{t}_i\|^2}{2\sigma^2}\right), \forall i=1,\ldots,q, \tag{4.1}$$

where $\|\mathbf{X}-\mathbf{t}_i\|$ is the Euclidian distance between the input vector $\mathbf{X}$ and the centre $\mathbf{t}_i$, and

σ is the spread parameter of the Radial Basis Function.

For a single neuron at the output layer, the output of the RBFN is given by,

$$f(\mathbf{X}) = \sum_{i=1}^{q} w_i g(\|\mathbf{X} - \mathbf{t}_i\|) \tag{4.2}$$

where w_i is the weight connecting the i^{th} neuron in the hidden layer to the output.

For the commonly used artificial neural networks such as the Multi Layer Perceptrons (MLP), described in Chapter 3, the design of the network involves all the layers of the network simultaneously. The design of the hidden and output layer of an RBFN can be carried out separately, at different points of time [53]. The hidden layer applies a non-linear transformation from the input space to the hidden space. The output layer is a linear combination of the activations in the hidden layer. The weights connecting the hidden layer to the output layer are found by using linear optimization techniques. The fact that the output layer can be designed separately and that the output is a linear combination of hidden activations, makes possible the use of a single RBFN for voltage stability monitoring for different contingencies [58]. As described in the next section, the centres of the RBFN for selected contingencies are chosen by using a sequential learning strategy. The optimal output weights are found for different contingencies, which linearly combine the activations of the same hidden layer to give the desired output for different contingencies.

4.3 Multicontingency online voltage stability monitoring

Loading margin is used in this research as an indicator to the proximity to the voltage collapse point, similar to the online voltage stability monitoring scheme proposed in Chapter 3. Real and reactive load power demands at the busses are taken as the input data set. It is to be noted here that other measurable power system parameters also can be used as inputs to the ANN [26-33]. In fact, parameters that highly affect the voltage stability may vary from one system to another. A purpose of the present research is to design an efficient ANN that should work as a mapping tool to estimate voltage stability margin for any suitable combination of inputs. A Radial Basis Function Network (RBFN) is used to predict the available MW margin to the point of voltage instability. The same RBFN is trained for different topologies; the number of outputs of the RBFN being equal to the number of topologies considered. Once trained, the RBFN can be used to predict the voltage stability margin for different contingencies. The basic architecture of the RBFN has much similarity with the Resource Allocating Network (RAN) described in [59] and the Minimum Resource Allocation Network (MRAN) proposed in [60]. Use of RAN or MRAN for the present problem was not found suitable since the ANN required a large number of hidden units due to the highly nonlinear nature of the mapping and inadequate capability of the ANN to interpolate unforeseen patterns. The possible reason for these drawbacks is the absence of any regularization technique in these networks. The architecture of RBFN proposed in this research uses the basic methodology of RAN and MRAN for selecting hidden neurons, and then uses a regularization technique before finding the optimal weights connecting hidden neurons and the outputs, by using a Least

Means Square (LMS) algorithm. The ANN can be upgraded or adapted when subjected to new patterns. The risk of network size growing bigger as a result of the adaptation process is eliminated by implementing a network pruning strategy as proposed in [60]. The basic online voltage stability monitoring scheme using RBFN is shown in Figure 4.1, followed by detailed description of the individual steps.

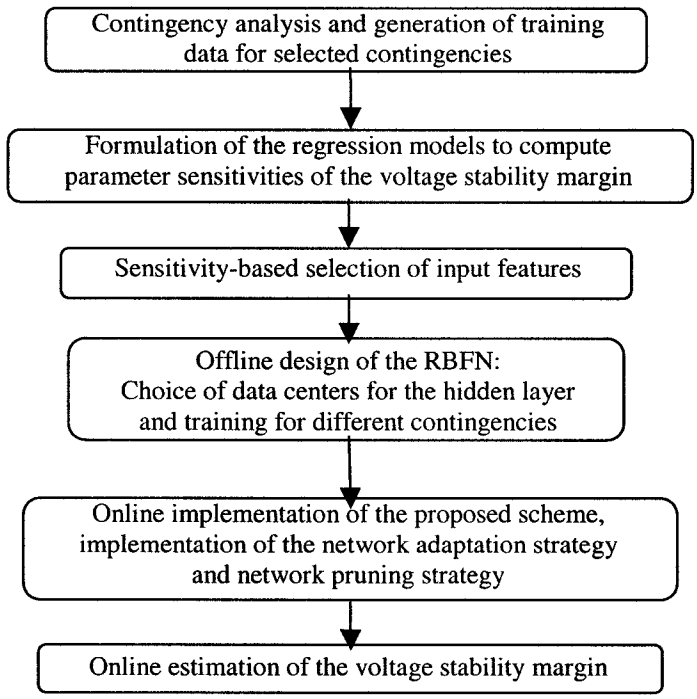

Figure 4.1: Online voltage stability monitoring for multiple contingencies using a single Radial Basis Function Network.

4.3.1 Identification of critical contingencies and generation of training data

Analysis of credible contingencies has been the standard practice in a power system [51]. A selected number of worst-case contingencies are considered in this study. Without loss of generality, any number of contingencies can be accommodated in the proposed

scheme. Training data sets for the RBFN are generated for the base case and the selected contingencies. The real and reactive power at all the load busses and the generator real power outputs are varied randomly within specific limits and the change in total load in the system is distributed among the available generators in proportion to their participation factors in the base case. The participation factor for a generator in the base case is taken as the ratio of the generator real power output to the total real power generation in the system. Real and reactive load powers are taken as the input vector to the RBFN. Corresponding to each loading pattern, the MW margin to the point of voltage instability is recorded for each network topology. The set of MW margins are taken as the outputs of the RBFN.

4.3.2 Selection of input features

The dimension of input features is reduced by the sensitivity-based feature selection method described in section 3.2.3 of Chapter 3. Separate regression models are first developed for each of the system topologies considered. Sensitivities of the voltage stability margin with respect to the load active and reactive power demands are found by differentiation of the regression models. An input qualifies as a feature for the RBFN when the sensitivity of the voltage stability margin with respect to that input exceeds the predefined cut-off value. Separate minimum cutoff values of sensitivity, viz., S^{j}_{pmin} and S^{j}_{qmin} are used to select the real and reactive power demands respectively, for the j^{th} contingency. The final set of input features are found by the union of the features selected for different topologies. The set T^{p}_{j} of active power demands included in the input feature

set for the j^{th} system topology is defined as:

$$T_j^p = \{p_i : \|S_i\| \geq S_{p\min}^j, i = 1,...,ld\}; j = 1,...,c \tag{4.3}$$

where 'ld' is the number of load busses in the system, and 'c' is the number of contingencies considered for voltage stability monitoring, including the base case.

Similarly, the set of reactive power demands chosen as input features for the RBFN is defined as:

$$T_j^q = \{q_i : \|S_i\| \geq S_{q\min}^j, i = 1,...,ld\}; j = 1,...,c \tag{4.4}$$

The final set of real power demands selected as input features to the RBFN is given as:

$$T^p = \bigcup_{j=1}^{c} T_j^p, \tag{4.5}$$

and the final set of reactive power demands chosen as input features is given as:

$$T^q = \bigcup_{j=1}^{c} T_j^q \tag{4.6}$$

4.3.3 Offline design of the RBFN

Let $\{\mathbf{X}_i, \mathbf{d}_i\}_{i=1}^n$ be the training patterns, where $\mathbf{X}_i \in \mathbf{R}^s$ is the vector of real and reactive load powers at busses, 's' being the dimension of the input vector; $\mathbf{d}_i \in \mathbf{R}^c$ is the corresponding MW margins for different system topologies, 'c' is the total number of contingencies considered, including the base case. The design of the RBFN begins with a single hidden unit. New units are added according to the sequential learning strategy described below. The first sample pattern from the training data set is chosen as the data

centre of the first neuron in the hidden layer, i.e.,

$$\mathbf{t}_1 = \mathbf{X}_1 \tag{4.7}$$

The spread parameter σ of the radial basis function shown in (4.1) is taken as,

$$\sigma = \sigma_{min} \tag{4.8}$$

where σ_{min} is the minimum specified value of the spread parameter.

The initial weight matrix is defined as,

$$\mathbf{W}^1 = \mathbf{d}_1^T, \tag{4.9}$$

where $\mathbf{d}_1 = (d_{11}, d_{21}, ..., d_{c1})^T$ is the vector of target MW margins for the input $\mathbf{X}_1$ for 'c' different contingencies.

The outputs of the RBFN are given by,

$$\mathbf{f}(\mathbf{X}) = [\mathbf{f}_1, \mathbf{f}_2, ..., \mathbf{f}_c] = g(\|\mathbf{X}_1 - \mathbf{t}_1\|)\mathbf{W}^1 \tag{4.10}$$

The q^{th} hidden unit for $q \geq 2$ is added for the i^{th} pattern when one or both of the following criteria are satisfied.

$$\min\{\|d_{ki} - \mathbf{f}_k(\mathbf{X}_i)\|, \forall k = 1, ..., c\} \geq e_{min} \tag{4.11}$$

and $$\|\mathbf{X}_i - \mathbf{t}_{nr}\| \geq \varepsilon_q \tag{4.12}$$

where $\mathbf{t}_{nr}$ is the data centre nearest to the input sample pattern $\mathbf{X}_i$ in terms of Euclidian distance, e_{min} is the minimum tolerable error for the output of the RBFN, and ε_q is defined as follows.

$$\varepsilon_q = \max\{\varepsilon_{max}\gamma^q, \varepsilon_{min}\} \tag{4.13}$$

where ε_{max} is the initial value of the distance parameter for adding a new hidden unit, γ is

the decay constant with $0<\gamma<1$, and ε_{min} is the minimum allowable value of the distance parameter.

The exponential decay criterion (4.13) of the distance parameter allows fewer basis functions with larger widths initially. As the number of hidden units grows, more basis functions with smaller widths are added to fine-tune the mapping.

The spread parameter σ for the newly added hidden unit is defined as follows [59, 60].

$$\sigma_q = \max\{\sigma_{min}, \kappa\|\mathbf{X}_i - \mathbf{t}_{nr}\|\} \tag{4.14}$$

where κ is a constant.

The process of adding a new unit to the hidden layer of the RBFN is described above. In the next step, an optimal set of weights is found, which connects the hidden units to the output layer. To improve the interpolating capability and to ensure a smooth mapping, the RBFN is regularized by penalizing large weights as shown in Appendix A.4. This regularization technique is similar to what is used in Ridge regression [61, 62] and is used here for its simplicity and effectiveness.

The optimal weight vector between the hidden layer and the output of the RBFN is determined by linear optimization. For the i^{th} training pattern, $\{\mathbf{X}_i, \mathbf{d}_i\}$, the optimum weight vectors connecting 'q' hidden units to the outputs are given by,

$$\mathbf{W}^q = [\mathbf{w}_1^q, \mathbf{w}_2^q, ..., \mathbf{w}_c^q] \tag{4.15}$$

Each column of $\mathbf{W}^q$ is defined as [Appendix A.4],

$$\mathbf{w}_t^q = (\mathbf{G}^{q^T}\mathbf{G}^q + \lambda_t \mathbf{I}_q)^{-1}\mathbf{G}^{q^T}\mathbf{D}_t \; ; \forall t = 1, ..., c \tag{4.16}$$

where $\mathbf{w}_t^q = [w_{1t}^q, w_{2t}^q, ..., w_{qt}^q]^T$ is the output weight vector connecting 'q' hidden units to

the output for the t^{th} contingency; $t = 1,...,c$; c being the number of contingencies considered,

$\mathbf{D}_t = [d_{t1}, d_{t2}, ..., d_{ti}]^T$ is the vector containing desired t^{th} outputs for all the patterns $\{\mathbf{X}_i, \mathbf{d}_i\}_{i=1}^n$.

$\mathbf{G}^q$ is the matrix of basis functions and is given by,

$$\mathbf{G}^q = \begin{bmatrix} g(\mathbf{X}_1,\mathbf{t}_1) & g(\mathbf{X}_1,\mathbf{t}_2) & \dots & g(\mathbf{X}_1,\mathbf{t}_q) \\ g(\mathbf{X}_2,\mathbf{t}_1) & g(\mathbf{X}_2,\mathbf{t}_2) & \dots & g(\mathbf{X}_2,\mathbf{t}_q) \\ \vdots & \vdots & & \vdots \\ g(\mathbf{X}_i,\mathbf{t}_1) & g(\mathbf{X}_i,\mathbf{t}_2) & \dots & g(\mathbf{X}_i,\mathbf{t}_q) \end{bmatrix} \tag{4.17}$$

λ_t =regularization parameter,

$\mathbf{I}_q$ is an identity matrix of dimension [q×q].

The regularization parameter λ_t ensures smoothness in the mapping and enhances the capability of the ANN to map unforeseen patterns. The desired value of the regularization parameter is found by iteration using (4.18), which is obtained by using Generalized Cross Validation of the prediction error of the RBFN [61-63]. Starting with an initial guess for λ_t, the weight vector $\mathbf{w}_t$ and other required quantities are computed. Using these quantities λ_t is computed again using the right hand side of (4.18). The iterations are continued untill no appreciable change is observed in λ_t.

$$\lambda_t = \frac{\mathbf{D}_t^T \mathbf{P}^2 \mathbf{D}_t \text{trace}(\mathbf{A}^{-1} - \lambda_t \mathbf{A}^{-2})}{\mathbf{w}_t^T \mathbf{A}^{-1} \mathbf{w}_t \, \text{trace}(\mathbf{P})} \tag{4.18}$$

where $\mathbf{P} = \mathbf{I}_i - \mathbf{G}^q \mathbf{A}^{-1} \mathbf{G}^{q^T}$ (4.19)

and $\mathbf{A}=(\mathbf{G}^{q^T}\mathbf{G}^q+\lambda_t\mathbf{I}_q)$ (4.20)

To find the output weight vectors $\mathbf{w}_t^q, t=1,...,c$, one needs to find the inverse of the matrix $\mathbf{A}$ in (4.20) as required in (4.16). Appendix A.4 shows that, after addition of a new training pattern or new basis function along with a training pattern, $\mathbf{A}^{-1}$ can be computed by simple matrix manipulations using its value from the previous step. This saves the effort of matrix inversion which is a demanding task for a large system and for multiple contingencies.

Once trained off-line with the example patterns $\{\mathbf{X}_i,\mathbf{d}_i\}_{i=1}^n$, outputs of the RBFN having 'Q' basis functions for any input $\mathbf{X}$ are given by,

$$\begin{aligned}\mathbf{f}(\mathbf{X}) &= [\mathbf{f}_1,\mathbf{f}_2,...,\mathbf{f}_c] \\ &= \left[g(\|\mathbf{X}-\mathbf{t}_1\|), g(\|\mathbf{X}-\mathbf{t}_2\|),..., g(\|\mathbf{X}-\mathbf{t}_Q\|)\right]\mathbf{W}\end{aligned} \quad (4.21)$$

where $\mathbf{W}=[\mathbf{w}_1,\mathbf{w}_2,...,\mathbf{w}_c]$ is the output weight matrix containing weight vectors connecting hidden units to different outputs.

4.3.4 Adaptive training of the RBFN

The proposed RBFN for voltage stability monitoring can be updated by training the network with new patterns that represent the new operating conditions or new loading scenario in the system. When subjected to a new training pattern $\{\mathbf{X},\mathbf{d}\}$, criteria (4.11) and (4.12) are evaluated to determine whether a new hidden unit needs to be added or not. In the next step, the output weight matrix is found by using (4.15) and (4.16). The MW margin is then estimated by (4.21). The risk of the number of hidden units growing

without bound as a result of network adaptation is eliminated by using a network pruning strategy described in the next section.

4.3.5 Network pruning strategy

The basic idea of the pruning strategy is that, a neuron from the hidden layer is removed if it does not make sufficient contribution to the output over a specified number of operations of the RBFN.

Let $\mathbf{o}_j = [o_{1j}, o_{2j}, ..., o_{cj}]^T$ be the output vector of the j^{th} hidden unit contributing to the outputs of the RBFN for an input **X**, where the k^{th} element of $\mathbf{o}_j$ is given by,

$$o_{kj} = w_{jk} \exp\left(-\frac{\|\mathbf{X}-\mathbf{t}_j\|^2}{2\sigma_j^2}\right); \forall k=1,...,c \tag{4.22}$$

The hidden unit 'j' is removed if and only if the value of every element in the output vector $\mathbf{o}_j$ provides an insignificant contribution to the output for a number 'P' of consecutive operations. The number 'P' is specified based on the past experience regarding the variation in the power system loading patterns and availability of computational resources. To avoid inconsistencies in comparing the contributions of different hidden units with a specified threshold, the elements of the output vector $\mathbf{o}_j$ are normalized as follows.

$$r_{kj} = \left\| \frac{o_{kj}}{\max(\text{abs}(\mathbf{o}_j))} \right\| \tag{4.23}$$

The j^{th} hidden unit is eliminated if it satisfies the following criterion 'P' successive times.

$$r_{kj} \leq r_{min}; \forall k = 1,...,c \tag{4.24}$$

where r_{min} is the threshold contribution to the output for pruning a hidden unit. Numerical value of r_{min} is decided in the present research by trial and error method to give the best result.

4.4 Simulation results

The proposed scheme for online voltage stability monitoring for multiple contingencies has been applied to the New England 39-bus test system [57]. The single-line diagram of this test power system is shown in Figure A.1 in Appendix A. For generating training data for the RBFN, active and reactive powers at the load busses are varied randomly within ± 20% of the base case values. The change in load is distributed among the available generators in proportion to their participation factors. For each operating condition, active and reactive load powers are recorded as input features. For each loading pattern, the MW margins corresponding to different contingencies are obtained by using PowerWorld Simulator [18] and are recorded as the outputs of the RBFN. The loads are assumed to be of constant power factor type. The training data set for the ANN and the sensitivity-based method of selecting important features are the same as in Chapter 3. Test results are reported in this section for the base case operating condition and four different contingencies as shown in Table A.1. The contingencies are selected in such a way that they reflect significant changes in system topology. For example, all the contingencies considered in this study involve outage of a radial line, which disconnects the corresponding generator also from the system. The lost generation is supplied by the available generators in proportion to their participation factors. Table A.3 shows the

number of features selected for different minimum cut-off values of the sensitivities. The subsequent results given in this section are based on the cut-off values of $S_{p\,min}$ and $S_{q\,min}$ given in Table A.4 for different contingencies. Following the method selection of features described in section 4.3.2, the final number of features is 21, which consists of 13 active load powers and 8 reactive load powers, as shown in the following sets T^p and T^q of features:

$$T^p = \{P1, P6, P7, P8, P9, P10, P11, P12, P13, P14, P15, P16, P17\}$$

$$T^q = \{Q2, Q3, Q4, Q5, Q14, Q15, Q16, Q17\}$$

These 21 features are used as inputs to the RBFN that is used for voltage stability monitoring for the base case and all the contingencies considered.

The design of the RBFN starts with a single neuron at its hidden layer. Initial values of the design parameters described in section 4.3.3 are given in Table 4.1. These values are found to give best results for the present case in terms of output errors. The initial high value of the distance parameter ε_{max} ensures that not too many units are added to the hidden layer and also has the effect of smoothing the mapping since spread parameter σ takes higher values initially. The distance parameter decays exponentially as new units are added, thus improving the mapping capability of the RBFN locally around the data centres in the hidden layer. After addition of each neuron to the hidden layer, the regularization parameter λ and the output weight matrix are updated. The size of the RBFN at the end of the off-line training is 21-27-5, with 21 input nodes that represent selected active and reactive powers as important features, 27 hidden nodes and 5 output nodes that give the MW margins for 5 different system topologies. The

estimated values of the MW margins based on the test patterns and the actual margins for the base case, Contingency C1, C2, C3 and C4 are shown graphically in figures 4.2 to 4.6. Table 4.2 shows the actual and estimated values of the MW margins plotted in figures 4.2 to 4.6. Table 4.3 gives the summary of simulation results for the base case, Contingency C1, C2, C3 and C4.

Table 4.1: Values of different design parameters for the RBFN

Parameters	σ_{min}	e_{min}	ε_{max}	γ	ε_{min}	κ	r_{min}
Values	300	20	2000	0.97	500	0.8	0.1

The adaptation process of the RBFN to changing loading scenarios was simulated by subjecting the network to a series of different loading patterns as inputs and corresponding MW margins for different contingencies as the outputs. The network pruning strategy described in section 4.3.5 was implemented with P = 5, i.e., a hidden node was eliminated if it did not make significant contribution to the output for 5 successive times. Fig. 4.7 shows the number of hidden units after subjecting the RBFN to every 5 new patterns. After performing adaptive training with 30 new patterns, 13 new units were added to the hidden layer and 5 old units were eliminated due to the pruning strategy, thus increasing the size of the hidden layer by 8 new units.

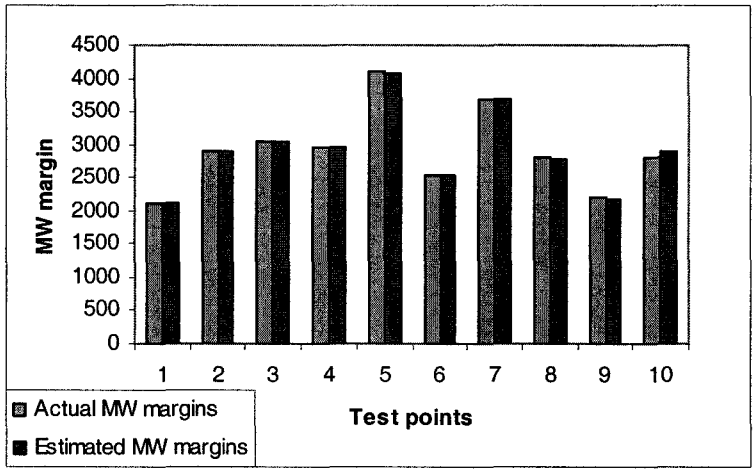

Figure 4.2: Estimated and actual values of the MW margins for the Base case of the New England 39-bus test system using single RBFN

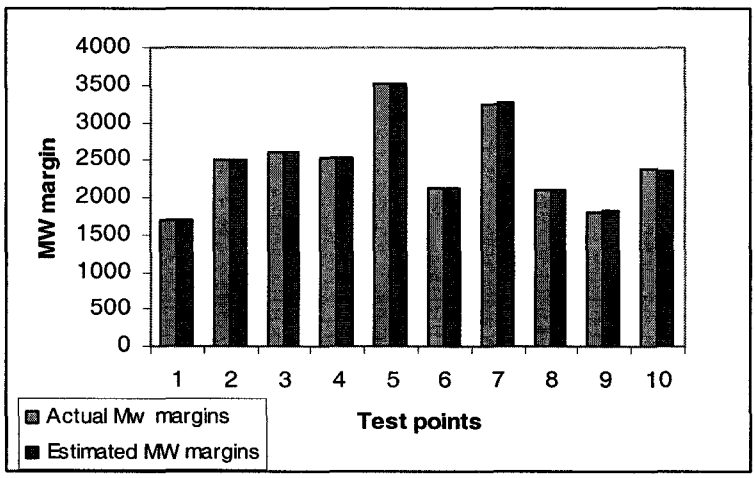

Figure 4.3: Estimated and actual values of the MW margins for the contingency C1 of the New England 39-bus test system using single RBFN

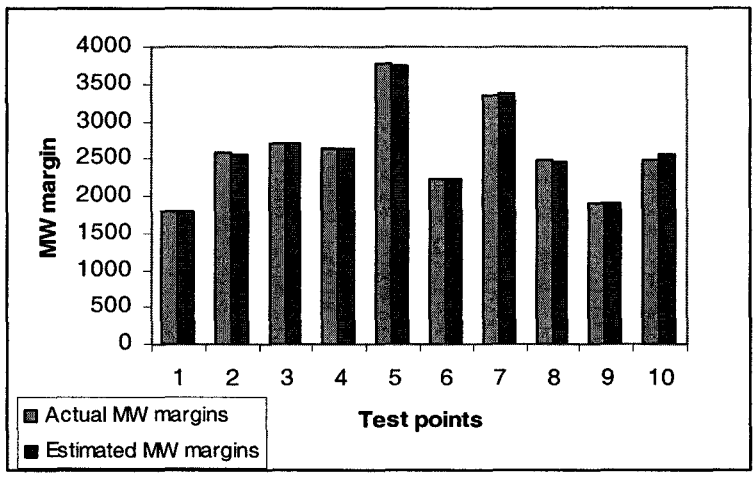

Figure 4.4: Estimated and actual values of the MW margins for the contingency C2 of the New England 39-bus test system using single RBFN

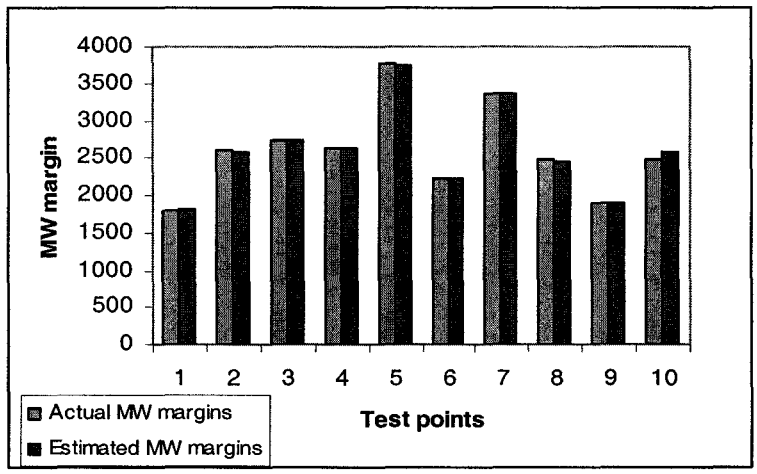

Figure 4.5: Estimated and actual values of the MW margins for the contingency C3 of the New England 39-bus test system using single RBFN

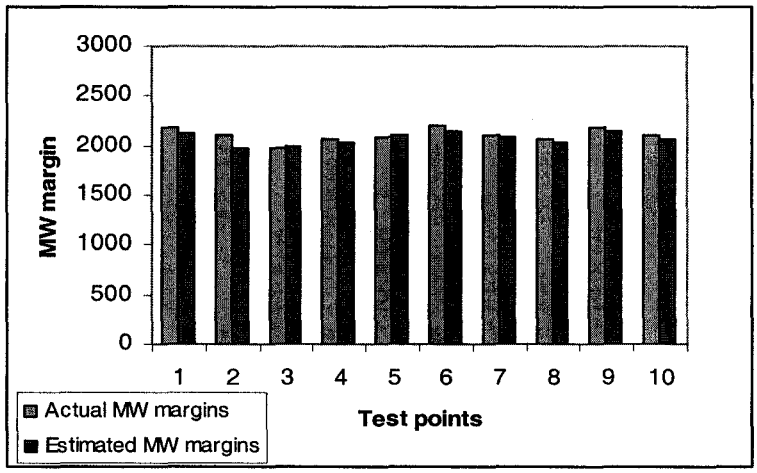

Figure 4.6: Estimated and actual values of the MW margins for the contingency C4 of the New England 39-bus test system using single RBFN

Table 4.2: Sample values of the actual and the estimated MW margins by the RBFN for different topologies for the New England 39-bus test system

Base case		Contingency C1		Contingency C2		Contingency C3		Contingency C4	
Actual	Estimated	Actual	Estimated	Actual	Estimated	Actual	Estimated	Actual	Estimated
2112	2122.3	1700	1698.9	1799	1807.1	1810	1818.2	2178	2131.9
2912	2886.9	2500	2502.4	2587	2564.6	2600	2577.6	2104	1983.5
3047	3048.8	2612	2610.6	2712	2714.8	2725	2727.7	1972	1995.5
2962	2968.1	2535	2536.1	2635	2637.9	2637	2640.2	2067	2040.5
4099	4084.5	3512	3515.9	3760	3746.8	3762	3748.8	2098	2111.7
2547	2546.1	2122	2122.9	2224	2221.6	2235	2233.6	2203	2153.4
3685	3695.4	3250	3258.4	3350	3358.3	3360	3370.2	2112	2081.7
2797	2770.8	2100	2103.5	2472	2446.3	2475	2449.5	2077	2028.8
2212	2168.4	1800	1833.4	1900	1887.8	1910	1894.7	2187	2143.3
2800	2895.9	2375	2345.9	2475	2566.8	2485	2576.3	2108	2075.7

Table 4.3: Summary of test results for the base case and the selected contingencies by using single RBFN

RBFN for different topologies	Maximum % error in MW margin	Average % error in MW margin
Base case	3.42	0.86
Contingency C1	1.85	0.39
Contingency C2	3.70	0.76
Contingency C3	3.67	0.77
Contingency C4	5.72	2.05

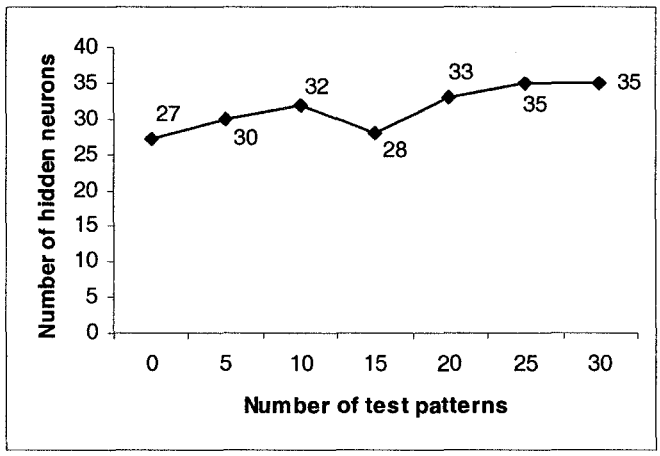

Figure 4.7: Variation in the total number of hidden neurons for the RBFN subjected to new test patterns representing the changing loading scenarios

4.5 Online implementation of the proposed scheme

A complete power system security analysis framework comprises of stability monitoring, security assessment, security enhancement, emergency control and restorative control. Online voltage stability monitoring, which is the focus of the present chapter, is considered as an integral part of the power system stability monitoring problem. Contingency analysis of a power system is done as a part of the security assessment. Evaluating N-1 contingencies with respect to the available MW margin is a standard procedure followed in many utilities. N-1 contingency means outage of one element in the system. MW margins for the base case and different selected line outages for specific loading patterns are computed in the control centre by using standard analytical tools. It is not feasible to have MW margins for all possible loading scenarios and corresponding

generation schedules. The ANN can interpolate the unforeseen or unstudied cases by capturing the functional relationships between the MW margin and the loading scenario of the power system. An important issue with the use of analytical methods for power system security assessment is the computational time [64], even with the state-of-the-art processor. Once trained offline with a wide range of loading scenarios, the proposed RBFN can be used for online voltage stability monitoring for different contingencies. The loading scenario in a power system may change with time. Designing a new ANN every time the loading scenario changes significantly is a demanding task. The proposed RBFN can be adapted to changing loading scenarios, as described in section 4.3.4, thus eliminating the need for a fresh ANN for voltage stability monitoring. The network pruning strategy described in section 4.3.5 keeps the size of the hidden layer of the RBFN within limit.

4.6 Comparison of the MLP and the RBFN for online voltage stability monitoring

Radial Basis Function Networks (RBFN) and Multilayer Perceptrons (MLP) are nonlinear layered feedforward networks. They are both universal approximators [53-55]. However, these two ANNs differ from each other in some important aspects regarding their architectures, and consequently in their applications for online voltage stability monitoring.

- The MLPs construct global approximations to nonlinear input-output mappings with the help of one or more hidden layers of neurons and synaptic weights.

RBFNs construct local approximations to nonlinear input-output mappings using nonlinear basis functions in the hidden layer and the connecting weights to the output. As a result of local learning, the RBFNs usually needs a greater number of parameters or hidden nodes to approximate a nonlinear mapping, compared to MLPs.

- The design of different layers of an MLP has to be done simultaneously. On the other hand, the design of different layers of RBFN can be done separately, at different points of time. This facilitates the use of a single RBFN for multicontingency voltage stability monitoring, as described in this chapter. The hidden layer is designed for multiple contingencies using a sequential learning strategy. The activations of the hidden layer are then combined by using linear optimization to give the output.
- One possible advantage of the MLP over the RBFN is the smaller number of hidden nodes needed for the nonlinear mapping. As shown in Chapter 3, the MLPs for different contingencies consist of 10 hidden neurons. The RBFN used in this chapter consists of 27 hidden nodes. Use of different MLPs for different contingencies however may be a disadvantage when a large number of potential contingencies need to be considered.
- Design of the MLP described in Chapter 3 is simple. The ANN can be used almost as a black-box for input-output mapping. Comparatively, the design of the RBFN proposed in this chapter is mathematically involved. It may therefore be

easier to use different MLPs for different contingencies for a smaller system with small number of potentially dangerous contingencies.

- An important advantage of the proposed RBFN is that, it can be adapted online, depending on the changing operating scenario of the power system. The MLP however, may need a fresh training if the operating conditions change considerably. For a large power system having numerous potentially dangerous contingencies, use of the proposed RBFN architecture is advisable for online voltage stability monitoring.

4.7 Conclusions

This chapter presents a scheme for online voltage stability monitoring for multiple contingencies using a single RBFN. In an RBFN, the output layer and the hidden layer can be designed separately, unlike other ANNs such as the MLPs. This allows optimization of the output weights for different contingencies with the same hidden layer.

Active and reactive load powers are chosen as input features to the ANN and the corresponding MW margins for the base case and different contingencies are taken as the outputs of the network. The proposed scheme should work for any other possible combinations of measurable power system parameters as inputs. For large power systems, training separate ANNs for all credible contingencies is a demanding task. The proposed method allows the use of a single ANN for different contingencies. The additional resource needed for monitoring voltage stability for a new contingency is the storage of an additional optimal weight vector in the output weight matrix in the off-line

training phase. Use of the same hidden layer for all contingencies saves much of the computational resources. The number of outputs of the RBFN can be limited by performing contingency analysis and selecting the required number of contingencies to be monitored. The sequential learning strategy used for designing the hidden layer minimizes the number of units in the hidden layer, resulting in a compact architecture for the ANN. Addition of a new training pattern or a new basis function along with a training pattern requires simple algebraic operation, without requiring extensive matrix inversion computations. The design procedure for the proposed RBFN is therefore computationally efficient. The proposed ANN can be adapted as the loading scenario changes in the power system. Growth of network size due to the adaptation process is limited by network pruning strategy. The test results indicate the effectiveness of the proposed method for online voltage stability monitoring for multiple contingencies.

A state-of-the art Dynamic Security Assessment (DSA) scheme of a power system works on real-time information or snapshots of the system. It comprises of measurement, modelling and state estimation, computation, and control actions. Intelligent systems technology is now being implemented in the computation module, in addition with conventional analytical solution tools. The proposed method can find its use in such modules as a tool for monitoring voltage stability of the system in real time.

Chapter 5

Sensitivity-based Generation Rescheduling for Multicontingency Voltage Stability Enhancement

5.1 Introduction

Chapters 3 and 4 describe proposed schemes for online voltage stability monitoring using ANN. At any point of time, the power system operating condition should be stable, meeting various operation criteria, and it should also be secure in the event of any possible contingency. There are different measures against voltage instability in real-time and in the planning and the design stage of a power system. The real-time measures can be of preventive or corrective in nature. To prevent immediate loss of voltage stability, corrective actions are needed. Preventive measures are then implemented to improve voltage stability margin of the system. The preventive and corrective control of voltage stability mainly constitute one or more of the following options: rescheduling real power generation, changing load tap changer (LTC) settings, adjusting phase shifter angles, reactive compensation and load shedding. In the present chapter, generator real power rescheduling is considered as the means for enhancing voltage stability of a power system. A sensitivity-based optimization method satisfying voltage stability constraints is implemented to reschedule the generations. The sensitivities of the voltage stability margin with respect to the generator real power outputs are found by using the ANN. The proposed method can be taken as a part of the preventive and corrective control of

voltage instability, along with other means of improving the voltage stability of a power system.

Most of the available methods of generation rescheduling for voltage stability enhancement use optimization to determine the correct amount of rescheduling needed to drive the operating point away from the potentially dangerous situation. The effect of change in control variables on the voltage stability of the system is usually included in the optimization process in the form of linearized sensitivities of the voltage stability margin with respect to the parameters of interest. Derivation of an accurate analytical expression for the sensitivities for multiple contingencies is a challenging task [37]. In the present research, the sensitivities for different network topologies are computed by using the enhanced Radial basis Function Network (RBFN) described in Chapter 4. Computation of sensitivities in this manner overcomes some of the limitations of the analytical method, as described in Chapter 3. The computed sensitivities are used in formulating the voltage stability constraints to be used in the optimization routine to find the optimal outputs of the generators to minimize the cost of total generation and improve the voltage stability margin of the system. The optimum generations for one topology may not ensure sufficient voltage stability margin for another. Hence, multiple contingencies are considered. Sensitivities for different contingencies are used to find optimum generations that ensure minimum voltage stability margin for multiple contingencies.

5.2 Sensitivity-based generation rescheduling

A voltage stability-constrained optimum generation rescheduling scheme aims at maintaining the voltage stability margin of the power system above some specified value, along with satisfying other operating criteria [65, 66]. The normal practice is to use the linearized sensitivities of the voltage stability margin with respect to generator outputs to formulate the voltage stability constraint in the optimization method [35-37, 67, 68]. The basic idea is that, a change in generator output results in a change in the voltage stability margin, which is estimated by the product of the change in generation with the corresponding sensitivity as shown below:

$$S_i \Delta p_i = \Delta M_i \tag{5.1}$$

where S_i is the sensitivity of the voltage stability margin with respect to the output of the i^{th} generator, Δp_i is the change in MW output of the i^{th} generator, and ΔM_i is the change in voltage stability margin due to the change in generation of the i^{th} generator.

The objective of the generation rescheduling is to find the optimum amounts and combination of changes Δp_i, such that the effective change in voltage stability margin is above or equal to what is required for a secure operation of the power system. If ΔM_{min} is the minimum MW margin enhancement required for the secure operation of the system, then the generation rescheduling should satisfy the following constraint:

$$\sum_{i=1}^{g} S_i \Delta p_i \geq \Delta M_{min} \tag{5.2}$$

where g is the number of generators participating in the generation rescheduling.

5.2.1 Multicontingency generation rescheduling

It is important to ensure secure operation of a power system in the event of potential contingencies. Generations rescheduled to enhance voltage stability margin for a particular operating condition may not serve to maintain the margin for some other contingency. Therefore it is necessary to make sure that the minimum voltage stability margin is maintained for all the critical contingencies, after rescheduling generations for a particular operating state. To this end, sensitivities of the voltage stability margin with respect to the generator outputs are computed for the base case, as well as for all the critical contingencies. The following inequality constraints are incorporated in the optimization program used for generation rescheduling, to maintain minimum voltage stability margins for the base case and all the contingencies considered:

$$\sum_{i=1}^{gk} \Delta p_i S_i^k \geq \Delta M_{k\min} \forall k = 1,...,c \tag{5.3}$$

where gk is the number of generators participating in the generation rescheduling for the k^{th} contingency,

S_i^k is the sensitivity of the voltage stability margin with respect to the i^{th} generator output for the k^{th} contingency,

$\Delta M_{k\min}$ is the minimum required enhancement in the MW margin for the k^{th} contingency to ensure the secure operation of the system,

'c' is the number of contingencies considered, including the base case.

5.3 Computation of sensitivities

The sensitivity information is needed to include in the optimization program the effect of change in generations on the voltage stability of the system. A commonly used method to compute the sensitivities of the voltage stability margin with respect to different parameters has been the use of the singularity of the powerflow Jacobian matrix at the point of voltage instability [4, 34]. The main drawbacks of the method are discussed in Chapter 2. A regression-based method of computing the sensitivities is proposed in Chapter 3. It is well-known that the ANNs have superior capability of mapping nonlinear relationships, compared to simple regression models [53-55]. To have a more accurate representation of the parameter sensitivities of the voltage stability margin, the ANN is used instead of the regression model to compute the sensitivities. The basic architecture of the ANN is the same as the RBFN proposed in Chapter 4. The only difference is that separate single-output RBFNs are used for finding sensitivities for different network topologies. The inputs to the RBFN are the generator MW outputs and the load real power demands, and the output is the MW margin to the point of voltage instability.

Let $y=F(\mathbf{x})$ be the mapping approximated by the RBFN, where y is the voltage stability margin and $\mathbf{x}$ is the vector of input parameters to the ANN. The sensitivities are computed by perturbing each input at a time by a finite amount and recording the corresponding change in output of the RBFN. The ratio of the two finite differences approximates the sensitivity S_x of the voltage stability margin with respect to the parameter x, i.e.,

$$S_x = \frac{\partial y}{\partial x} \approx \frac{\Delta y}{\Delta x} \tag{5.4}$$

where Δx is the change in input x, and Δy is the change in output of the RBFN.

A strategy is needed to maintain uniformity in the required perturbations Δx for inputs of different magnitudes. A fixed percentage 'p' of each input is taken as the corresponding perturbation. For the input x, the value of Δx is computed as:

$$\Delta x = \frac{xp}{100} \tag{5.5}$$

Special care has to be taken to decide the size of Δx, and consequently, of 'p'. A large value of 'p' may fail to account for the nonlinear mapping due to over-linearization around the point of interest. Starting with an initial value, the size of 'p' is reduced until no appreciable change is observed in the calculated values of the sensitivities. The following steps are taken to determine the appropriate value of 'p', and consequently, of the step size for Δx :

1. Choose an initial value of p: $p = p_0$ .Compute the sensitivities $S_x|_p$ of the output of RBFN at p, using (5.4) and (5.5)
2. Reduce p by a small amount: $p = p - \Delta p$; compute the sensitivities, $S_x|_{p-\Delta p}$.
3. Compute the magnitudes of the differences: $\Delta S_x = \left\| S_x|_p - S_x|_{p-\Delta p} \right\|, \forall x$.
4. If $\min_x \{\Delta S_x\} \geq \Delta S_{min}$, where ΔS_{min} is the minimum specified tolerance for the changes in sensitivities, go to step 2, otherwise, go to step 5. Numerical value of

ΔS_{min} is chosen by trial and error process to ensure convergence of 'p' within a value of +/- 10.

5. Stop the iterations.

In the sensitivity-based generation rescheduling scheme presented in this chapter, the sensitivities of the voltage stability margin with respect to the generator MW outputs are found by the above method. An RBFN is trained for each network topology with the generator MW outputs and the load real power demands as the inputs, and the MW margins to voltage instability as the corresponding outputs. The training data are generated by randomly varying the load active power demands and the generator MW outputs within specific limits. Corresponding to each operating condition, the available MW margin to the point of voltage instability is recorded as the output of the RBFN. Once the RBFN is trained with sufficient varieties of sample training patterns representing different possible operating conditions, the sensitivities of the voltage stability margin with respect to the generator outputs can be found using (5.4).

The sensitivities are found for the base case and all other contingencies considered. It is to be noted that the above-described procedure for finding the sensitivities does not depend on any particular choice of direction of increase in system stress. Although a certain direction is assumed for increasing system stress while generating the training data, different directions can be assumed for different operating conditions and the directions do not have to be linear as commonly used in the case of sensitivity expression given in (2.7). One more advantage is that one does not have to

find the Jacobian matrix exactly at the point of voltage instability, which is numerically a difficult task.

5.4 Formulation of the generation rescheduling problem

The most economic amount of generation rescheduling to enhance the voltage stability margin by at least a specified amount is found by using optimization [69, 70]. The sensitivities of the voltage stability margin with respect to the generator real power outputs are found by using trained RBFNs as described above. The voltage stability constraints for multiple contingencies are incorporated in the form of inequalities stated in (5.3). Other operating constraints of a power system, such as the real and reactive power balance, voltage constraints at the busses, generator output limits are included in the optimization routine. The total cost of generation is taken as the objective function to be minimized. The optimization problem is stated as follows:

Minimize $$\sum_{i=1}^{g} F(p_i) \tag{5.6}$$

subject to

$$p_i = |V_i| \sum_{j=1}^{N} |V_j| |Y_{ij}| \cos(\delta_i - \delta_j - \theta_{ij}), \forall i = 1, ..., g \tag{5.7}$$

$$p_{ldi} = |V_i| \sum_{j=1}^{N} |V_j| |Y_{ij}| \cos(\delta_i - \delta_j - \theta_{ij}), \forall i = 1, ..., ld \tag{5.8}$$

$$q_i = |V_i| \sum_{j=1}^{N} |V_j| |Y_{ij}| \sin(\delta_i - \delta_j - \theta_{ij}), \forall i = 1, ..., N \tag{5.9}$$

$$\sum_{i=1}^{g} p_i = \sum_{i=1}^{ld} p_{ldi} + P_{loss} \tag{5.10}$$

$$p_{i\min} \le p_i \le p_{i\max}, \forall i = 1,...,g \tag{5.11}$$

$$V_{i\min} \le V_i \le V_{i\max}, \forall i = 1,...,N \tag{5.12}$$

$$\sum_{i=1}^{gk} \Delta p_i S_i^k \ge \Delta M_{k\min}, \forall k = 1,...,c \tag{5.13}$$

where $F(p_i)$ is the operating fuel cost of the i^{th} generator and is given by the quadratic equation, $F(p_i)=a_i p_i^2 + b_i p_i + c_i$, with a_i, b_i and c_i as constants,

p_{ldi} is the real power demand of the i^{th} load,

q_i is the reactive power injection at the i^{th} bus,

$V_i = |V_i| \angle \delta_i$ is the voltage of bus i,

$Y_{ij} = |Y_{ij}| \angle \theta_{ij}$ is the ij^{th} element of the bus admittance matrix,

P_{loss} is the total real power loss in the system,

$P_{i\min}$ and $P_{i\max}$ are the minimum and maximum MW limits of the i^{th} generator,

$V_{i\min}$ and $V_{i\max}$ are the minimum and maximum voltage limits of the i^{th} bus,

Δp_i is the change in MW output of the i^{th} generator in the base case,

$\Delta M_{k\min}$ is the required minimum MW enhancement in voltage stability margin for the k^{th} contingency,

gk is the number of participating generators for the k^{th} contingency,

S_i^k is the sensitivity of the voltage stability margin with respect to the i^{th} generator for the k^{th} contingency,

c is the total number of contingencies considered, including the base case.

Inequality constraints (5.13) ensure that the rescheduling of generations in the base case results in a safe voltage stability margin for the base case as well as for different potential contingencies.

5.5 Simulation results

The proposed scheme of generation rescheduling for voltage stability enhancement for multiple contingencies has been applied to the New England 39-bus test system [57]. The single-line diagram of this test power system is shown in Figure A.1 in Appendix A. The sensitivities of the voltage stability margin with respect to the generator real power outputs are found by using separate RBFNs for the base case and different contingencies. For generating training samples for the RBFN, the active and reactive powers at the load busses and the generator MW outputs are varied randomly within ± 20% of the base case values. The MW outputs of the generators and the active load powers are taken as the inputs to the RBFN. For each operating condition, the MW margin is obtained by using PowerWorld Simulator [18] and is recorded as the outputs of the RBFN. Separate RBFNs are designed for different contingencies. For a contingency involving the outage of a generator, remaining generators are allowed to increase the generation in proportion to their participation factors in the base case, to compensate for the lost generation. The participation factors are taken as the ratio of a generator output to the total generation.

Test results are reported in this section for the base case operating condition and four different contingencies as shown in Table A.1. The contingencies are selected in such a way that they reflect significant changes in system topology. For example, all the

contingencies considered in this study involve outage of a radial line, which disconnects the corresponding generator also from the system.

The sensitivities are found with the help of the RBFNs trained with sufficient variety of training samples consisting of the generator real power outputs and the load real power demands. Separate RBFNs are used for each network topology. Table 5.1 gives the values of the designed parameters of the RBFN. The values are determined by trial and error method to give best results. Table 5.2 gives the number of hidden units for the RBFNs for the base case and different contingencies.

Table 5.1: Values of different design parameters for the RBFN used for computing the parameter sensitivities of the voltage stability margin for the New England 39-bus test system

Parameters	σ_{min}	e_{min}	ε_{max}	γ	ε_{min}	κ
Values	200	50	1000	0.97	100	0.8

Table 5.2: Number of hidden units for the RBFNs used for different topologies for finding the parameter sensitivities of the voltage stability margin for the New England 39-bus test system

Topologies	Number of hidden units
Base case	57
Contingency C1	59
Contingency C2	54
Contingency C3	52
Contingency C4	51

The sensitivities of the voltage stability margin with respect to the generator outputs are found by using the RBFNs for corresponding network topology, as described in section 5.3. Step size of the perturbations given to the generator outputs to compute the sensitivities are found using the iterative scheme described at the end of section 5.3. The

ratio of the change in output of the RBFN to the change in generator output is taken as the sensitivity corresponding to that particular generator. Table 5.3 shows the sensitivities of the voltage stability margin with respect to different generator outputs, for the base case and different contingencies.

Table 5.3: Sensitivities of the voltage stability margin with respect to outputs of participating generators, found by using separate RBFNs for different topologies

Topologies	Sensitivities of the voltage stability margin with respect to the output of generators								
	G30	G32	G33	G34	G35	G36	G37	G38	G39
Base case	-0.3118	-0.8011	-0.8173	-0.5225	-0.8997	-0.8348	-0.6691	-0.7931	-0.8544
Contingency C1	-0.3294	-0.8653	-0.9565	-0.8268	-0.9649	-0.7904	-0.8720	---	-0.9916
Contingency C2	-0.2239	---	-0.7261	-0.7721	-0.8173	-0.8588	-0.7178	-0.9054	-0.9658
Contingency C3	-0.4335	-1.2609	---	-1.2855	-0.7553	-1.2181	-0.8042	-1.4264	-1.4664
Contingency C4	-0.3828	-0.9901	-0.8238	-1.2742	-0.9879	-0.7179	---	-1.3667	-1.3809

The sensitivities are used in the optimization routine for generation rescheduling to enhance the voltage stability margin for multiple contingencies. The MATLAB based power system simulation package MATPOWER [71] is used to find the optimum values of the generator outputs for voltage stability enhancement. It uses linear programming as optimization method. Voltage stability constraints are included in the MATPOWER programs to implement the proposed algorithm. Table 5.4 shows the voltage stability margins in MW before and after generation rescheduling for three different base case configurations. Base case 1 represents the original configuration of the New England 39-bus test system. Base case 2 and 3 are generated by increasing and curtailing the load respectively in the load area formed by the busses 18, 17 and 27. In both the cases, the change in the load active power demand is distributed among the participating generators in proportion to their participation factors. Table 5.5 shows the base case 1 and the

rescheduled generations. It is assumed that the generator outputs can be easily adjusted, as dictated by the proposed generation rescheduling scheme.

Table 5.4: MW margins to the point of voltage instability, for different base cases and after generation rescheduling for the New England 39-bus test system

	MW margin		% increase in MW margin
	Base case	After rescheduling	
Base case 1	2809	2956	5.23 %
Base case 2	2543	2687	5.66 %
Base case 3	3187	3375	5.90 %

Table 5.5: Base case 1 and the rescheduled generations for the New England 39-bus test system

Generators	MW generation	
	Base case	After rescheduling
30	250	350
32	650	662
33	632	548
34	508	559
35	650	536
36	560	531
37	540	548
38	830	843
39	1000	892

The hourly costs of the generators are determined by the following cost model:

$$C(P_{gi}) = 10 * P_{gi} + 0.1 * P_{gi}^2 \ \$/hr \tag{5.14}$$

where P_{gi} is the generation of the i^{th} generator and $C(P_{gi})$ is the cost in \$/hr.

The total hourly cost of generation in the base case 1 operating condition is \$103801 /hr, while that after rescheduling as shown in Table 5.5 is \$102636 /hr. Column 3 of Table 5.5 shows the generations that results in minimum total cost per hour, satisfying the minimum voltage stability margin requirement, along with other constraints. Table 5.6

shows the voltage stability margins in MW for different contingencies, before and after generation rescheduling. Column 2 in Table 5.6 shows the MW margins to the point of voltage instability when a contingency occurs with the base case generation settings as given in column 2 of Table 5.5. Column 3 of Table 5.6 shows the MW margins when a contingency occurs with the optimal generation settings as shown in column 3 of Table 5.5. As observed from Table 5.4 and 5.6, significant increase in MW margin is obtained by the proposed method of generation rescheduling, for different operating conditions in the base case topology and also for different contingencies.

Table 5.6: MW margins to the point of voltage instability before and after generation rescheduling for different contingencies for the New England 39-bus test system

Contingencies	MW margin		% increase in MW margin
	Base case	After rescheduling	
Contingency C1	2393	2556	6.81 %
Contingency C2	2481	2643	6.53 %
Contingency C3	2493	2556	2.53 %
Contingency C4	2537	2698	6.35 %

5.6 Conclusions

A sensitivity-based generation rescheduling method for voltage stability enhancement considering multiple contingencies is presented in this chapter. The sensitivities of the voltage stability margin with respect to the outputs of the participating generators are computed by using separate RBFNs for each topology. A simple algorithm is also proposed to determine the appropriate perturbations to the inputs to the RBFNs to compute the sensitivities. The ANN-based method of computing sensitivities overcomes

the limitations of the analytical method of finding the sensitivity, as mentioned in Chapter 3, and provides an efficient way to compute the sensitivities. The proposed scheme considers multiple contingencies while rescheduling the generations. It ensures that the generation rescheduling for a particular contingency or base case does not violate the minimum MW margin requirement for other potential contingencies considered.

In the context of preventive and corrective control against voltage instability, the proposed method can be taken as a preventive measure against voltage instability by driving the present operating condition of a power system away from the point of voltage instability. The test results show that effectiveness of the proposed method of generation rescheduling for multiple contingencies. There are different control actions against the voltage instability in a power system such as generation rescheduling, changing the load tap changer (LTC) settings, adjusting the phase shifter angles, reactive compensation, and the load shedding. The proposed method of finding sensitivities using ANN can be extended to all of these control actions. It has been discussed earlier that the ANN-based computation of the sensitivities gives more accurate and realistic representation of the dependency of the voltage stability margin on the control actions, compared to the conventional analytical method. The proposed method therefore helps in developing a more accurate and effective voltage stability enhancement scheme for the utilities.

Chapter 6

Contributions of this Thesis and Directions for Future Research

6.1 Contributions of this Research

The significant contributions of this thesis are in the area of online voltage stability monitoring using the ANN, and also in the area of voltage stability enhancement of the electric power systems. Online voltage stability monitoring using the ANN is the area of focus for a major part of the research. In the later part of the research, a sensitivity-based multicontingency voltage stability enhancement scheme is proposed. The sensitivities are computed efficiently by using the ANN architecture proposed in the earlier part of the research. The main contributions of the research are summarized as follows:

- Numerous measurable power system parameters can be used as input features to the ANN for online voltage stability monitoring. A method of selection of important features is therefore essential for a large power system. Sensitivities of the voltage stability margin with respect to different power system parameters are used widely to select features that highly affect the voltage stability margin. There are, however, limitations of the conventional methods of finding the sensitivities, as discussed in Chapter 2. A new regression-based method of finding sensitivities is proposed in Chapter 3. A second-order regression model is developed for each topology to estimate the voltage stability margins. The regression model offers the advantages of differentiability. Sensitivities of the voltage stability margin with

respect to different parameters can be found by differentiating the regression model. It also eliminates the need for obtaining the powerflow Jacobian matrix at the point of bifurcation, which is numerically difficult. Once trained for sufficient varieties of operating conditions, the regression model can serve as a means to find the sensitivities needed to select important features.

- Using the sensitivity-based selection of input features, a scheme for online voltage stability monitoring using a Multilayer Perceptron (MLP) network is proposed in Chapter 3. The efficient method for the selection of features results in a compact and efficient ANN architecture. Separate ANNs are used for voltage stability monitoring for different system topologies. Contingency analysis is performed at the beginning to choose a limited number of critical contingencies to be monitored. The test results indicate the effectiveness of the proposed scheme for online voltage stability monitoring.
- Chapter 4 proposes a scheme for online voltage stability monitoring for multiple contingencies using an enhanced Radial Basis Function Network (RBFN). For a large power system with numerous potentially dangerous contingencies, it may be a demanding task to design separate ANNs for different contingencies. The proposed RBFN can be trained and used to estimate voltage stability margins for multiple contingencies. The only additional resource needed for monitoring a new contingency is an additional weight vector at the output layer of the RBFN. Designs of the architectures of the ANNs used in the existing literature are mostly based on trial and error methods to find the optimum network size. The number of

neurons in the hidden layer of the proposed RBFN is decided automatically using a sequential learning strategy. As the operating conditions and loading scenario keep changing in a power system, the ANN should have the facility to adapt online. The proposed RBFN can be adapted online, without requiring fresh training of the network. A network pruning strategy is used to limit the growth of the network size as a result of the adaptation process. Application of the proposed method on test systems gives satisfactory results.

- It is well-known that the ANN works as a more accurate mapping tool than a simple second-order regression model, as used in Chapter 3. When a more accurate and robust method of finding sensitivities is required, use of the ANN is advisable in place of the simple regression-based method described earlier. A sensitivity-based generation rescheduling scheme for enhancement of voltage stability of a power system is proposed in Chapter 5. The sensitivities of the voltage stability margin with respect to the participating generators are computed by using the RBFN proposed in Chapter 4. A simple and effective algorithm is also proposed to determine the step size of the perturbations that one needs to impart on the generator outputs to compute the sensitivities.
- The sensitivity-based generation rescheduling scheme proposed in Chapter 5 aims at enhancement of the voltage stability margin for multiple contingencies. Voltage stability constraints are incorporated into the optimization routine for generation rescheduling by utilizing the sensitivity information obtained by using the RBFN. The generations rescheduled to enhance voltage stability margin for one

contingency may not be applicable for other contingencies. Hence multiple contingencies are considered while formulating the optimization problem, which aims at minimizing the total cost of generation in the system, while meeting various operational constraints. Application of the proposed method on test system proves its effectiveness in improving the voltage stability margins for multiple contingencies.

The operating conditions in a modern-day power system change continuously, depending on the demand scenario and economic considerations. The assessment of the voltage stability of the power system for any operating condition is essential for the secure operation of the system. The ANN-based online voltage stability monitoring scheme proposed in Chapter 3 can serve as a tool for estimating the available voltage stability margin for different contingencies for a relatively smaller power system. The voltage stability monitoring scheme proposed in Chapter 4 estimates the available voltage stability margins for multiple critical contingencies using a single ANN. The ANN has the features of automatically determining the network size and getting adapted online with changing operating conditions. Once trained with a sufficient variety of operating conditions, it can be used as a black box to estimate the voltage stability margin of a power system. The proposed method may therefore prove to be an attractive alternative to the utilities for online voltage stability assessment, compared to the time-consuming and complicated analytical methods.

Chapter 5 proposes a sensitivity-based method of enhancement of the voltage stability margin using the optimization technique. The sensitivities of the voltage stability margin with respect to the generator real power outputs are found using the ANN, which overcomes many limitations of the conventional method of finding the sensitivities. A complete preventive and corrective control scheme against the voltage instability in a utility incorporates different control actions such as generation rescheduling, changing load tap changer (LTC) settings, adjusting phase shifter angles, reactive compensation, and load shedding. The proposed method of finding sensitivities using an ANN can be extended to the control actions other than generation rescheduling as well, and therefore can assist in a more accurate and realistic representation of the control actions in the overall voltage stability enhancement scheme for the utility.

6.2 Directions for Future Research

The research presented in this thesis is an effort to contribute to the ongoing investigation by the scientific community in the interesting and very important area of monitoring and enhancement of voltage stability in a power system. Following are some of the suggestions regarding the future directions of research, based on or related to the current research:

- The proposed research on online voltage stability monitoring and enhancement has been tested successfully on the widely used New England 39-bus test system. Future research will apply the proposed methods on power systems of larger dimensions.

- Analytical methods in power system security assessment have their limitations due to modelling inaccuracies, computational burdens, and complex natures. In many cases human expertise is the last resort in taking vital decisions regarding secure operation of the power system. An expert system can provide a solution to this type of problems on its own, or at least, it can enhance the reliability of the human intervention in the security assessment problem by acting as a decision support system. There have been some discrete efforts to develop an expert system for power system security assessment problems [26, 72]. An integrated approach reaping the benefits of both conventional analytical methods and intelligent systems technology still needs to be worked out.
- The sensitivity-based multicontingency generation rescheduling scheme described in Chapter 5 considers only the generator real power rescheduling as the means to enhance voltage stability of a system. Future research will incorporate other methods of voltage stability enhancement, such as changing load tap changer (LTC) settings, adjusting phase shifter angles, reactive compensation, and load shedding, into the optimization process.
- Optimum operation of a power system meeting various economical and operational constraints is a basic requirement in the modern-day highly stressed power system. Conventional optimization methods, although being accurate, pose significant computational burdens as the system becomes larger. Another problem associated with the conventional methods of optimization is the convergence to local minima. A number of evolutionary programming techniques such as Genetic

Algorithm, Particle Swarm Optimization, and Ant Colony System Optimization have proved to be efficient in finding global solutions to the complex optimization problems of large dimensions [73]. While there is always an amount of uncertainty or error associated with the evolutionary algorithms, a hybrid approach including the conventional methods may prove to be a more efficient and accurate tool for power system optimization problems.

References

[1] C. W. Taylor, *Power System Voltage Stability*, McGraw-Hill, 1994.

[2] P. Kundur, *Power System Stability and Control*, McGraw-Hill, 1993.

[3] IEEE/CIGRE Joint Task Force on Stability Terms and Definitions, "Definition and Classification of Power System Stability", *IEEE Transactions on Power Systems*, Vol. 5, No. 2, May 2004, pp. 1387–1401.

[4] T. V. Cutsem, C. Vournas, *Voltage Stability of Electric Power Systems*, Kluwer Academic Publishers, 1998.

[5] IEEE/PES Power System Stability Subcommittee Special Publication, *Voltage Stability Assessment, Procedures and Guides*, Final Draft, January 1999.

[6] S. C. Savulescu, *Real-time Stability in Power Systems*, Springer, 2006.

[7] J. Machowski, J. W. Bialek, J. R. Bumby, *Power System Dynamics and Stability*, John Wiley & Sons, 1997.

[8] J. A. Diaz de Leon II, C. W. Taylor, "Understanding and Solving Short-Term Voltage Stability Problems', *IEEE Power Engineering Society Summer Meeting*, 2002, pp. 745-752.

[9] I. Dobson, "Observations on the Geometry of Saddle Bifurcation and Voltage Collapse in Electrical Power Systems", *IEEE Transactions on Circuits and Systems*, Vol. 39, No. 3, March 1992, pp. 240-243.

[10] H. D. Chiang, I. Dobson, R. Thomas, J.S. Thorp, L. F. Ahmed, "On Voltage Collapse in Electric Power Systems", *IEEE Transactions on Power Systems*, Vol. 5, No. 2, May 1990, pp.601–611.

[11] F. Dong, B. H. Chowdhury, M. Crow, L. Acar, "Cause and Effects of Voltage Collapse-Case Studies with Dynamic Simulations", *IEEE Power Engineering Society General Meeting*, 2004, pp. 1806-1812.

[12] I. Dobson, "The Irrelevance of Load Dynamics for the Loading Margin to Voltage Collapse and Its Sensitivities", *Bulk Power System Voltage Phenomena-III, Voltage Stability, Security and Control*, Davos, Switzerland, August, 1994.

[13] I. Dobson, "Towards a Theory of Voltage Collapse in Electric Power Systems", *Systems and Control Letters* 13, 1989, pp. 253-262.

[14] B. Gao, G.K. Morison, and P. Kundur, "Voltage stability evaluation using modal analysis," *IEEE Transactions on Power Systems*, Vol. 7, No. 4, November 1992, pp.1529–1542.

[15] R. Seydel, *From Equilibrium to Chaos*, Elsevier, New York, 1988.

[16] F. Milano, "An Open Source Power System Analysis Toolbox," *IEEE Transactions on Power Systems*, Vol. 20, No. 3, August 2005, pp.1199–1206.

[17] G. K. Morison, B. Gao and P. Kundur, "Voltage stability analysis using static and dynamic approaches", *IEEE Transactions on Power Systems*, Vol. 8, No. 3, August 1993, pp. 1159–1171.

[18] PowerWorld Simulator, Version 10.0 SCOPF, PVQV, PowerWorld Corporation, Champaign, IL 61820, 2005.

[19] T. S. Dillon, D. Neibur, *Neural Networks Applications in Power Systems*, CRS Publishing Ltd, 1996.

[20] PSERC Publication 01-05, " Automated Operating Procedures for Transfer limits", Power Systems Engineering Research Center, Cornell University, Final report, May 2001.

[21] PSERC Publication 03-06, " Integrated Security Analysis", Power Systems Engineering Research Center, Cornell University, Final report, May 2003.

[22] N. Balu et al., " On-line Power system Security Analysis", *Proceedings of the IEEE*, Vol. 80, No. 2, February 1992, pp. 262-280.

[23] K. Warwick, A. Ekwue, R. Aggarwal, *Artificial Intelligence Techniques in Power Systems*, IEE, 1997.

[24] L. A. Wehenkel, *Automatic Learning Techniques in Power Systems*, Kluwer Academic Publishers, 1998.

[25] D. J. Sobajic, *Neural Network Computing for the Electric Power Industry*, Lawrence Erlbaum Associates, Publishers, 1993.

[26] J. A. Momoh, M. E. El-Hawary, Electric Systems, *Dynamics and Stability with Artificial Intelligence Applications*, Marcel Dekker, Inc, 2000.

[27] D. Popovic, D. Kukolj, F. Kulic, "Monitoring and Assessment of Voltage Stability Margins Using Artificial Neural Networks with a Reduced Input Set", *IEE Proceedings*, Vol. 145, No. 4, July 1998, pp. 355-362.

[28] D. Popovic, F. Kulic, "On Line Monitoring and Preventing of Voltage Stability Using Reduced system Model", *Bulk Power System Dynamics and Control V-Security and Reliability in a Changing Environment,* Onomichi, Japan August, 2001, pp. 387-400.

[29] B. Jeyasurya, "Artificial Neural Networks for Power System Steady-State Voltage Instability Evaluation", *Electric Power Systems Research*, Vol. 29, 1994, pp. 85-90.

[30] B. Jeyasurya, "Artificial Neural Networks for On-line Voltage Stability Assessment", *IEEE Power Engineering Society Summer Meeting*, 2000, pp. 2014-2018.

[31] A. A. El-Keib, X. Ma, "Application of Artificial Neural Networks in Voltage Stability Assessment", *IEEE Transactions on Power Systems*, Vol. 10, No. 4, November 1995, pp. 1890-1896.

[32] L. Chen, K. Tomsovic, A. Bose, R. Stuart, "Estimating Reactive Margin for Determining Transfer Limits", *IEEE Power Engineering Society Summer Meeting*, July 2000, pp. 490-495.

[33] S. Chakrabarti, B. Jeyasurya, "On-line Voltage Stability Monitoring Using Artificial Neural Network", *Large Engineering Systems Conference on Power Engineering*, Halifax, Canada, July 2004.

[34] S. Greene, I. Dobson, F. L. Alvarado, "Sensitivity of the Loading Margin to Voltage Collapse with respect to Arbitrary Parameters," *IEEE Transactions on Power Systems*, Vol. 12, No. 1, February 1997, pp. 262-272.

[35] X. Wang, G. C. Ejebe, J. Tong, J. G. Waight, "Preventive/ Corrective Control for Voltage Stability Using Direct Interior Point Method," *IEEE Transactions on Power Systems*, Vol. 13, No. 3, August 1998, pp. 878-883.

[36] Z. Feng, V. Ajjarapu, D. J. Maratukulam, "A Comprehensive Approach for Preventive and Corrective Control to Mitigate Voltage Collapse," *IEEE Transactions on Power Systems*, Vol. 15, No. 2, May 2000, pp. 791-797.

[37] F. Capitanescu, T. V. Cutsem, "Preventive Control of Voltage Security Margins: A Multicontingency Sensitivity-Based Approach," *IEEE Transactions on Power Systems*, Vol. 17, No. 2, May 2002, pp. 358-364.

[38] T. V. Cutsem, "An Approach to Corrective Control of Voltage Instability using Simulation and Sensitivity," *IEEE Transactions on Power Systems*, Vol. 10, No. 2, May 1995, pp. 616-622.

[39] H. Song, B. Lee, S. Kwon, V. Ajjarapu, "Reactive Reserve-Based Contingency Constrained Optimal Power Flow (RCCOPF) for Enhancement of Voltage Stability Margins", ," *IEEE Transactions on Power Systems*, Vol. 18, No. 4, November 2003, pp. 1538-1546.

[40] F. Dong, B. H. Chawdhury, M. L. Crow, L. Acar, "Improving Voltage Stability by Reactive Power Reserve Management", *IEEE Transactions on Power Systems*, Vol. 20, No. 1, February 2005, pp. 338-345.

[41] W. Rosehart, C. Canizares, V. Quintana, "Optimal Power Flow Incorporating Voltage Collapse Constraints," *Proceedings of the 1999 IEEE Power Engineering Society Summer Meeting*, July 1999, pp. 820-825.

[42] M. E. El-Hawary, L.G. Dias, "Bus Sensitivity to Load-model Parameters in Load-flow Studies," *IEE proceedings*, Vol. 134, Pt. C, No. 4, July 1987, pp. 302-305.

[43] L.G. Dias, M. E. El-Hawary, "Static Load Modeling in Electric Power Systems," *IEE proceedings*, Vol. 136, Pt. C, No. 2, March 1989, pp. 68-77.

[44] T. Ohyama, A. Watanabe, K. Nishimura, S. Tsuruta, "Voltage Dependence of Composite Loads in Power Systems", *IEEE Transactions on Power Apparatus and Systems,* Vol. 104, No.11, November 1985, pp. 3064-3073.

[45] E. Vaahedi, M.A. El-Kady J. A. Libaque-Esaine, V. F. Carvalho, "Load Models for Large Scale Stability Studies from End User Consumption", *IEEE Transactions on Power Systems*, Vol. 2, No. 4, November 1987, pp. 864-871.

[46] W. W. Price, K. A. Wirgau, A. Murdoch, J. V. Mitsche, E. Vaahedi, M. A. E-Kady, "Load Modeling for Power Flow and Transient Stability Computer Studies", *IEEE Transactions on Power Systems*, Vol. 3, No. 1, February 1988, pp. 180-187.

[47] W. Xu, E. Vaahedi, Y. Mansour, J. Tamby, " Voltage Stability Load Parameter Determination from Field Tests on B. C. Hydro's System", *IEEE Transactions on Power Systems*, Vol. 12, No.3, August 1997, pp. 1290-1297.

[48] M. K. Pal, "Voltage Stability Conditions Considering Load Characteristics", *IEEE Transactions on Power Systems*, Vol. 7, No. 1, February 1992, pp. 243-249.

[49] M. K. Pal, "Voltage Stability: Analysis needs, Modeling Requirement, and Modeling Adequacy", *IEE proceedings*, Vol. 140, No. 4, July 1993, pp. 279-286.

[50] S. Chakrabarti, B. Jeyasurya, "Effect of Load Modeling on the Performance of Power System Voltage Stability Indices", *IEEE NECEC Conference*, St. John's, Newfoundland, Canada, November, 2004.

[51] Canada-U.S. Power System Outage Task Force, "Final Report on the August 14, 2003 Blackout in the United States and Canada: Causes and Recommendations", April 2004.

[52] R. H. Myers, *Classical and Modern Regression with Applications*, PWS-KENT, 1990.

[53] S. Haykin, *Neural Networks: A Comprehensive Foundation*, Pearson Education, 2002.

[54] M. H. Hassoun, *Fundamentals of Artificial Neural Networks*, MIT Press, Cambridge, 1995.

[55] S. Kumar, *Neural Networks: A Classroom Approach*, Tata McGraw Hill Publishing Company Limited, New Delhi, 2004.

[56] Neural Network Toolbox, MATLAB version 6.5.0, MathWorks Inc., June 18, 2002.

[57] M. A. Pai, *Energy Function Analysis for Power System Stability*, Kluwer Academic Publishers, 1989.

[58] S. Chakrabarti, B. Jeyasurya, "Multicontingency Voltage Stability Monitoring of Power Systems Using Radial Basis Function Network", *13th International Conference on Intelligent Systems Application to Power Systems*, Washington DC, USA, November, 2005.

[59] V. Kadirkamanathan, M. Niranjan, "A Function Estimation Approach to Sequential Learnings with Neural Networks", *Neural Computation*, Vol. 5, 1993, pp. 954-975.

[60] N. Sundararajan, P. Saratchandran, L. Y. Wei, *Radial Basis Function Neural Networks with Sequential Learning*, World Scientific, 1999.

[61] M. J. L. Orr, Introduction to Radial Basis Function Networks, http://www.anc.ed.ac.uk/~mjo/intro/intro.html.

[62] H. W. Engl, M. Hanke, A. Neubauer, *Regularization of Inverse Problems*, Kluwer Academic Publishers, 1996.

[63] D. M. Trujillo, H. R. Busby, *Practical Inverse Analysis in Engineering*, CRC Press, 1997.

[64] P. Hirsch, D. Sobajic, N. Hatziargyriou, "Real Time DSA and AI: Next Steps?", *IEEE Power Engineering Society General Meeting*, June 2005.

[65] J. A. Momoh, *Electric Power System Applications of Optimization*, Mercel Dekker, New York, 2001.

[66] D. P. Kothari, *Power System Optimization*, Prentice Hall of India, New Delhi, 2004.

[67] S. Chakrabarti, B. Jeyasurya, "Sensitivity-based Generation Rescheduling for Voltage Stability Enhancement", *IEEE Power Engineering Society General Meeting*, 2005, pp. 1267-1271.

[68] S. Chakrabarti, B. Jeyasurya, "Sensitivity-based Generation Rescheduling for Multicontingency Voltage Stability Enhancement", accepted for publication in the Proceedings of *IEEE Power Engineering Society General Meeting*, 2006.

[69] F. S. Hillier, G. J. Lieberman, *Introductions to Operations Research*, McGraw Hill, Boston, 2001.

[70] S. S. Rao, *Engineering Optimization: Theory and Practice*, Wiley, New York, 1996.

[71] MATPOWER, Version 3.0.0, Power Systems Engineering Research Center, School of Electrical Engineering, Cornell University, Ithaca, 2005.

[72] J. Giarrantano, G. Riley, *Expert Systems, Principles and Programming*, PWS Publishing Company, Boston, 1994.

[73] Tutorial on Intelligent Optimization and Control for Power Systems, *13th International Conference on Intelligent Systems Application to Power Systems*, Washington DC, USA, November, 2005.

[74] A. Horn, C. R. Johnson, *Matrix analysis*, Cambridge University Press, 1985.

Appendix A

A.1 Single line diagram of the 39-bus test power system

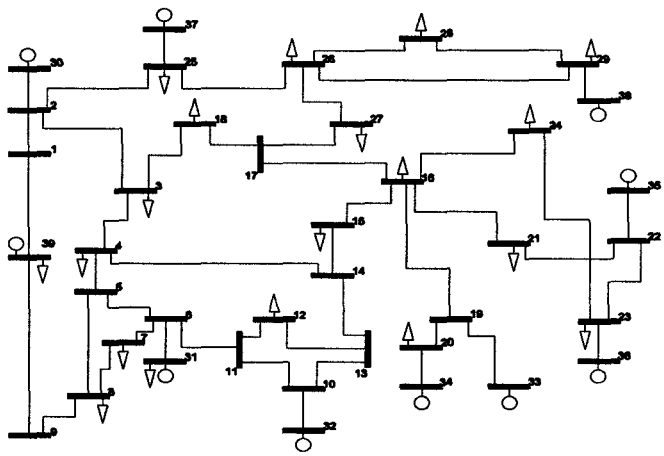

Figure A.1: New England 39-bus test power system

A.2 Table of contingencies

Table A.1: Selected contingencies for the case studies on the New England 39-bus test power system

Contingency	Description
C1	Outage of line between busses 29 and 38 and generator 38
C2	Outage of line between busses 10 and 32 and generator 32
C3	Outage of line between busses 19 and 33 and generator 33
C4	Outage of line between busses 25 and 37 and generator 37

A.3 Results of sensitivity analysis of the voltage stability margin

Table A.2: Sensitivities of the voltage stability margin with respect to the active and reactive power demands of the loads for different contingencies

Load P, Q	Base case	Contingency C1	Contingency C2	Contingency C3	Contingency C4
P3	-0.2441	-0.2297	-0.2284	-0.2311	-0.2302
P4	-0.2069	-0.1947	-0.1980	-0.1971	-0.1956
P7	-0.1758	-0.1654	-0.1711	-0.1677	-0.1668
P8	-0.1806	-0.1699	-0.1751	-0.1718	-0.1709
P12	-0.1818	-0.1710	-0.1837	-0.1767	-0.1761
P15	-0.2459	-0.2314	-0.2322	-0.2381	-0.2338
P16	-0.2570	-0.2418	-0.2415	-0.2498	-0.2452
P18	-0.2567	-0.2415	-0.2374	-0.2427	-0.2410
P20	-0.2621	-0.2466	-0.2510	-0.2664	-0.2555
P21	-0.2583	-0.2430	-0.2451	-0.2528	-0.2491
P23	-0.2565	-0.2414	-0.2459	-0.2530	-0.2502
P24	-0.2589	-0.2435	-0.2437	-0.2519	-0.2475
P25	-0.2575	-0.2423	-0.2267	-0.2309	-0.2459
P26	-0.2905	-0.2733	-0.2425	-0.2481	-0.2556
P27	-0.2812	-0.2646	-0.2445	-0.2509	-0.2538
P28	-0.3300	-0.3105	-0.2481	-0.2533	-0.2621
P29	-0.3327	-0.3131	-0.2458	-0.2508	-0.2598
Q3	-0.0238	-0.0223	-0.0089	-0.0123	-0.0093
Q4	-0.0390	-0.0367	-0.0251	-0.0263	-0.0217
Q7	-0.0452	-0.0425	-0.0355	-0.0329	-0.0288
Q8	-0.0436	-0.0410	-0.0339	-0.0316	-0.0277
Q12	-0.0376	-0.0354	-0.0336	-0.0272	-0.0223
Q15	-0.0241	-0.0227	-0.0099	-0.0153	-0.0090
Q16	-0.0171	-0.0161	-0.0043	-0.0089	-0.0040
Q18	-0.0234	-0.0220	-0.0062	-0.0104	-0.0063
Q20	-0.0037	-0.0035	-0.0010	-0.0037	-0.0009
Q21	-0.0117	-0.0110	-0.0024	-0.0057	-0.0022
Q23	-0.0058	-0.0055	-0.0006	-0.0025	-0.0005
Q24	-0.0152	-0.0143	-0.0035	-0.0077	-0.0032
Q25	-0.0133	-0.0125	-0.0012	-0.0027	-0.0016
Q26	-0.0339	-0.0319	-0.0014	-0.0039	-0.0010
Q27	-0.0309	-0.0290	-0.0031	-0.0065	-0.0030
Q28	-0.0437	-0.0412	-0.0003	-0.0016	0.0001
Q29	-0.0439	-0.0413	-0.0003	-0.0012	-0.0000

Table A.3: Reduction of the input data dimension using the sensitivity of the MW margin with respect to the load real and reactive power demands

Topologies	Initial number of inputs	Number of inputs selected for $S_{pmin} = 0.15$ and $S_{qmin} = 0.01$	Number of inputs selected for $S_{pmin} = 0.2$ and $S_{qmin} = 0.02$	Number of inputs selected for $S_{pmin} = 0.25$ and $S_{qmin} = 0.03$
Base case	38	32	25	19
Contingency C1	38	32	24	11
Contingency C2	38	21	17	4
Contingency C3	38	24	17	9
Contingency C4	38	21	17	6

Table A.4: Selected cut-off values of the sensitivities for different contingencies

Topologies	S_{pmin}	S_{qmin}
Base case	0.25	0.03
Contingency C1	0.25	0.03
Contingency C2	0.20	0.02
Contingency C3	0.20	0.02
Contingency C4	0.20	0.02

A.4 Important computational steps for the RBFN

The important matrix operations and computational steps for the Radial Basis Function Networks (RBFN) used in Chapter 4 and 5 are given below:

A.4.1 Computation of optimal output weight vectors

Let $\{\mathbf{X}_i, \mathbf{d}_i\}_{i=1}^{n}$ be the training patterns, where $\mathbf{X}_i$ is the input to the RBFN and $\mathbf{d}_i = (d_{1i}, d_{2i}, ..., d_{ci})^T$ are the corresponding outputs. To improve the interpolating capability of the RBFN and smoothness in mapping, larger weights are penalized and the cost function to be minimized for the weight vector connecting hidden units to the t^{th}

output is given by,

$$C_t = \sum_{i=1}^{n} (d_{ti} - f_t(\mathbf{X}_i))^2 + \lambda_t \sum_{j=1}^{q} w_{jt}^2 ; \forall t = 1,...,c \qquad \text{(A1)}$$

where w_{jt} is the weight connecting j^{th} hidden neuron to the t^{th} output; q is the number of neurons in the hidden layer, λ_t is the regularization parameter.

The t^{th} output of the RBFN for the input $\mathbf{X}_i$ is given by,

$$f_t(\mathbf{X}_i) = \sum_{j=1}^{q} w_{jt} g_{ij} \qquad \text{(A2)}$$

where g_{ij} is defined as follows:

$$g_{ij} = g(\mathbf{X}_i, \mathbf{t}_j) = g(\|\mathbf{X}_i - \mathbf{t}_j\|) = \exp\left(-\frac{\|\mathbf{X}_j - \mathbf{t}_j\|^2}{2\sigma_j^2}\right) \qquad \text{(A3)}$$

where $\mathbf{t}_j$ is the data centre of the j^{th} hidden unit.

To find the optimal weight vector $\mathbf{w}_t$ for the t^{th} output of the RBFN, the cost function in (A1) is differentiated against each element of $\mathbf{w}_t$ and made equal to zero. Differentiating (A1) with respect to w_{jt},

$$\frac{\partial C_t}{\partial w_{jt}} = -2\sum_{i=1}^{n} (d_{ti} - f_t(\mathbf{X}_i)) \frac{\partial f_t(X_i)}{\partial w_{jt}} + 2\lambda_t w_{jt} \qquad \text{(A4)}$$

Now, from (A2), $\frac{\partial f_t(X_i)}{\partial w_{jt}} = g_{ij}$. Using this in (A4) and equating to zero for optimality condition,

$$-2\sum_{i=1}^{n} (d_{ti} - f_t(\mathbf{X}_i)) g_{ij} + 2\lambda_t w_{jt} = 0$$

Rearranging above and using (A2),

$$\sum_{i=1}^{n}(\sum_{j=1}^{q} w_{jt}g_{ij})g_{ij} + \lambda_t w_{jt} = \sum_{i=1}^{n} d_{ti}g_{ij} \tag{A5}$$

There are 'q' equations as (A5), for 'q' hidden units and all such equations can be expressed in the form of following matrix equation.

$$\mathbf{G}^T\mathbf{G}\mathbf{w}_t + \lambda\mathbf{w}_t = \mathbf{G}^T\mathbf{D}_t$$

Or, $$\mathbf{w}_t = (\mathbf{G}^T\mathbf{G} + \lambda\mathbf{I}_q)^{-1}\mathbf{G}^T\mathbf{D}_t \tag{A6}$$

where **G** is the matrix of basis functions and is given by,

$$\mathbf{G} = \begin{bmatrix} g_{11} & g_{12} & \cdots & g_{1q} \\ g_{21} & g_{22} & \cdots & g_{2q} \\ \vdots & \vdots & & \vdots \\ g_{n1} & g_{n2} & \cdots & g_{nq} \end{bmatrix} \tag{A7}$$

$\mathbf{D}_t = [d_{t1}, d_{t2}, ..., d_{tn}]^T$ is the vector containing desired t^{th} outputs for all the patterns $\{\mathbf{X}_i, \mathbf{d}_i\}_{i=1}^{n}$.

$\mathbf{I}_q$ is an identity matrix of dimension [q×q].

The weight vectors $\mathbf{w}_t$ as in (A6) are assembled for 'c' outputs in the output weight vector matrix **W** as in (4.15).

A.4.2 Addition of a new training pattern

Addition of a new training pattern to the existing design matrix $\mathbf{G}^q$ having 'q' basis functions based on 'n' training patterns has the effect of adding a new row as follows.

$$\mathbf{G}^{q+1} = \begin{bmatrix} \mathbf{G}^q \\ \mathbf{G}_{21} \end{bmatrix} \tag{A8}$$

where $\mathbf{G}^{q+1}$ is the new design matrix based on 'n+1' training patterns,

$$\mathbf{G}_{21} = \left[g_{n+1,1}, g_{n+1,2}, \ldots, g_{n+1,q} \right]$$

The variance matrix $\mathbf{A}^{q+1}$ after addition of the new training pattern can be constructed as follows.

$$\mathbf{A}^{q+1} = \mathbf{G}^{q+1^T}\mathbf{G}^{q+1} + \lambda_t \mathbf{I}_q = \left[\mathbf{G}^{q^T} \;\; \mathbf{G}_{21}^T \right] \begin{bmatrix} \mathbf{G}^q \\ \mathbf{G}_{21} \end{bmatrix} + \lambda_t \mathbf{I}_q \tag{A9}$$

Or, $$\mathbf{A}^{q+1} = \left[\mathbf{A}^q + \mathbf{G}_{21}^T \mathbf{G}_{21} \right] \tag{A10}$$

where $\mathbf{A}^q = \mathbf{G}^{q^T}\mathbf{G}^q + \lambda_t \mathbf{I}_q$

Using small rank adjustment formula for inverse of a matrix [74],

$$\mathbf{A}^{q+1^{-1}} = \mathbf{A}^{q^{-1}} - \frac{\mathbf{A}^{q^{-1}}\mathbf{G}_{21}^T\mathbf{G}_{21}\mathbf{A}^{q^{-1}}}{1 + \mathbf{G}_{21}\mathbf{A}^{q^{-1}}\mathbf{G}_{21}^T} \tag{A11}$$

Equation (A11) shows, with a prior knowledge of $\mathbf{A}^{q^{-1}}$, one can compute $\mathbf{A}^{q+1^{-1}}$ without inverting $\mathbf{A}^{q+1}$.

A.4.3 Addition of a new basis function

Addition of a new basis function and the corresponding training pattern to the existing design matrix $\mathbf{G}^q$ having 'q' basis functions based on 'n' training patterns has the effect of adding a new row and column as follows.

$$\mathbf{G}^{q+1} = \begin{bmatrix} \mathbf{G}^q & \mathbf{G}_{12} \\ \mathbf{G}_{21} & \mathbf{G}_{22} \end{bmatrix} \tag{A12}$$

where G^{q+1} is the new design matrix consisting of 'q+1' basis functions,

$$\mathbf{G}_{12} = \left[g_{1,q+1}, g_{2,q+1}, \ldots, g_{n,q+1} \right]^T$$

$$\mathbf{G}_{21} = \left[g_{n+1,1}, g_{n+1,2}, \ldots, g_{n+1,q} \right]$$

$$\mathbf{G}_{22} = g_{n+1,q+1}$$

The variance matrix $\mathbf{A}^{q+1}$ after addition of the new basis function and training pattern can be constructed as follows.

$$\begin{aligned} \mathbf{A}^{q+1} &= \mathrm{G}^{q+1^T}\mathrm{G}^{q+1} + \lambda_t \mathrm{I}_{q+1} \\ &= \begin{bmatrix} \mathbf{G}^{q^T} & \mathbf{G}_{21}^T \\ \mathbf{G}_{12}^T & \mathrm{G}_{22} \end{bmatrix} \begin{bmatrix} \mathbf{G}^q & \mathbf{G}_{12} \\ \mathbf{G}_{21} & \mathrm{G}_{22} \end{bmatrix} + \lambda_t \mathrm{I}_{q+1} \end{aligned} \tag{A13}$$

The above can be expressed as a partitioned matrix as follows.

$$\mathbf{A}^{q+1} = \begin{bmatrix} \mathbf{A}_{11} & \mathbf{A}_{12} \\ \mathbf{A}_{21} & \mathbf{A}_{22} \end{bmatrix} \tag{A14}$$

where $\mathbf{A}_{11} = \mathbf{A}^q + \mathbf{G}_{21}^T \mathbf{G}_{21}$

$$\mathbf{A}_{12} = \mathbf{G}^{q^T}\mathbf{G}_{12} + \mathrm{G}_{22}\mathbf{G}_{21}^T$$

$$\mathbf{A}_{21} = \mathbf{G}_{12}^T\mathbf{G}^q + \mathrm{G}_{22}\mathbf{G}_{21}$$

$$\mathbf{A}_{22} = \mathbf{G}_{12}^T\mathbf{G}_{12} + \mathrm{G}_{22}^2$$

Inverse of $\mathbf{A}^{q+1}$ can be found by using the formula for finding inverse of a partitioned matrix [74] as follows.

$$\mathbf{A}^{q+1^{-1}} = \begin{bmatrix} \mathbf{A}_{11}^{-1} + \mathbf{A}_{11}^{-1}\mathbf{A}_{12}\Delta^{-1}\mathbf{A}_{21}\mathbf{A}_{11}^{-1} & -\mathbf{A}_{11}^{-1}\mathbf{A}_{12}\Delta^{-1} \\ -\Delta^{-1}\mathbf{A}_{21}\mathbf{A}_{11}^{-1} & \Delta^{-1} \end{bmatrix} \tag{A15}$$

where $\Delta = \mathbf{A}_{22} - \mathbf{A}_{21}\mathbf{A}_{11}^{-1}\mathbf{A}_{12}$

$\mathbf{A}_{11}^{-1}$ in (A15) can be computed using small rank adjustment formula for finding inverse of a matrix.

$$\mathbf{A}_{11}^{-1} = \mathbf{A}^{q^{-1}} - \frac{\mathbf{A}^{q^{-1}}\mathbf{G}_{21}^{T}\mathbf{G}_{21}\mathbf{A}^{q^{-1}}}{1+\mathbf{G}_{21}\mathbf{A}^{q^{-1}}\mathbf{G}_{21}^{T}} \tag{A16}$$